DISSERTATION

Chiral Metallocene/Lewis Acid Hybrid Polymerization Catalysts And Heterobimetallic Polypyridine Substituted Dioxocyclams

Submitted by
Andrew David Bolig
Department of Chemistry

In partial fulfillment of the requirements
for the degree of Doctor of Philosophy
Colorado State University
Fort Collins, CO
Summer, 2005

COLORADO STATE UNIVERSITY

April 21, 2005

WE HEREBY RECOMMEND THAT THE DISSERTATION PREPARED UNDER OUR SUPERVISION BY ANDREW BOLIG ENTITLED CHIRAL METALLOCENE / LEWIS ACID HYBRID POLYMERIZATION CATALYSTS AND HETEROBIMETALLIC POLYPYRIDINE SUBSTITUTED DIOXOCYCLAMS BE ACCEPTED AS FULFILLING IN PART REQUIREMENTS FOR THE DEGREE OF DOCTOR OF PHILOSOPHY.

Committee on Graduate Work

Oren P. Anderson

Debbie C. Crans

Laurence A. Belfiore

Eugene. Yi-X. Chen / Co-advisor

Louis S. Hegedus / Co-advisor

Anthony K. Rappe / Department Head / Director

ABSTRACT OF DISSERTATION

CHIRAL METALLOCENE / LEWIS ACID HYBRID POLYMERIZATION CATALYSTS AND HETEROBIMETALLIC POLYPYRIDINE SUBSTITUTED DIOXOCYCLAMS

The investigation of *ansa*-zirconocene catalysts for the polymerization of polar monomers is described, revealing striking differences in mechanism and the stereochemistry of products obtained depending on the nature of the Lewis Acid cocatalyst, $M(C_6F_5)_3$ (M=B,Al). Whereas borane-mediated processes proceed via a cationic active site, the aluminates apparently operated by a novel anionic mechanism. This observation led to the production of stereo-diblock copolymers of MMA via sequential catalyst addition. Further, stereo-multiblock copolymers were produced by judicious blending of catalysts. This represents catalysis wherein both cation and anion operate in tandem, generating distinct stereoregular segments. Model studies are presented which support the proposed mechanisms. Towards this end, the first chiral *ansa*-metallocene (mono- and bis-) ester enolates were prepared and characterized, and demonstrated to be competent catalysts and useful model compounds.

The complexation of a new class of ligands, wherein polypyridine functionality is covalently appended onto capped dioxocyclams, was investigated. Coordination linkage of these species was then achieved through Ru(II) and Co(II) of terpyridine capped cyclams. Further investigations revealed an N,C,N variant of terpyridine was more practical. This new (dipyridyl benzene, dpb) capped dioxocyclam readily cyclometallated Ru. The resultant products were then subjected to metal complexation of the dioxocyclam cavity, resulting in heterobimetallic products containing an Ru photosensitizer group covalently linked to cobalt and copper dioxocyclams.

Andrew David Bolig
Department of Chemistry
Colorado State University
Fort Collins, CO 80523
Summer, 2005

TABLE OF CONTENTS

Chapter 1

Introduction

I. Early Metal Catalyzed Polymerizations

A significant paradigm shift in polymer chemistry began fifty years ago with the appearance of metal-catalyzed processes for the production of polyolefins. First, Ziegler[1] demonstrated the feasibility of the approach, polymerizing ethylene with catalyst systems typically comprised of an early transition metal halide (typically $TiCl_4$ or $TiCl_3$) and a Group I-III component (AlR_3, R= methyl, ethyl most common). The resultant polymers had substantially improved physical properties compared to those produced by free radical processes. It is widely accepted that the transition metal "catalyst" is acted upon by the main-group "cocatalyst" in two critical ways[2], illustrated in scheme 1: 1) alkylation of the metal center to provide a suitable initiating group for monomer, and 2) halide (or alkide) abstraction by the Lewis acid to generate open coordination sites.

Exchange Reactions to Alkylate the TM catalyst

$$AlR_3 + TiCl_4 \rightarrow AlR_2Cl + TiRCl_3$$

$$AlR_2Cl + TiCl_4 \rightarrow AlRCl_2 + TiRCl_3$$

$$AlR_3 + TiRCl_3 \rightarrow AlR_2Cl + TiR_2Cl_2$$

Representative Lewis Acid Abstraction

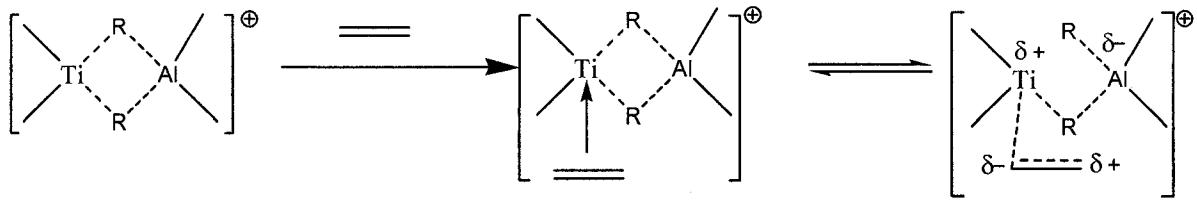

Scheme 1. Representative Interactions of catalyst system components

Although these two reaction pathways are believed to produce active catalytic species for coordination polymerizations, it should be noted that many mechanistic questions remain. The matter is complicated by several additional reactions, including homolytic cleavage of transition metal-alkyl bonds to yield reduced metal species and alkyl radicals, both of which engage in further chemistry. Most commercial processes employ supported catalysts, wherein the species discussed above are adsorbed onto solid supports such as MgO or $MgCl_2$, further complicating the situation. In short, despite massive efforts, there is still debate over the nature of the true active species in these polymerization processes. While this has not hindered their commercial success, it has frustrated mechanistic study and rational design and improvements of new generation systems.

The one feature required for activity in these systems, however, upon which consensus has largely been reached[3] is the cationic transition metal center. It is widely accepted that this species is required for π-complexation of the olefin, activating it to migratory insertion in the case of olefins, as illustrated in scheme 2. In the case of polar monomers, we will see a slightly different mechanism, but the cationic transition metal has still been considered a requisite for activity.

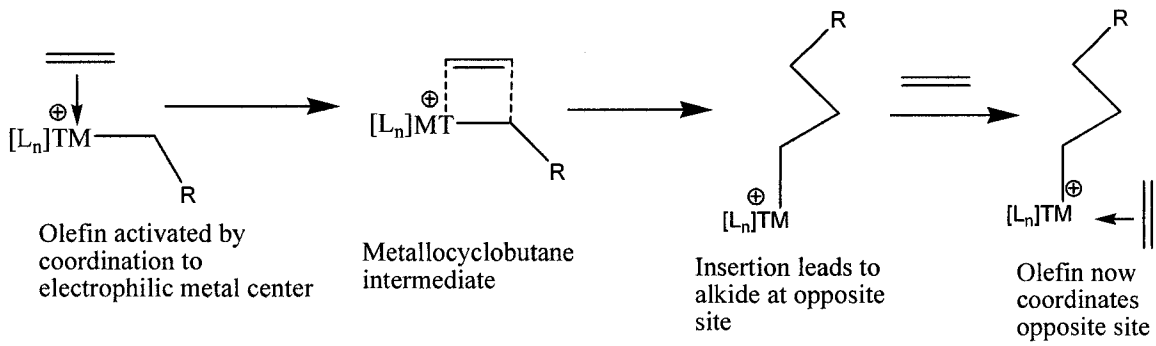

Scheme 2: Role of cationic transition metal site

II. Stereoregular Polymers

Shortly after Ziegler's publication appeared, Natta[4] applied catalysts of this type to the prochiral α-olefins, which opened the possibility of stereoregular synthetic polymers. Not only do these monomers fail to react with radical or conventional ionic initiators, but there was considerable doubt that stereoregular polymers could be prepared synthetically. He showed both that they were accessible, and that the polymeric products were highly crystalline, with higher melting points, density, and lower solubility, than the analogous amorphous products. This illustrates a powerful aspect of the application of coordination chemistry to polymerizations; the stereochemistry, or tacticity, can be regulated by suitable choice of metals and ligand systems. As will be seen, this has dramatic effects on the physical properties of the resultant materials. For the purposes of the present work, there are two major types of stereoregular polymers, illustrated in figure 1; those with a random sequence of stereocenters are termed atactic.

Isotactic
SAME relative configuration at adjacent stereocenters

Syndiotactic
OPPOSITE relative configuration at adjacent stereocenters

Figure 1: Two major types of stereoregular polymers (illustrated for PMMA)

The first type, isotactic, indicates that adjacent stereocenters have the same relative configuration. This is denoted "m", or meso, referring to the mirror plane bisecting the methylene group between stereocenters. Alternatively, the adjacent stereocenters may have the opposite relative configuration, denoted "r", or racemic, referring to the R, or S isomers that are possible at each site. It should be noted that, for high molecular weight polymers, the polymer chain substituents on either side of the stereocenters effectively become identical, so these are usually termed pseudo-asymmetric centers.

These various configurations are not simply academic curiosities; they have dramatic effects on the physical properties of the resultant polymeric materials. The award of the 1963 Nobel Prize in Chemistry to Ziegler and Natta attests to the importance of stereoregular polymers. A practical aspect of the various tacticities can be seen in the glass transition temperatures (T_g) of the resultant polymers. Polymeric materials may exhibit crystalline and amorphous regions. In an ideal sense, a purely crystalline polymer would exhibit a melting transition, analogous to (but broader than) that observed for a crystalline small molecule. This is the case for certain forms of linear polyethylene, which pack very well into crystalline domains. However, less ordered polymers exhibit amorphous regions wherein long range movements of the backbone of the chain, or

"segmental motion" can occur, when sufficient thermal energy is present[5]. On the macro scale, T_g is observed as a temperature above which a polymeric material loses its glasslike properties (rigidity, stiffness, and brittleness), and behaves more as a rubbery material. It is not a melting transition, but rather a point at which the free volume of the solid increases; large segments of polymer chain begin to slide past each other, and more long range motion is possible, resulting in rubbery behavior, or "softening". This has large consequences for the processing and applications of the plastic. For instance, poly(methyl methacrylate) (PMMA) is commonly employed as a "safety glass" in the cockpits of fighter jets. For this and other uses, it is critical that the plastic maintain its structural integrity, and not behave as a rubbery material. For this reason, higher T_g materials are desirable for most applications. Typically, it is observed that isotactic material have very low glass transitions, and it is conventional wisdom that atactic and syndiotactic materials of similar molecular weight exhibit similar T_g's. For example, i-PMMA undergoes this transition at 38°C, whereas s-PMMA and a-PMMA do so at 105°C[6]. However, it will be shown in this work that substantially higher transition temperatures can be obtained in s-PMMA relative to the atactic variant, so there are exceptions to these general trends. Hence, highly syndiotactic PMMA is an attractive synthetic target.

III. Heterogeneous Catalyst Systems: Challenges

The Ziegler-Natta type catalysts that have dominated the industrial production of polyolefins have been largely of the solid, supported type, as this allows for facile separation of the product from catalyst residues. However, there are disadvantages to this approach from an academic perspective. Heterogeneous catalysis (catalyst and reactant

in separate phases) is difficult to characterize relative to homogeneous processes, for which more advanced analytical techniques emerged earlier (notably, solution NMR). In addition, these catalysts systems are extraordinarily complicated, as noted above. Interactions of the original addends produce (at least) three different oxidation states of the transition metal (e.g. Ti II, III, and IV), several of which may be in equilibrium, and reacting with each other through comproportionation and disproportionation reactions. The solid support material may be involved in the process, or may interact with the catalyst species. Halide and alkyl groups are readily exchanged between the metal centers, further complicating the situation. In addition, homolytic cleavage of metal-alkyl bonds results in reduced metal species and organic radicals which greatly exacerbate the problem of characterizing the reaction. In short, there is still no generally applicable mechanistic model for heterogeneous Ziegler-Natta type catalysts.

IV. Metallocenes and Model Studies

Hence there is a strong driving force to create soluble systems for homogeneous catalysis (reactant and catalyst in same phase), which could be studied by the relatively more advanced solution-phase analytical techniques. Surface characterization processes, though advancing rapidly, are still much less widely applicable. Advances in homogeneous catalysis began shortly after the original disclosures regarding homogeneous systems in the literature. Natta extended the previous strategy to include soluble metallocene complexes, and even isolated what he believed to be a model compound.[7]

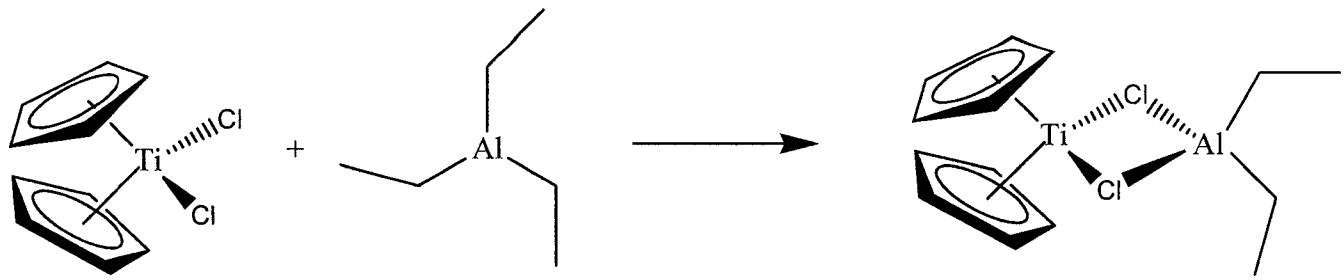

Figure 2: Natta's early soluble catalyst model

Again, this formulation relies on the use of a transition metal halide with a main group metal-alkyl Lewis acid. The analogy to the proposed active species shown in figure one is direct. The use of metallocene compounds proved fortuitous for further developments in homogeneous catalysis, as will be shown. The initial investigations presumably stemmed from the greater solubility of this versus other Ti(IV) species. That the product was isolable and crystalline turned out to be a very significant advance over previous systems. Although its activity for production of polyethylene was less than that of the simple $TiCl_4$/ triethylaluminum formula, it lent credence to the bimetallic hypothesis (since neither of the components on their own show any activity), and opened up this new class of compounds to investigation. Other workers soon revealed[8] very similar investigations had been ongoing in industry, utilizing the same titanocene dichloride with triethylaluminum as above, or with diethylaluminum chloride as the main group component. They proposed that the true active species was an adduct (not the bridging structure shown above) of $(Cp)_2Ti(III)(Cl)$ with diethyl aluminum chloride. While the two were indistinguishable in the absence of a crystal structure, this assignment highlights the oxidation state of the active site. Significantly, they were able to show that the presence of traces of oxygen enhanced the activity of this isolated species by more than one order of magnitude, demonstrating for the first time that these species were

catalytically competent as the active species for coordination polymerizations, which had been left in doubt by Natta's study, and suggesting that Ti(IV) species may be relevant. Therefore, the introduction of metallocene species was significant in that it allowed the isolation and characterization of intermediates. Although there is still debate over the mechanisms of these processes, much of the current understanding derives from studies using these soluble catalyst precursors.

V. Methylalumoxane: Next Generation Activator

Although mechanistic insights were obtained by the substitution of metallocene ligands on the transition metal component, greater advances in catalytic activity were obtained by changing the nature of the main group cocatalyst, or "activator". As noted above, these were typically aluminum alkyl species, or aluminum(alkyl)halides. The synthesis and handling of these species is typically performed with rigorous exclusion of oxygen and moisture, due to their pyrophoric nature. However, the serendipitous interaction of trace moisture (as a contaminant due to sloppy handling) to trimethyl aluminum (TMA) resulted in the discovery of an extremely potent activator.[9]

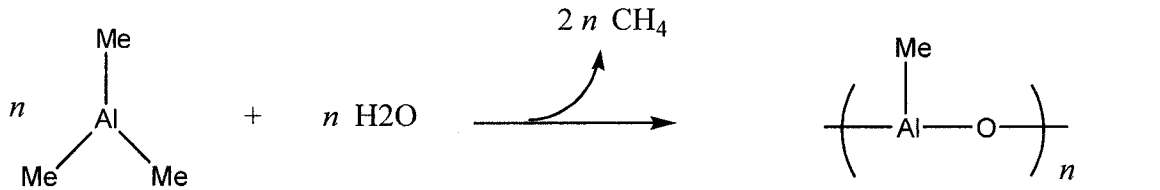

Methylaluminoxane "MAO"
(one proposed structure)

Scheme 3: Synthesis of MAO

As shown in scheme 3, controlled hydrolysis of trimethylaluminum generates a series of oligomers. The authors employed $(Cp)_2Zr(CH_3)_2$ as the soluble transition metal

component. This is a more robust precursor than its titanium analog discussed above, as the II and III oxidation states are much less accessible, simplifying study. Previous work had shown it to be highly active for ethylene polymerization, but not for higher α-olefins. Also, the transition metal bears alkyl groups (initiators), not halides as shown previously, presumably obviating the alkylation step required with the halide precursors. However, the precatalyst was only moderately active when coupled with aluminum alkyls. Use of MAO as the (accidentally discovered) main group component changed this dramatically, giving activities (g polyethylene/g Zr precatalyst) in excess of 10^7 in 2 hours. The authors calculated that the time between insertion steps must therefore be comparable to that of the fastest known enzymes, indicating remarkable catalytic activity. Although MAO demonstrated the extreme reactivity possible in homogeneous polymerization catalysis, it was not without its drawbacks. First, a very large excess of the aluminum species was required for activity (typically, a Zr:Al ratio of 1:100 up to 1:10,000). More discouraging from a mechanistic viewpoint, the exact nature of MAO is still not known. It exists as a series of oligomers of various chain lengths, with cyclic and linear structures, all in equilibrium. Further complicating matters, many commercial formulations contain 30-40% free trimethylaluminum. Only a few of the metal centers appear to be active for the desired reaction (abstraction of alkyl (or halide) group from the transition metal center to generate active cationic sites). Therefore, although this species has been utilized as an activator to great advantage in industrial chemistry, it continues to remain a mechanistic "black box". Catalyst systems employing MAO activation allowed the chemist to produce more polymer than was previously possible, but with less understanding of how it was formed.

A. MAO: Insight into activation processes

Research in this field continues to this day, and some progress has been made. Barron was able to produce t-Butyl alumoxanes which crystallized into discrete cage structures.[10] These studies are intriguing from a fundamental organometallic perspective, as they demonstrated that aluminum could retain its Lewis acidity in a four-coordinate environment. Conventional wisdom holds that the acidity is due to the unfilled octet in three-coordinate Al. Nevertheless, Barron's structures had four-coordinate aluminum centers, with oxygen atoms bridging between three aluminum atoms, and yet when combined with metallocene alkyls ($(Cp)_2ZrX_2$, X=Cl or Me), they exhibited activities on the order of commercial MAO/metallocene formulations. This unique reactivity is attributed to the ring strain of the cage structures, and was termed "latent Lewis acidity". Using these discrete Al-based activators, NMR studies with $(Cp)_2Zr(Me)_2$ indicated that the MAO model compounds abstracted methide anion from the zirconium center, generating cation-like species which were active for ethylene polymerization. This lent credence to the hypothesis that cationic transition metal centers are the active sites for polymerization, and that the role of the cocatalyst, or activator, was primarily to abstract an alkyl group to generate the active cationic complex. It should be noted however, that these studies are hindered by the fact that they use model compounds; t-Butyl alumoxane does not exist in the same forms as the methyl derivative, MAO, so conclusions about structure and reactivity should be extended to the parent compounds only with caution.

Marks was able to provide strong evidence to support the hypothesis of MAO serving simply as an alkide abstractor (to generate unsaturated transition metal centers), although in this case his model compounds proved to be even more interesting than the

system under investigation. By vacuum drying commercial MAO (to remove free TMA), a solid was obtained, and its interaction with $(Cp)_2Zr(^{13}Me)_2$ was monitored by solid phase NMR[11]. The results were taken to indicate that the primary interaction was indeed methide abstraction, as proposed.

$$Cp_2Zr(CH_3)_2 + [Al(CH_3)O]_n \rightleftharpoons [Cp_2Zr(CH_3)]^{\oplus}\,{}^{\ominus}[(CH_3)Al(CH_3)O]_n$$

Scheme 4: Primary role of MAO: methide abstraction

The assignment of the structure as a cationic zirconium species was made by analogy to a discrete, crystalline material which had very recently been synthesized and characterized.[12]

VI. Isolable Lewis Acids: Discrete Activators

As discussed, the traditional Ziegler-Natta formulation consisted of a transition metal component and a main-group Lewis acid, typically an aluminum alkyl. However, the latter are typically pyrophoric liquids, so Marks set out to use the solid, crystalline tris(pentafluorophenyl)borane in their stead. These species had been known for some time[13], but apparently had escaped the attention of polymer chemists. It is a strong Lewis acid, intermediate in strength between BCl_3 and BF_3, but transfer of the bulky aryl groups is less facile than halide exchange, minimizing competing reaction pathways. Mark's work was a significant breakthrough for catalysis, not simply because he generated a highly active catalyst system which only required a 1:1 ratio of "catalyst" and "cocatalyst", but because the resultant product was the first isolable polymerization catalyst to be characterized via x-ray crystallography. This was a major advance, relative to the traditional Ziegler-Natta systems, wherein the active species has yet to be

convincingly elucidated, and over the MAO-based systems, which require large excess of the Lewis acid, and are not discrete or homogeneous.

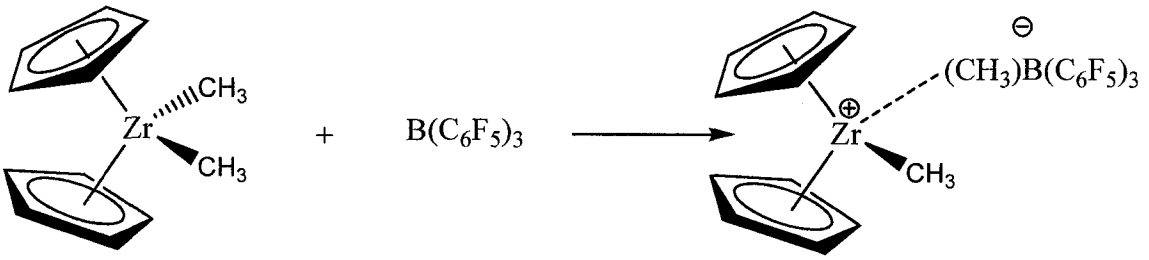

Scheme 5: Lewis acid "activation" to produce discrete, isolable catalysts

As shown in scheme 5, the borane abstracts the methyl group, generating a weakly coordinated anion. For the first time, the catalyst/cocatalyst interaction could be directly observed, in the form of an x-ray crystal structure. The "abstracted" methyl group is considered to be bridging the Zr and B centers, with a Zr-C bond length 0.3 angstroms longer than that in the neutral zirconocene, (and that of the remaining, bonded methyl). The complex exhibited very similar reactivity to zirconocene/MAO systems for polyethylene, indicating that transition metal cations are kinetically competent for polymerization. The advantage of isolable, discrete catalyst systems cannot be overstated, as their characterization provides a "picture" of the active site, which can then be utilized to rationally design and optimize catalysts for related reactions. Since this work, it has become widely accepted that catalyst systems for olefin polymerization by coordination/insertion mechanisms rely on generation of cationic transition metal centers. In the case of traditional Ziegler-Natta systems (heterogeneous and homogeneous), metallocene/MAO systems, and the ion pairs shown above, the chemistry is believed to be similar: a neutral transition metal species is transformed into an active cationic site by interaction with a Lewis acid that effects alkide abstraction. Hence, the term "activator"

has been applied to the main-group component, as its role is primarily thought to be that of abstractor, generating an active cation and a weakly coordinated anion. As Marks' elegant work shows, the cationic zirconocene has an open site into which olefins can coordinate (form a π-complex) by displacing the borate anion. Insertion into the adjacent Zr-C bond initiates polymerization and re-opens the coordination site, allowing coordination of another monomer. Repetition of this coordination/insertion process generates high polymer very rapidly.

Direct observation and isolation of discrete catalyst active species proved useful for mechanistic investigations, but also dramatically improved the reactivity and selectivity of the resultant processes. The term "single site" catalysts is utilized to refer to cationic metallocene derivatives[14], of which $[(Cp)_2Zr(Me)]^+$ $[(Me)B(C_6F_5)_3]^-$ shown above, is the prototype. This terminology distinguishes the soluble, discrete homogeneous catalysts which can be isolated, from their heterogeneous relatives, which exhibit several different active sites with different specificities and reactivities, none of which can be thoroughly characterized. As a result, the polymers produced by these single site catalyst systems are dramatically different from those resulting from heterogeneous processes[15]. Synthetic polymers are formed with a range of molecular weights. This range is known as the polydispersity, and physical properties and processing depend are improved by narrowing the range of chain lengths. Metallocene-based catalysts produce polyolefins with polydispersities 1/3 to ½ of those produced in heterogeneous systems. In addition, activities are improved by one to two orders of magnitude. This enhanced reactivity opens up the possibility of polymerizing cyclic

substrates, such as norbornene, which are resistant to reaction under heterogeneous Ziegler-Natta conditions.

VII. Other Activation Processes[16]: Trityl Abstraction and Weak Acid Protonolysis

The discovery that cationic, soluble transition metal species were highly active for olefin polymerization led to a paradigm shift in catalyst synthesis, and an ensuing renaissance of research in the field. An electron deficient, coordinatively unsaturated metal center (often zirconium) was now the target, and subsequent advances were targeted at generating more "naked" cations, which would make monomer coordination more facile, thereby enhancing reactivity. $[(Me)B(C_6F_5)_3]^-$ may be considered as a weakly coordinating anion, but as seen above, when paired with metallocenium cations, there is a bridging interaction of the methyl group between metal centers. Hence, the next generation of catalysts employed the analogous tetrakis(borate) anion, $B(C_6F_5)_4^-$. This was achieved by two new strategies for activation: protonolysis, and abstraction by trityl salts. The first strategy was employed notably by Marks[17], who first utilized trialkylammonium tetraphenylborates to generate cations from actinide metallocene alkyl species by protonation. This differs from the above strategy of abstraction, because the leaving group is a neutral alkane (gas), and the counteranion is the gegenion from the ammonium salt, not the anion resulting from the abstraction process. Since the phenyl derivatives ($B(C_6H_5)_4^-$) formed rather tight ion pairs with the transition metal centers, the perfluoro analogs were investigated[18], as shown in scheme 6.

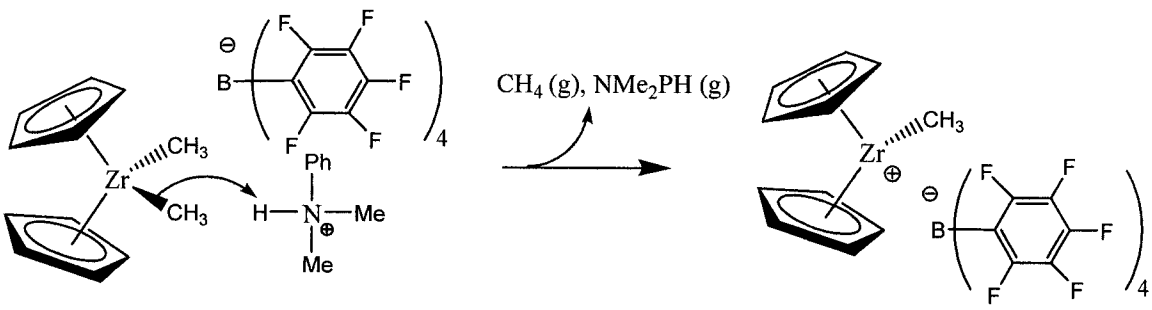

Scheme 6: Alternative metallocene activation strategy: Protonolysis

These species were highly active catalysts, as expected, and the investigation of "BArF" salts (an acronym for perFluoroAryl Borane) ensued.

Chien and Rausch[19] approached these highly reactive intermediates by another route, employing trityl BArF salts as abstraction reagents.

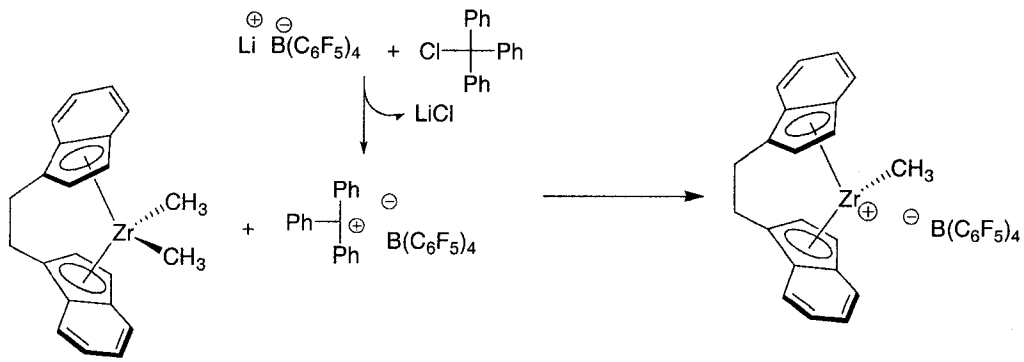

Scheme 7: Alkide abstraction with trityl BArF

This disclosure was a significant advance on several fronts. First, it revealed an alternative method for production of highly active metallocenium cations paired with extremely weakly coordinating anions. Second, they showed that this strategy could be extended to the *ansa*-metallocenes (ligands with bridging groups). The Zr catalyst precursor shown in scheme 6 is known as *rac*-(EBI)Zr(Me)$_2$, (EBI=Ethylene bridged bisIndenyl). *"rac"* refers to the orientation of the indenyl rings; as drawn, it is C_2 symmetric, and can exist as two enantiomers, as opposed to the meso form, which is C_S

symmetric, and only has one isomer. Several variants of the *ansa*-metallocenes have been synthesized, some of which are pictured in figure 3. The indenyl and fluorenyl ring systems can be thought of as substituted analogs of the Cp rings discussed in other catalyst systems.

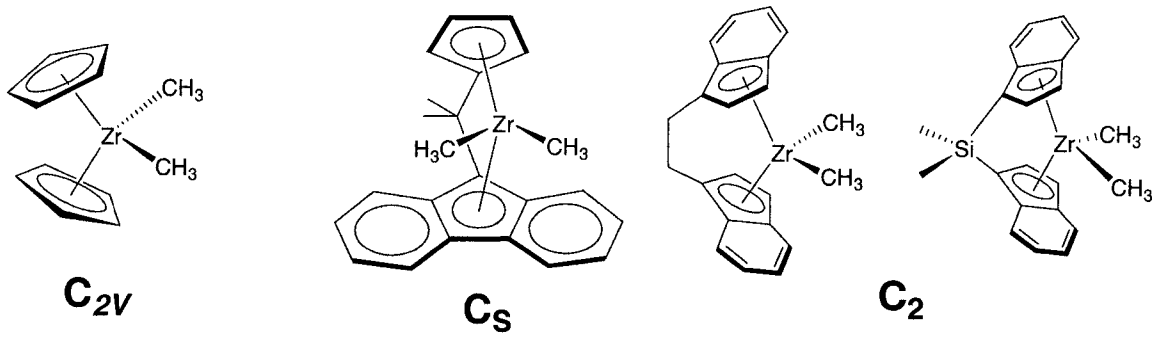

Figure 3: Representative metallocene dialkyls with their respective symmetries

The unique feature of this class of catalyst precursors is that, by tethering the various ring systems together, various geometrical environments can be attained around the metal center. Chien and Rausch's extension of the discrete activation strategy to *ansa*-metallocenes was revolutionary, in that now the polymer chemist had access to a multitude of "single-site" cations, each of which could influence the orientation of monomer coordination and hence enchainment, to allow access to various different stereoregular polymers. In fact, they were able to show that the EBI metallocenium cation was not only highly active for ethylene polymerization (similar to non-bridged metallocenes paired with MAO), but unlike the unbridged analogs (activated by MAO or abstraction), it also exhibited good reactivity for production of polypropylene, and was selective for the commercially useful isotactic variant (the few unbridged species that are reactive with propylene give atactic material). Bridged metallocenes had been known for some time; the first report was in 1985[20] from Germany, detailing the synthesis of the

dichlorides and their polymerization trials when coupled with MAO. The *rac*-(EBTHI)$ZrCl_2$ (dimethyl derivatives shown in figure 3; EBTHI is a variant of EBI in which the C6 rings of the indenyl systems are hydrogenated) and *rac*-(SBI)$ZrCl_2$ (SBI=dimethyl Silyl bridged Bis Indenyl)[21] were the earliest generation ansa metallocenes. The former exhibited only modest activity for ethylene polymerization, and only gave low molecular weight oligomers of polypropylene. This once again reveals the power of the "single site" approach in which the true active species can be independently synthesized and used directly for catalysis, allowing rational determination of structure-activity relationships. In these early examples, it was unclear whether the failure to produce high polymer was due to the metallocene chloride, the MAO, or some interaction (or lack thereof) between the two.

VIII. Bulky Counterions: Problems and Improvements

As noted above, BArF gegenions were thought to be highly desirable for some time, due to their limited coordination to the active cationic species. Unfortunately, after a flurry of investigations, it became apparent that this was perhaps too much of a good thing[22]. The tetrakis (pentafluorophenyl)borate anion is in fact so weakly coordinated that its metallocenium salts show poor solubility in hydrocarbon solvents, are thermally unstable, and notoriously resistant to crystallization. Conversely, the methyl tris(pentafluorophenyl)borate anion remains in the coordination sphere of the metallocene cation until displaced by monomer (as shown in scheme 4, for example), stabilizing the electron deficient metal and enhancing the solubility (and thus activity). As a result, attention was focused back in the direction of neutral Lewis acidic perfluoro borane and alane species. Particular attention was paid to enhancing the steric bulk of the aryl

systems to afford anions which would be more loosely coordinated to the cationic center than in the parent methyl tris(pentafluorophenyl)borate species. Again, the Marks group was at the forefront of this field, generating bulky abstraction agents such as the prototypes PBB[23] and PNB[24], shown in figure 4.

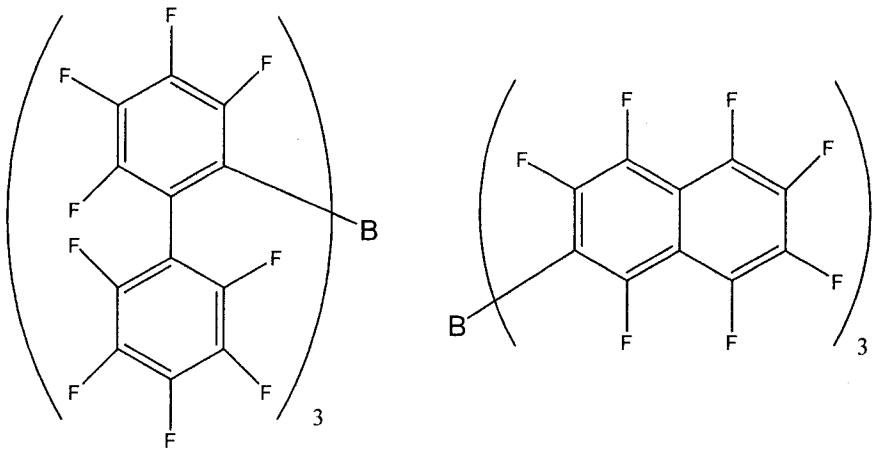

PBB **PNB**

Figure 4: Bulky Borane Lewis Acids

It has been mentioned that homogeneous catalytic systems are preferable to heterogeneous systems, as they are more amenable to characterization and monitoring of reactions. Perfluoroaryl-based Lewis acids are particularly well suited to chemical observation, due to their ^{19}F NMR handle. In stark contrast to the previous generation MAO activators, these species and their reaction products can be readily monitored. Chen and Marks showed that PBB indeed was less coordinating that the parent acid. However, its abstraction reactions were very sluggish (up to one hour for $SBIZrMe_2$), and it had a tendency to form μ-methyl products at room temperature (e.g. $[Cp_2ZrMe(\mu\text{-}Me)MeZrCp_2]$. Although these ion pairs were active for olefin polymerizations, they effectively require two equivalents of transition metal to generate one active site, unlike the ideal 1:1 stoichiometry displayed by the parent Lewis Acid. PNB proved to be a

somewhat stronger Lewis acid that tris(pentafluorophenyl)borane, and when coupled with certain metallocene derivatives, exhibited marginally higher catalytic activity.

Shortly after the disclosure of the next generation of bulky borane cocatalysts, Chen and Marks[25] thoroughly investigated the abstraction chemistry of PBB with a broad range of metallocene catalyst precursors, characterized the resultant complexes, and screened their polymerization activity. The main focus of the work was "anion engineering" to directly measure the effect of the anion on the polymerization activity of various "single site" cationic active species. To this end, PBB was compared against an aluminum based activator, triphenyl carbenium tris(2, 2', 2''-nonafluorobiphenyl) fluoroaluminate (Ph_3C^+)(PBA^-). The abstraction chemistry here is based on the potent trityl cation, which removes alkide anions from the transition metal center, with the aryl aluminate anion already formed. This was an early example of the trend back to investigating aluminum based activators, which were involved in the traditional Ziegler systems, but were of less interest once the discrete nature of the active cations generated with borane reagents became known.

IX. Alane Lewis Acids Rediscovered

Despite the fact that borane reagents were very well established as activators for homogeneous metallocene catalysts, the analogous alane species were predicted to be much more effective Lewis acids[26]. In fact, aluminum alkyls were utilized in industrial homogeneous polymerizations employing metallocene/borane catalyst systems. Since it would be impractical to rigorously dry the massive volumes of solvent used for these commercial processes, trialkylaluminum species (alkyl = methyl, ethyl typically) are commonly added to function as moisture scavengers to avoid decomposition (hydrolysis)

of the highly sensitive metallocenium active species, generated in situ. TMA is not sufficiently acidic to effectively abstract alkide groups from neutral metallocene alkyls[27] in useful concentrations. However, given that the reaction product of the two catalyst components was discrete and well characterized, the question arose whether the aluminum additives, which are known to be reactive alkylating agents, might interact with either the electrophilic borane or the cationic transition metal center. Bochmann[28] performed an elegant study of these reactions. The reaction of trityl borate with TMA resulted in a series of stepwise ligand exchange reactions, eventually forming tris(pentafluorophenyl) aluminum, as shown in scheme 8.

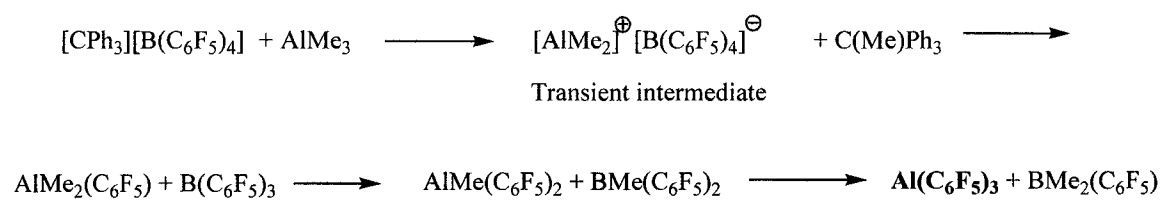

Scheme 8: Interaction of aluminum alkyls with borane Lewis Acids

Given that aluminum alkyls are significantly more potent Lewis acids than the analogous boranes, it was reasonable to suppose that this the final product of this series of reactions might prove to be an extremely useful alkide abstractor. However, Bochmann went on to show a side reaction that seemed to prevent the application of this alane as a cocatalyst, illustrated in scheme 9.

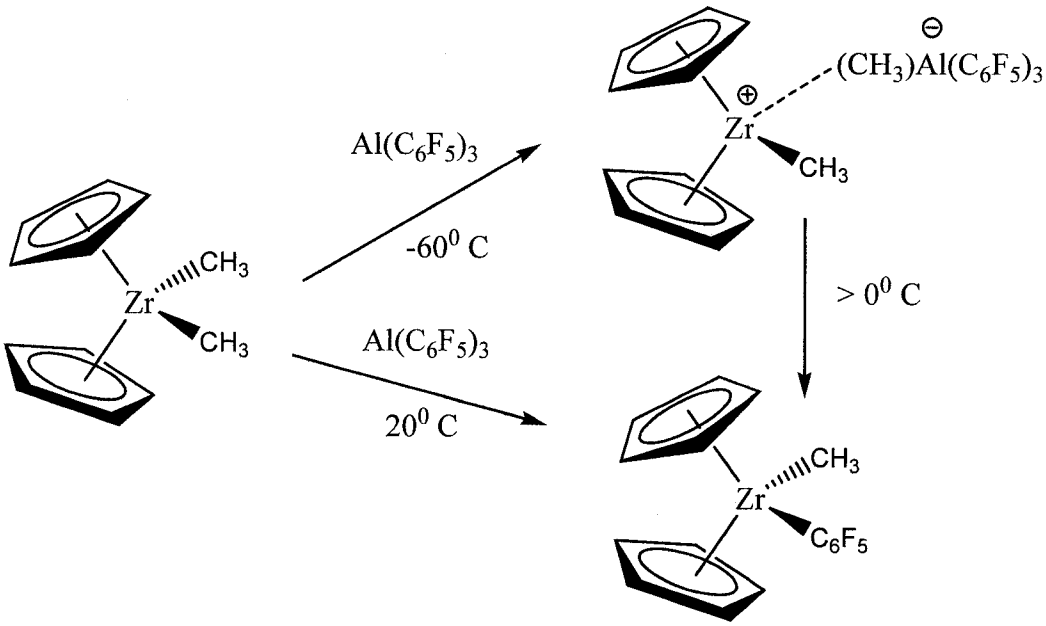

Scheme 9: Abstraction and deactivation of metallocene precatalyst

Since the desired species for olefin polymerization is the metallocene cation, the upper reaction was desirable (as observed for the analogous borane, scheme 4). However, the fact that this species transfers a fluoroaryl group to the metallocene cation means that this is effectively a catalyst de-activation process. The end result is a neutral, inactive metallocene, and a neutral methyl alane species, less acidic than the starting material. This is highly undesirable, and this observation presumably prevented more research groups from investigating the reactivity of the novel aluminum Lewis acid.

X. $Al(C_6F_5)_3$: Synthesis, Structure and Reactivity

Despite this, tris(pentafluorophenyl)aluminum was investigated by a few academic and industrial research groups. It was initially reported in 1965[29], shortly after the perfluoroaryl borane species was synthesized. Interestingly, the material is so strongly acidic that it was isolated as the diethyl etherate, not the free alane. Curiosity about the material was dampened somewhat by the initial discoverer's report that

attempts to remove the coordinated ether with heat caused it to detonate violently. However, three decades later, H.W. Roesky revealed a new route to this material, synthesized as the free Lewis acid. Crystallization from THF yielded the THF adduct, which was characterized by x-ray crystallography[30]. The authors noted that, "$B(C_6F_5)_3$ is used as cocatalyst in the field of metallocene-catalyzed olefine (sic.) polymerization, e.g. with $Cp^*_2ZrH_2$, so that 1 (tris(pentafluorophenyl)alane) can be expected to act as cocatalyst in these systems". However, they again noted that the material "tends to explode under circumstances not exactly determined," deterring potential investigators. Interest was not abated in industry, however, and a patent[31] appeared for preparation of $Al(C_6F_5)_3$, wherein the authors revealed that synthesis in the presence of aromatic hydrocarbons afforded the Lewis acid an adduct of the aromatic compound, typically toluene. This coordination is sufficiently labile to provide an active catalyst, but strong enough to stabilize the extremely electrophilic aluminum center.

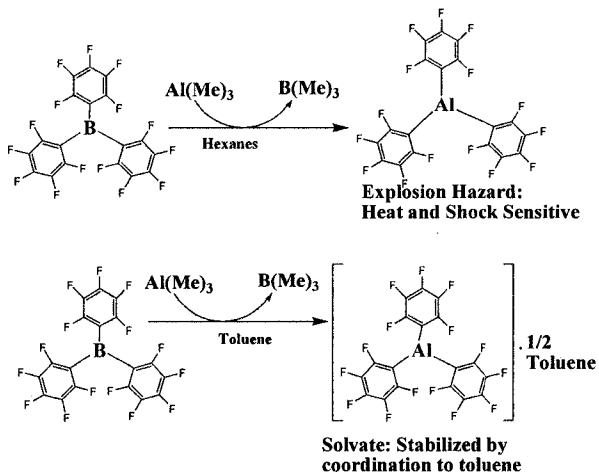

Scheme 10: Improved synthesis of $Al(C_6F_5)_3$ and its toluene adduct

This modified procedure relies on the sequential ligand exchange reactions shown in scheme 8, and the equilibrium is driven by the loss of BMe_3, which is a gas. It may seem somewhat surprising that the strongly electron withdrawing fluoroaryl groups are

preferentially transferred to the more Lewis acidic Al center, but it is believed that they stabilize the metal center by interaction of the π-electrons with the electrophilic metal. The toluene adduct is a relatively stable, white crystalline material which may be safely handled using standard Schlenk and glovebox techniques, allowing the chemistry of this novel alane to be explored with caution. It has been characterized by x-ray diffraction[32], revealing coordination of the Al to the para position of toluene. The authors note that the nature of the Al-toluene bonding may be thought of as a hybrid between π-arene complexation and a Wheland intermediate, shown below.

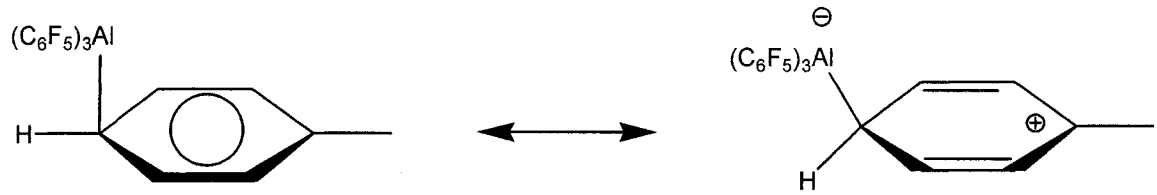

Figure 5: Resonance contributors of $Al(C_6F_5)_3$ toluene adduct

The structure on the left features coordination to a formally sp^2 carbon, and hence the expected angle Al-C-C(para) is 90°, relatively close to the observed value of 96.1°. The right-hand structure is a σ-complex, proposed as transient intermediates in electrophilic aromatic substitution reactions. Such species have been observed by NMR[33], and even characterized by x-ray diffraction[34]. Evidence for the Wheland resonance contributor lies in the shortening of the C-C bonds between the ortho and meta positions of toluene relative to the other positions, suggesting more single bond character to the other bonds. Although the effect is rather subtle, it was recently demonstrated that this coordination can indeed affect enhancement of the acidity of the para proton, resulting in C-H

activation of the Friedel-Crafts sort[35]. Other novel reactivity of the Lewis acid includes C-X activation in the form of halide abstraction from methylene chloride to form $(Al(C_6F_5)_2)_2(\mu\text{-}Cl)_2$, which has been characterized crystallographically[36].

For catalytic purposes, it is advantageous to use the safer toluene solvated form of the alane. According to the patent literature, this coordinated solvent can be removed by drying in vacuuo at 80°C, to afford the free alane, though this is perhaps inadvisable due to the explosive nature of the compound. Cowley revealed that the coordination is retained in solution, by NMR experiment. Highly relevant to the present work, however, was the discovery that the aromatic solvent could be readily displaced by THF, presumably a manifestation of the high oxophilicity of the molecule. Mass spectral evidence (negative ion CI) indicates that the aromatic solvent is retained in the vapor phase. In spite of this, Korean workers report[37] that vacuum drying at room yields a species which is the ½ toluene adduct, based on CH analysis. It is proposed that extensive vacuum drying yields this form, whereas the species studied by Cowley (containing a full equivalent of toluene for each Al center) was not dried in vacuuo. Hence, for synthetic purposes, it will be assumed that the material is isolated as the former form (½ toluene adduct). Another surprising result was revealed in this paper, regarding the Lewis acid strength of the species in question. As mentioned earlier, it is conventional wisdom that Al species should be more strongly Lewis acidic than the corresponding boranes. NMR studies in our labs support this idea, based on chemical shifts of methyl methacrylate on coordination to the various Lewis acids[38]. However, these authors report, based on IR data of the benzonitrile adducts of the borane and alane, that the alane is only a slightly stronger Lewis acid than trimethylaluminum, and is

substantially weaker than tris(pentafluorphenyl)borane. The origin of this discrepancy is unclear. In any event, the activity of this novel Lewis acid has remained a largely unexplored area, in spite of the fact that its boron analog is very well studied. The present work will highlight recent advances in our laboratories along these lines.

A. $Al(C_6F_5)_3$: Applications to Polymer Chemistry

The first indication that $Al(C_6F_5)_3$ was more than a curiosity, and had novel reactivity which would be useful for olefin polymerization appeared in the literature in 2001[39]. Chen *et al.* at Dow Chemical compared the activation efficacy of $Al(C_6F_5)_3$ with the more common $B(C_6F_5)_3$ when coupled with the metallocene *rac*-SBI-$ZrMe_2$ and CGC-$TiMe_2$. The latter is a mono-Cp precatalyst featuring a silyl bridge between the permethylated Cp and a bulky amido group which coordinates to the transition metal center. It has proven to be a highly active precatalyst for olefin polymerization due to its less congested coordination sphere relative to the bis-Cp, and ansa-metallocenes. Treatment of either species with 1 equivalent $B(C_6F_5)_3$ effects abstraction of one methyl group, producing a monocation, as has been shown. Similarly, use of $Al(C_6F_5)_3$ lengthens the Zr-C distance, generating a μ-methyl derivative, e.g. SBI-$ZrMe(\mu\text{-}Me)Al(C_6F_5)_3$. Surprisingly, in contrast to the abstraction behavior with non-bridged metallocenes demonstrated by Bochmann (back-transfer of pentafluorobenzene to Zr cation, destroying polymerization activity), this corresponding ansa-derivative is stable in solution for weeks, and isolable. This in itself would bode well for catalytic applications of the alane, although tests showed that the complex was somewhat less active for olefin polymerization than the analogous borate. This is attributed to somewhat closer association of the abstracted methyl group with the transition metal center, in spite of the

fact that computations predict a higher alkide affinity for the alane. Much more significant, however, was the phenomenon observed when further equivalents of Lewis acidic borane were added. Up to four equivalents of the cocatalyst effect removal of one methyl group, and exhibit no further chemical change (or alteration of polymerization activity). In stark contrast, addition of a second equivalent of $Al(C_6F_5)_3$ removes the second methyl group from the transition metal center, producing stable, isolable dicationic, pseudo-12 electron catalysts which are extremely potent for olefin polymerization.

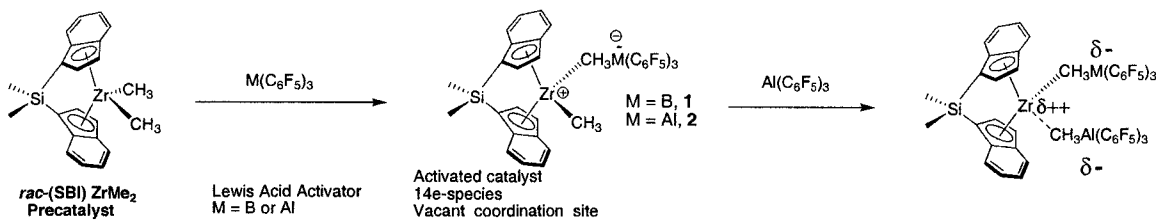

Scheme 11: Single and "Double Activation" of ansa-metallocene dialkyls

These studies demonstrated another facet of the unique reactivity of this less-studied Lewis acid, and revealed that, when coupled with bridged metallocene species, it has great potential for polymerization catalysis, stirring new interest in the field.

XI. Polar Monomers: Metal Mediated Polymerizations

Although both heterogeneous and homogeneous Ziegler-Natta polymerizations have been developed for production of high polymers of various tacticities from a broad range of α-olefins, polar monomers remained a largely unmet challenge. This derives from the high oxophilicity of both Group IV metal compounds (e.g. Ti, Zr), the cations of which are believed to be the active catalysts, and the Group 13 compounds (B, Al) which

are typically used as activators. The oxygen-containing functionalities of most polar monomers were expected to coordinate to either the activator, drastically reducing its Lewis acidity, or to form inert bonds to the cationic Group IV metal, shutting down propagation. Hence it was long held that polymerization of heteroatom-containing monomers, notably the commercially important methyl methacrylate (CH_2=$C(CH_3)CO_2CH_3$), would not be feasible by coordination mechanisms involving traditional Ziegler-Natta catalysts. The first example of such a process appeared in 1969[40], wherein the conventional Ziegler-Natta system of $Cp_2TiCl_2/AlEt_3$ was shown to polymerize several polar monomers when a very large excess of the aluminum species was added. However, the yields and molecular weight distributions were disappointing, in contrast to later works. Yasuda first reported production of highly syndiotactic, narrow polydispersity PMMA in the American literature in 1992[41]. While this was a landmark achievement, his catalyst was a lanthanide hydride ($[Cp^*_2SmH_2]_2$) without activator. Lanthanides are substantially less oxophilic than the Group IV precatalysts employed in Ziegler-Natta processes, which was presumably a key factor in the success of this approach. Given the considerable difference in the catalytic system, this work will be considered outside of the scope of the present report.

A significant advance on this front was made in the early 1990's by the Canadian research group of Scott Collins[42]. He demonstrated that cationic zirconocene species would indeed produce high molecular weigh poly(methyl methacrylate) (PMMA) in the presence of neutral zirconocene. Furthermore, the resultant polymers exhibited stereoregularity, with approximately 80% r diads produced at 0°C. As opposed to the traditional coordination/insertion mechanism postulated for olefin polymerizations, it was

believed that these polymers were produced by Michael addition. Interestingly, the cationic zirconocene itself did not produce polymer without addition of neutral zirconocene dimethyl as initiator. The proposed mechanism is shown below.

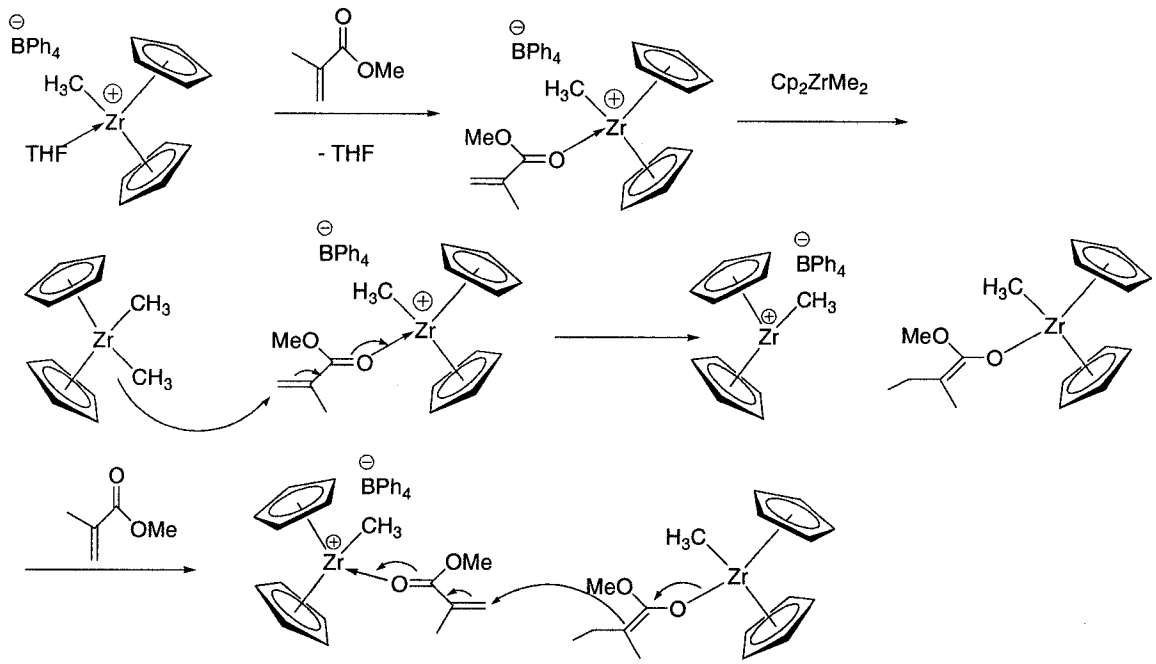

Scheme 12: Bimetallic polymerization of MMA with metallcenes

The cationic active species was generated by alkide abstraction from Cp_2ZrMe_2 with trityl (tetrakis(phenyl)borate), and is isolated as the stabilized THF adduct. Studies initially were focused on the application of this cationic metallocene to MMA polymerization, based on the well-established activity of similar species for conventional olefins. In this case, however, addition of MMA does displace the coordinated THF, but does not begin polymerization in the absence of neutral zirconocene. In the second step, the MMA-cation adduct is subjected to Cp_2ZrMe_2, which functions as an initiator. Hence the coordinated monomer, which is activated by its association with the electrophilic metal center, is attacked by methide anion via intermolecular 1,4- Michael addition. Labeling studies employing $Cp_2Zr(^{13}CH_3)_2$ confirm this initiation step by the presence of

labeled carbon in the resultant enolate. This generates a neutral metallocene (methyl) enolate, and regenerates a metallocene cation. Added MMA then is subsequently activated by coordination to the latter. Kinetic studies[43] demonstrated that the process is the process is first order in neutral enolate and cationic metallocene, supporting the proposed bimetallic mechanism. Hence, initiation and propagation do not appear to proceed by intra-molecular attack on coordinated monomer, but rather via inter-molecular Michael addition. The next step is perhaps the most surprising and unique. As discussed above, the Zr-O bond is particularly strong, and it had been supposed that such metallocene enolates would be inactive. However, propagation indeed ensues, with the enolate attacking activated monomer. The driving force for cleavage of this bond is presumably the formation of another, equally strong, Zr-O bonded enolate, with concomitant formation of a C-C bond. This final step in the above scheme is the proposed propagation mechanism, and is repeated multiple times to produce polymer. The anionic propagating chain is hence shuttled back and forth between Zr centers in a bimetallic mechanism analogous to group transfer polymerization[44].

XII. Stereochemical Considerations

Transition metal catalyzed polymerization of polar monomers was a significant advance; the fact that Collins' system produced the desirable syndiotactic form of PMMA (s-PMMA) at 0°C made it even more attractive. Commercial production of this important material relies on radical processes that must be conducted at low temperatures (-78°C) to be sufficiently syndiospecific. Therefore, this disclosure raised the prospect of metal catalyzed polymerizations which would be considerably safer and more convenient

to perform on an industrial scale. NMR techniques have existed for decades for the stereochemical analysis of PMMA, first introduced by Bovey[45]; their basis and applications warrant some mention. The two major forms of stereoregular PMMA are illustrated in figure 1. Proton NMR experiments reveal that the methyl groups of the various configurations can be readily distinguished from one another. Standard terminology refers to the case where adjacent stereocenters bear the same configuration as m (meso), and those with opposite stereochemistry as r (racemic). The methyl groups are sensitive to their electronic environment, which is affected by the relative proximity of adjacent methyl groups. Hence conventional ^{1}H-NMR spectra of PMMA are sufficiently resolved to show the effects of adjacent stereocenters on either side of the backbone from the methyl group of interest. A typical sample will thus show well-distinguished peaks for these "triads" into mm (three adjacent stereocenters of same configuration; isotactic segment), mr (and rm; the two are indistinguishable via NMR) (two adjacent stereocenters of same configuration, followed by another of opposite configuration (and vice versa); heterotactic segment), and rr (three adjacent stereocenters of opposite configuration; syndiotactic segment). Integration of the corresponding peaks allows facile determination of the degree of the various tacticities present in any given sample.

Furthermore, statistical analysis of the relative quantities of each type of enchainment gives information regarding the manner of control over stereochemistry. Although more complicated models are possible, two major types are relevant to the present discussion: "chain end control", or Bernoullian distribution, and "enantiomorphic site control. In the previous case, the last inserted monomer unit is the only influence on

the orientation of the incoming monomer, and is ideally described at the triad level by the equation $4[rr][mm]/[mr]^2 = 1$.

The derivation of this relationship is as follows. If we assume that only one factor (last inserted monomer unit) controls the orientation of incoming monomer, we can denote the probability of enchainment in the same orientation as σ. Thus, the probability of an mm (isotactic) triad (denoted P_i) is σ^2. There are only two possibilities for the orientation of an incoming monomer; the same as the previous, or opposite. Hence, the probability of opposite enchainment is simply $(1-\sigma)$, and thus the probability of an rr (syndiotactic) triad (denoted P_i) is $(1-\sigma)^2$. The sum of all probabilities must equal one; therefore, the probability of heterotactic triads (mr) is therefore $(1- P_i- P_s)=[1- \sigma^2-(1-\sigma)^2]=[2(\sigma- \sigma^2)]$. Since heterotactic triads may manifest as mr or rm, this probability is squared to determine the overall probability of heterotactic enchainment. Therefore, $[mr]^2 = [2(\sigma- \sigma^2)] = [4\sigma^2-8\sigma^3-4\sigma^4]$. Substituting the values for P_i in for [rr], and P_s for [mm] and multiplying the two yields $[\sigma^2-2\sigma^3-\sigma^4]$. Therefore, $[rr][mm]=1/4([mr]^2)$. Rearrangment yields $4[rr][mm]/[mr]^2 = 1$. Hence, in cases where the preference for orientation of incoming monomer is only affected by the last inserted unit, this relationship should hold, within experimental error.

The next major model for stereocontrol of monomer enchainment is that of "enantiomorphic site control", wherein the geometry of the catalyst active site determines the orientation of insertion. In this case, there is not just a preference for m or r diads; there is an overall configuration which will fit into the active site more readily. The difference in this model is seen primarily in the behavior after a mis-insertion event. In the above model (chain-end control), propagation simply continues after this occurs. For

example, in an isospecific chain-end controlled process, an r diad ("misinsertion") will be most likely to simply be followed by an m diad, as the chain end prefers this orientation. This is not the case in the site control model. Here, the chain end fits into the catalyst active site in a preferred orientation. Hence, an r diad misinsertion in an isospecific process will most often be followed by another r diad, so that the stereochemistry of the following stereocenters will be identical to that of the previous chain, as preferred by the active site.

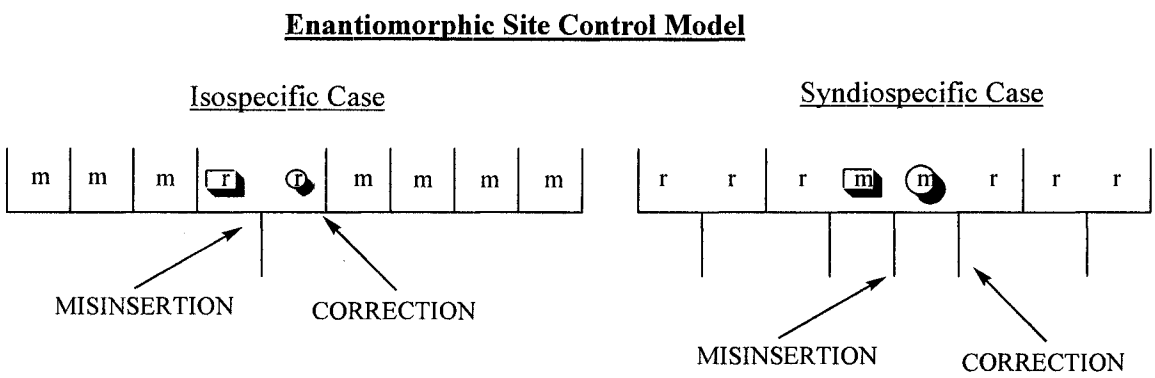

Figure 6: Misinsertion and ensuing propagation in the Site Control Model

Here we see that, for the isospecific site, an r misinsertion is followed by another to correct the stereochemistry of the following chain, generating one rr triad and two mr triads. Hence, 2[rr] = [mr], or 2[rr]/[mr] = 1. Similarly, for the syndiospecific catalyst site, an m misinsertion is followed by another m diad to correct back to the preceding configuration, generating one mm triad and two mr triads. Therefore, 2[mm] = [mr], or 2[mm]/[mr] = 1. These formulae are used to fit statistical NMR data to models for stereochemical control, giving ready insight into the mechanism of propagation.

Based on NMR studies and statistical analysis as shown above, Collins was able to demonstrate that his s-PMMA was apparently produced via a chain-end control mechanism. Interestingly, his 1994 publication includes trials with the bridged

metallocene, rac-EBTHI-$ZrMe_2$, activated by protonolysis to afford the cationic species. In this case, the resultant polymer was predominantly isotactic, and the NMR data fit the enantiomorphic site control model. Further workers have shown that these processes involve intra-molecular Michael addition for initiation and propagation steps, resulting in a mono-metallic mechanism, as opposed to the bimetallic process active with the non-bridged metallocenes. This phenomenon has been dubbed the "ansa effect" to denote the different mechanism operative with the ansa, or bridged metallocenes. While this approach is somewhat more amenable to scale-up and mechanistic study, due to the simpler stoicheometry and consequent requirement of only one transition metal center per propagating chain, the resultant i-PMMA, as a low T_g material, is considerably less attractive as a synthetic target than that produced by Collins system.

XIII. Stereocomplex PMMA

Early work with PMMA led Fox[46] to propose that three stereoregular forms could be produced; isotactic, syndiotactic, and "stereoblock". In spite of crude IR and NMR characterization techniques, this concept became widely accepted. Later workers showed that materials nearly identical to the "stereoblock" polymers could be produced simply by blending homopolymers of the isotactic and syndiotactic forms of PMMA[47]. Crystallographic evidence revealed helical interactions of the stereoregular forms in the ratio of 2:1 (iso- to syndio- tactic) when the two are mixed in polar solvents. These helical coils maximize hydrophobic interactions of the polymer chains and alter the glass transition temperature and hydrodynamic volume of the resultant blends, producing unique and robust materials. Distinguishing between stereoblock and stereocomplex polymers has remained difficult and contentious. However, it is believed that true

stereoblock copolymers should be able to be induced to form stereocomplexes, further enhancing the physical properties over either the blended stereocomplex or the pure stereoblock material.

XIV. PMMA via metallocenes: Recent Advances

In 1994, the Marks group[48] published a paper comprehensively detailing the activity of tris(pentafluorophenyl)borane as an activator of several unbridged and bridged metallocenes. The isolable, characterizable nature of the resultant cations, their high polymerization activity, and structural features were revealed in great detail. Inspired by developments in this field, Soga's group sought to re-investigate the polymerization of MMA with metallocenes[49]. It was supposed that the discrete cations resulting from the use of $B(C_6F_5)_3$ with dimethyl zirconocene or the ansa derivative, *rac*-EBI-$ZrMe_2$, which Marks had shown to be isolable and active for olefins, would provide a more discrete active system than that employed by Collins. Surprisingly, they found these compounds to be inactive, but addition of several equivalents of diethylzinc to the reaction mixture resulted in polymerization systems with similar stereospecificity (but reduced activity) to those investigated by Collins. While the goal of the work had been to demonstrate the application of a simpler, discrete system relative to Collins work, the result was in fact the exact opposite, and the interpretation of this data puzzled chemists for many years. A reasonable explanation was provided in 2000 by Gibson[50], also offering insight into Collins' earlier work. These workers noted that Soga had mixed the monomer and activator prior to adding the metallocene. It was proposed that the monomer simply coordinated to all of the $B(C_6F_5)_3$, so that there was no free Lewis acid present to abstract alkide groups from the metallocene. Hence, with this order of addition, there was no

possibility of producing active Group IV cations unless a large excess of another Lewis acid, namely diethyl zinc, was added to coordinate monomer and free up the borane to function as the metallocene activator for which it is intended. This illustrates the importance of attention to detail, and control over experimental variables that is crucial to success in catalysis. Gibson also made salient observations regarding Collins system. He noted that the latter employed CPh_4- as a counterion. Compared to the BArF anions discussed above, this is a relatively strongly coordinating anion. In addition, the presence of the strongly coordinating solvent THF complicated matters, presumably tying up catalyst active sites. Indeed, by premixing the activator with a broad range of zirconocenes (to form active cations, as isolated by Marks), and employing less coordinating solvents (methylene chloride and toluene), the authors were able to produce extremely active catalyst systems, which gave nearly quantitative conversion of MMA in one hour, though polymerizations were often complete within minutes. This work greatly simplifies the field of MMA polymerizations. Unfortunately, the authors did not perform kinetic studies to determine the dependence of the reaction rates on metallocene and activator concentration. Hence it is conceivable that, in their discrete, well defined system, propagation may occur via intra-molecular Michael addition, not the inter-molecular variant proposed by Collins. Evidence against this, however, was presented by Chen and Marks[51], who claimed that preformed $Cp_2ZrMe_2^+$ $(MeB(C_6F_5)_3^-$ gave no conversion of MMA in 6h in toluene. The discrepancy could be explained by the presumption that some free neutral zirconocene is present in Gibson's system to function as initiator, and this was not the case in the more rigorously activated system employed by Chen.

Hence, in spite of five decades of extensive research into transition metal catalyzed polymerizations of olefins, many questions remain regarding processes suitable for conversion of polar monomers, notably methyl methacrylate, into stereoregular high polymers. It is towards this end that the present work is directed.

Results and Discussion

XV. MMA Polymerizations with $Al(C_6F_5)_3$ and $B(C_6F_5)_3$ cocatlysts

Homopolymerizations

Given the literature precedent for the preparation of Group IV cationic metallocene polymerization catalysts with $B(C_6F_5)_3$, we sought to investigate the reactivity of the less well known Lewis acid, $Al(C_6F_5)_3$. In particular, we were interested in investigating the polymerization of the polar monomer, methyl methacrylate. Although group trends might lead one to suspect that identical activation pathways would lead to zirconocenium aluminates with similar reactivity, it seemed feasible that these species might be more reactive polymerization catalysts, given the noted higher methide affinity of the Al species versus its B relative. Early polymerization trials revealed much more surprising behavior. Table 1 shows relevant data comparing the reaction products from the metallocenium -aluminate and -borate catalysts.

No.	complex	T_p (°C)	Yield (%)	M_n	PDI	T_g (°C)	[*rr*] (%)	[*mr*] (%)	[*mm*] (%)	2[*rr*]/[*mr*]	4[*rr*] [*mm*]/[*mr*]^2
1	*rac*-(SBI)-$ZrMe_2$	23	0								
2	$B(C_6F_5)_3$	23	0								
3	$Al(C_6F_5)_3$	23	0								
4	**1**	23	80	30 300	1.13	56	2.6	4.7	**92.7**	**1.1**	43.6
5	**2**	23	100	39 800	1.25	113	**60.4**	35.7	3.9	3.4	**0.8**
6	**2**	0	100	73 900	1.32	127	**60.8**	34.6	4.6	3.5	**0.9**
7	(i) $B(C_6F_5)_3$ (ii) *rac*-(SBI)-$ZrMe_2$	23	80	28 400	1.12	55	3.1	6.5	**90.4**	**1.0**	26.5
8	(i) $Al(C_6F_5)_3$ (ii) *rac*-(SBI)-$ZrMe_2$	23	85	28 800	1.19	111	**60.6**	35.1	4.3	3.5	**0.8**

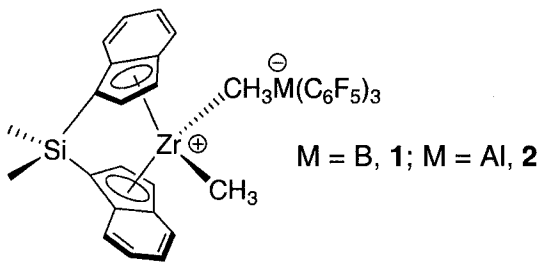

Table 1: MMA Polymerization Results and PMMA properties

All polymerizations were run for 2 hours (except run 6 = 4 hours) with 46.7μmol catalyst, in 10 ml toluene (initial solvent: monomer ratio of 10:1 (v:v)), with monomer/catalyst molar ratio 200:1 (target MW= 20 kD). Runs 1, 2, and 3 are control reactions to demonstrate that neither the neutral metallocene nor the Lewis acid component are active for polymerization in the absence of the other. Run 4 shows the expected activity of the zirconocenium borate catalyst, 1. In agreement with earlier workers, we demonstrated that the resultant PMMA had a relatively narrow polydispersity, consistent with "single site" catatlysis. It was highly isotacic, with 92.7% mm triads based on NMR integration. The triad data is well fit to the enantiomorphic site control model described above (2[rr]/[mr] = 1.1; vs. 1.0 for ideal), and does not fit the chain end control mechanism (calculated value 43.6 vs. 1.0 for ideal chain end control). Again, this is precedented, and

is consistent with the hypothesis that the cationic zirconocene center is the site of propagation. C_2 symmetric metallocene cations are the prototypical isospecific catalytic species, first revealed by Ewen's work in propylene polymerization[52]. Considerable mechanistic evidence suggests that the propagating polymer chain switches between two coordination sites in each insertion event. In a C_2 symmetric catalyst, these two sites are identical by symmetry.

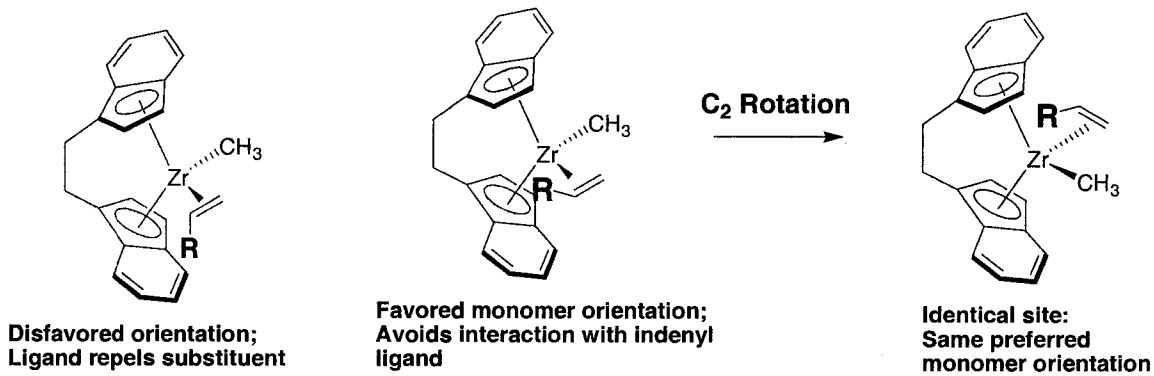

Figure 6: Origin of isospecificity in C_2 symmetric cations

Hence, the steric interactions between the ligand framework and coordinated monomer are identical in the two different active sites. This leads to enchainment of monomer with preferential placement of substituents on one side (only) of the polymer backbone (same relative configuration at stereocenters, isotactic polymer). The number average molecular weight of the sample (M_n) is larger than the targeted value, indicating that catalyst efficiency is somewhat less than 100%. The polymer produced by this experiment is otherwise unremarkable; it is produced in moderate yield, and exhibits the expected low glass transition temperature expected of isotactic PMMA (i-PMMA).

Strikingly, the material produced by the aluminate analog is different in many regards. First, it contains a high percentage of rr triads (60.4%), indicating that it is

syndio-enriched. Given the well established isospecificity of the zirconocenium cation, this suggests that this may in fact not be the active site for this process. The material has a relatively high T_g (113°C), as is expected for s-PMMA. As mentioned, this confers a greater utility in the resultant plastic, as its temperature application window is substantially increased over the isotactic variant. Furthermore, the triad data is well fit to the chain-end control model ($4[mm][rr]/[mr]^2 = 0.8$, vs. 1.0 ideal chain-end model), and is not fit to the site control mechanism ($(2[rr]/[mr] = 3.4$; vs. 1.0 for ideal). This further reinforces the emerging picture of a process that is not mediated by the cationic, isospecific site. Nevertheless, the polydispersity is still rather low, suggesting a well-defined process. The yield is now quantitative, indicating somewhat higher activity of this catalyst system. However, the M_n is almost exactly double the target molecular weight (39.8 kD vs. 20kD target). This suggests either very poor catalyst efficiency, or that the cationic zirconocenium is indeed not the active site, and that a bimetallic mechanism (employing only aluminum metal) is operative.

Run 6 illustrates the effect of lowering the temperature to 0°C with the aluminate catalyst and all other conditions held constant. In free radical polymerizations of MMA, lower temperatures markedly improve the degree of syndiotacticity. In this case, only a moderate improvement was observed, although this significantly raises the glass transition temperature of the product. The data fit the chain-end control model somewhat more closely. The most marked change, however, is in the number-average molecular weight, which is virtually doubled again (73.9 kD vs. 39.8 kDvs. 20 kD target). This suggests that lower temperatures retard either initiation, or formation of the active catalyst species. Either possibility would necessarily involve a different mechanism from

the borate analog. In the former case (slow initiation), the methyl zirconocenium is identical to the borate analog, so coordination of monomer to the cation, and initiation should be identical for either anion. Since an analogous molecular weight change is not seen with the borate, this suggests that a different mechanism is operative in the two systems. Alternatively, if the higher molecular weight is the result of a retarded formation of active species, this again implies that the cation is not the active site, since it is preformed before monomer is added. Therefore, these data, and the previous points, suggest that an alternative mechanism is operative in the aluminate catalyzed processes. Since the resultant polymer is syndio-enriched, a material of considerable commercial importance, this warranted further study to determine the origin of the syndiospecific nature of the catalyst, and if this might be improved.

Given the emerging hypothesis that the cation may not be the species of interest, we sought to explore order of addition effects, illustrated in runs 7 and 8. These are termed "activated monomer" polymerizations, because the Lewis acid is added first to monomer, to activate it to 1,4 conjugate addition, a well known strategy in small molecule catalysis. The physical properties of the polymers were essentially unchanged from those of the respective materials synthesized via the activated catalyst approach, with the exception of slightly lower conversions and a lower molecular weight from the $Al(C_6F_5)_3$ catalyzed polymer. This can be interpreted either in terms of more efficient initiation (resulting in more propagating chains) with this order of addition, or in terms of faster generation of catalyst active species.

To more rigorously demonstrate a cationic active site was not relevant to the alane catalyzed polymerizations, metallocenes with various symmetry ligand sets were

synthesized. It is well known that cation mediated processes are very sensitive to the symmetry of the active metal catalyst. Collins has shown that C_{2V} symmetric bis-Cp zirconocenes produce isotactic polymer via a chain-end controlled mechanism, but that C_2 catalysts produce isotactic polymer via enantiomorphic site control. C_S catalysts, wherein the two possible sites for monomer coordination are not symmetrically equivalent, generate syndiotactic polymers, also via site control.

entry	complex	T_p (°C) T_p (h)	yield (%)	[*rr*] (%)	[*mr*] (%)	[*mm*] (%)	2[*rr*]/ [*mr*]	4[*rr*][*mm*] /[*mr*]^2
1	**$Cp_2ZrMe_2 + B(C_6F_5)_3$**	23 (1)	100	66.7	30.8	2.5	4.3	0.7
2	**$Cp_2ZrMe_2 + Al(C_6F_5)_3$**	23 (1)	100	**62.1**	34.0	3.9	3.7	0.8
3	**$Me_2C(Cp)(Flu)ZrMe_2 + B(C_6F_5)_3$**	25 (16)	0					
4	**$Me_2C(Cp)(Flu)ZrMe_2 + Al(C_6F_5)_3$**	25 (16)	17	**62.4**	34.2	3.4	3.6	0.7
5	***rac*-(EBI)$ZrMe_2$ + $B(C_6F_5)_3$**	23 (2)	100	1.2	2.8	**96.0**	0.9	59
6	***rac*-(EBI)$ZrMe_2$ + $Al(C_6F_5)_3$**	23 (2)	100	**60.2**	35.8	4.0	3.4	0.8

Table 2: Effects of Metallocene symmetry on polymer tacticity

Runs 1, 3, and 5 (metallocenium borate catalyzed processes) illustrate the expected trends. In the C_{2V} case, run 1, the product is iso-enriched, and the data is fit to a chain-end controlled model. Run 5, the C_2 case, as previously discussed, produced isotactic PMMA, with a much lower degree of misinsertions, as is expected for the enantiomorphic site control mechanism to which the data are well fit. Interestingly, run 3 produced no polymer; presumably, the steric bulk of the two reagents is too great to allow methyl abstraction by the borane. This is consistent with the findings of Gibson, *et al.* [53] Thus, the variation in polymer properties (assuming a metallocenium active site) expected was indeed observed in metallocenes activated with the perfluoroaryl borane.

The processes involving tris (pentafluorophenyl) aluminum, however, were remarkably insensitive to metallocene geometry. In all three cases (runs 2, 4, and 6), syndio-enriched PMMA was produced. rr triads were nearly identical within experimental error, and all three cases are well fit by the chain-end control model, reinforcing the hypothesis that cationic sites are not active in this process. In addition, run 4 illustrates the higher reactivity of catalyst systems based on the alane. It is tempting to rationalize this based simply on a higher methide affinity of the alane versus the borane. However, steric bulk was invoked to explain the failure of the latter to activate the metallocene, and the aluminum analog is even larger, suggesting that it should be even less reactive. However, all evidence thus far suggests that the aluminum catalyzed reactions do not require a cationic active site. Hence it is probable, and currently hypothesized, that the neutral metallocene simply acts as an initiator (source of nucleophilic methide anion) for monomer activated by coordination to the aluminum Lewis acid. Hence, in this case (unlike the borane catalyzed processes, wherein the acid must interact with the transition metal directly to produce active cationic species) the bulky activator itself need not interact with the Zr-Me group, which is sterically inaccessible. In any event, the fact that metallocene symmetry produces no effect on the tacticity or fit of the data to a mechanistic model (chain-end control) suggests that MMA polymerizations involving $Al(C_6F_5)_3$ do not proceed via cationic mechanisms.

B. Non-Metallocene Initiators

Given that several various metallocenes gave nearly identical results, we sought to directly demonstrate that the transition metal component (and associated ligand) was not a requirement for production of s-PMMA mediated by $Al(C_6F_5)_3$. This was of academic

interest, to show that the cationic component was a "spectator" to the polymerization process, but also of practical interest; *rac*-(EBI)$ZrMe_2$ has a formula weight of 377.7 g/mol, and it only appears to function as a source of methide anion to initiate polymerization. This certainly does not qualify as an "atom economical" process. Furthermore, on an industrial scale it is simply not feasible to remove catalyst residues from the plastic product, so they are left in the final product. While the activity of commercial catalyst formulations is sufficiently high that this does not correspond to a significant contamination issue, it would be beneficial to use initiators which leave more benign residues. To this end, lithium based initiators were investigated.

entry	complex	T_p (°C) T_p (h)	yield (%)	M_n	*PDI*	T_g (°C)	[*rr*] (%)	[*mr*] (%)	[*mm*] (%)
1	**Me_2C=C(OMe)OLi**	23 (2)	52	14 700	18.8		10.7	22.5	66.8
2	**Me_2C=C(OMe)OLi**	-78 (10)	0						
3	**Me_2C=C(OMe)OLi + 2Al(C_6F_5)$_3$**	23 (5 min)	100	52 100	1.08	127	78.4	20.6	1.0
4	**Me_2C=C(OMe)OLi + 2Al(C_6F_5)$_3$**	-78 (1.75)	46	37 000	1.35	**138**	**94.2**	5.8	0.0

Table 3: MMA polymerizations initiated by Lithium enolates

Based on the work of Collins and Yasuda, it is generally believed that metal-mediated polymerizations of MMA involve metal-enolate species, generated from 1,4 Michael addition to the α,β-unsaturated monomer. Hence, the lithium enolate of methyl isobutyrate was synthesized to generate a simple, low molecular weight initiator. The close relationship between this species and the expected propagating anion suggested that it might be kinetically competent to replace metallocenes as initiator. In addition, since each step of propagation regenerates an enolate (albeit oligomeric and eventually polymeric), these species could be seen as crude "catalysts", since their functionality will remain intact after each step. Concentrations and conditions are identical to those shown

for table 1, allowing for direct comparison. Run 1 shows that, in the absence of Lewis acid, these compounds do initiate polymerization. However, the process is ill defined, producing polymers with a very broad range of molecular weights, which are enriched in isotactic portions. In addition, this is a slow process, and hence the isolated yield is very low. Lowering the temperature to -78°C (run 2) shuts down the initiation completely. Premixing the monomer with 2 equivalents of Al Lewis acid to activate the monomer produces several dramatic changes. First, the activity is significantly enhanced, giving quantitative conversion in 5 minutes at room temperature (vs. 52% in 2 hrs w/o activator). Next, the polydispersity is markedly improved, to values suggesting a living character. Most importantly, the stereoselectivity of the process is reversed, revealing a propensity for syndiotactic enchainment, as opposed to the isospecific process active without Lewis acid additive. The percentage of rr triads is significantly improved over the analogous run catalyzed by metallocenes (Table 1, run 5). Lowering the temperature to -78°C (run 4) greatly improves the percentage of rr triads, up to 94.2%, resulting in a material with the unusually high T_g value of 138°C. This is a substantial improvement over the materials produced using metallocenes as initiators, in spite of the fact that the enolate-initiated polymers have lower molecular weights (which lowers the glass transition temperature). It is clear that Lewis acid catalysis turns the ill-defined, slow, iso-specific process promoted by enolates alone into a discrete, highly efficient, syndio-specific process. Furthermore, these experiments demonstrate that metallocenes are not crucial to MMA polymerizations in these systems, and that, in fact, far better results can be obtained in their absence.

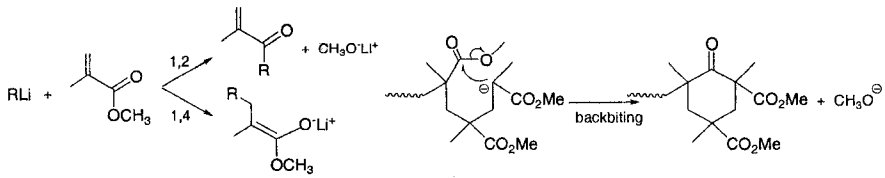

In the absence of Lewis acid, 1,2 addition (LH side, upper pathway), and backbiting compete with the desired propagation mechanism, Michael addition (LH lower pathway)

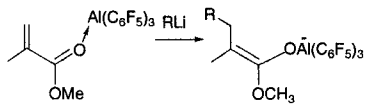

$Al(C_6F_5)_3$ catalysis promotes 1,4 Michael Addition

Scheme 13: MMA polymerizations: competing processes and Lewis acid catalysis

Given the improvements gained by simplifying the gegenion (from metallocenium to lithium), the next experiments were directed at exploring even simpler, commercially available alkyl lithiums as initiators. The obvious choice would be methyllithium, since the metallocene dimethyls apparently provide methide anion as an initiator. However, this species has an oligomeric form with reasonably strong intermolecular forces[54]. More importantly, it is insoluble in hydrocarbon solvents, which would reduce its ability to function as an initiator in toluene, the solvent of choice for MMA polymerizations in our labs. Hence, *tert*-butyllithium was selected; it is soluble in hydrocarbons, and has somewhat weaker intermolecular forces than MeLi, suggesting better initiation activity in spite of its greater steric bulk. Alkyllithiums have been used as initiators previously; Bovey[55] achieved similar results with n-BuLi at -62°C in 1960. Given the lack of utility of the i-PMMA due to its low softening temperature, however, this is not a particularly interesting accomplishment.

entry	complex	T_p (°C) T_p (h)	yield (%)	M_n	*PDI*	T_g (°C)	[*rr*] (%)	[*mr*] (%)	[*mm*] (%)
1	***t*BuLi**	23 (2)	29	16 200	21.7		7.4	14.7	77.9
2	***t*BuLi**	-78 (10)	80	53 600	14.4		7.3	17.7	75.0
3	**(i) $2Al(C_6F_5)_3$ (ii) *t*BuLi**	23 (5 min)	100	85 800	1.73	135	76.6	22.3	1.1
4	**(i) $2Al(C_6F_5)_3$ (ii) *t*BuLi**	-78 (4)	84	59 800	1.33	**140**	**95.0**	5.0	0.0

Table 4: MMA polymerizations initiated with alkyl lithium reagents

Table 4 illlustrates similar trends to those just shown for lithium enolate initiated polymerizations. Somewhat surprisingly, the yield is somewhat lower at room temperature (run 1) than that achieved with the enolates. In spite of this, the species is an effective initiator at -78°C (run 2), in contrast to the enolate. In the absence of Lewis acid, the range of molecular weights is very broad, and the product is predominantly isotactic (higher % mm triads than observed with enolates). Lowering the temperature markedly improves the polydispersity index (PDI), but the value (14.4) is still far too large for most commercial applications. As before, addition of two equivalents Lewis acid produces a very highly active catalyst system, with relatively narrow PDI (though noticeably broader than that achieved with the enolate initiator). Lowering the reaction temperature (run 4) produced very highly syndiotactic PMMA (95% rr triads), with correspondingly high T_g. In fact, this material exhibited the highest percentage rr triads and highest glass transition of any material synthesized in our labs, clearly demonstrating the concept that s-PMMA can be produced via an unexpected, metallocene-free mechanism.

Interestingly, attempts to substitute $B(C_6F_5)_3$ for the alane used above completely shut down polymerization activity with both lithium alkyls and enolates. Since, as shown, enolates themselves are active initiators for MMA polymerization, this does not simply correspond to a failure to catalyze the process, but indicates some interaction that

prevents polymerization. Fluorine and proton NMR experiments to probe the interaction of the borane with lithium enolates revealed very complicated mixtures, and failed to shed any light on the competing processes. Erker[56] and coworkers have shown with crystallographic evidence that $B(C_6F_5)_3$ coordinates to the α-carbon in MVK (methyl vinyl ketone, a related polar monomer) metallocene complexes. While the comparison is not direct, it does suggest that this reagent has much lower oxophilicity than $Al(C_6F_5)_3$. The latter strongly prefers to form O-bound enolates, whereas Erker's work shows that the borane forms C-bound enolates, at least under certain conditions. If this hypothesis could be extended to lithium enolates, and the borane indeed coordinated to the unsaturated β carbon, then it would 1) not be present as free Lewis acid to activate monomer via coordination, and 2) consume all of the enolate in formation of a C-bound adduct, thereby preventing initiation.

C. Mechanistic Considerations

As discussed in the introduction, conventional wisdom holds that the role of the Lewis acid cocatalyst in metallocene-based polymerizations is to abstract alkide (or halide) from the transition metal center to generate cations. Having shown that such cations were not active in the Al-based systems of interest, it became apparent that the direct interaction of the monomer with the Lewis acid was the crucial interaction. Towards this end, Dr. Chen was able to isolate the MMA-$Al(C_6F_5)_3$ adduct, and characterize this species via x-ray diffraction[57]. One unique feature of this structure is that the α,β-unsaturated moiety is locked into the s-cis configuration. As expected, the carbonyl oxygen is bound to the oxophilic aluminum center. Coordination to the electrophilic metal activates the monomer to 1,4 conjugate addition, so isolation of this

species represents interception of an activated monomer species. It is important to recall, however, the Lewis acid itself does not produce polymer (table 1, run 3). Hence, pre-mixing of this Lewis acid with monomer forms this activated species in situ, but propagation does not ensue without initiator (as in Collins system). With this structure in hand, it is reasonable to propose that an anionic initiator would Michael add to the activated monomer, generating an enolaluminate anion. The Lewis acidity of the four-coordinate Al would be negligible, and the enolate itself should be an active nucleophile (provided sufficient driving force to break the strong Al-O bond). Hence, if another equivalent of activated monomer were present, the enolate could attack the coordinated monomer via 1,4 conjugate addition.

While this is a very attractive mechanistic proposal, it features a puzzling aspect in that it requires the presence of free $Al(C_6F_5)_3$. The analogous borane abstracts methide from metallocene methyls, and forms an inactive borate anion, which does not further interact under polymization conditions. Indeed, the term "spectator anion" has been applied to these borates because they are robust, chemically inert, and do not interfere in cationic coordination polymerizations. Given that the Al analog has been predicted to have a higher methide affinity than the more established B Lewis acid, it was unclear how free alane might appear under polymerization conditions, given that preformed zirconocenium aluminates were typically used. NMR studies were useful in this regard, and we observed an unexpected back-transfer of methide anion to the cationic zirconocene center in the presence of MMA monomer.

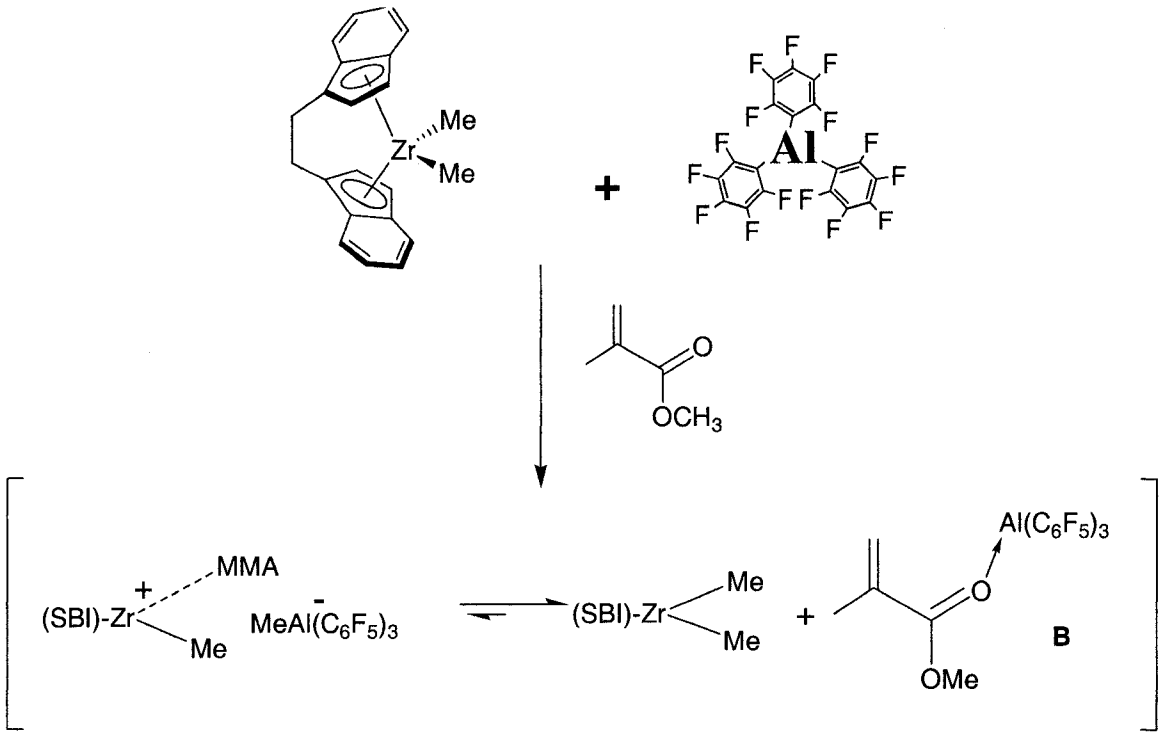

Scheme 14: Interaction of metallocene and Lewis acid in the presence of MMA

Hence, when the neutral metallocene and $Al(C_6F_5)_3$ are mixed in the presence of monomer, the expected abstraction product is observed, resulting from methide abstraction, forming metallocenium cation, with coordinated monomer, and methyl aluminate anion. However, an equilibrium is established, and the aluminate is the minor product. Methide is transferred back to the zirconocene cation, regenerating neutral metallocene and free alane, to which monomer coordinates. Even if the metallocenium aluminate is preformed, addition of MMA causes the observed methyl transfer. While this is somewhat surprising at first, it may be rationalized based on the high oxophilicity of the aluminum species. Apparently, coordination of the electron rich (but neutral) carbonyl oxygen stabilizes the elecrophilic center better than the (anionic) methide anion. This observation provides a pathway for generation of free aluminum Lewis acid under polymerization conditions, allowing proposal of a working hypothesis for the mechanism for anionic group-transfer type polymerization, shown below.

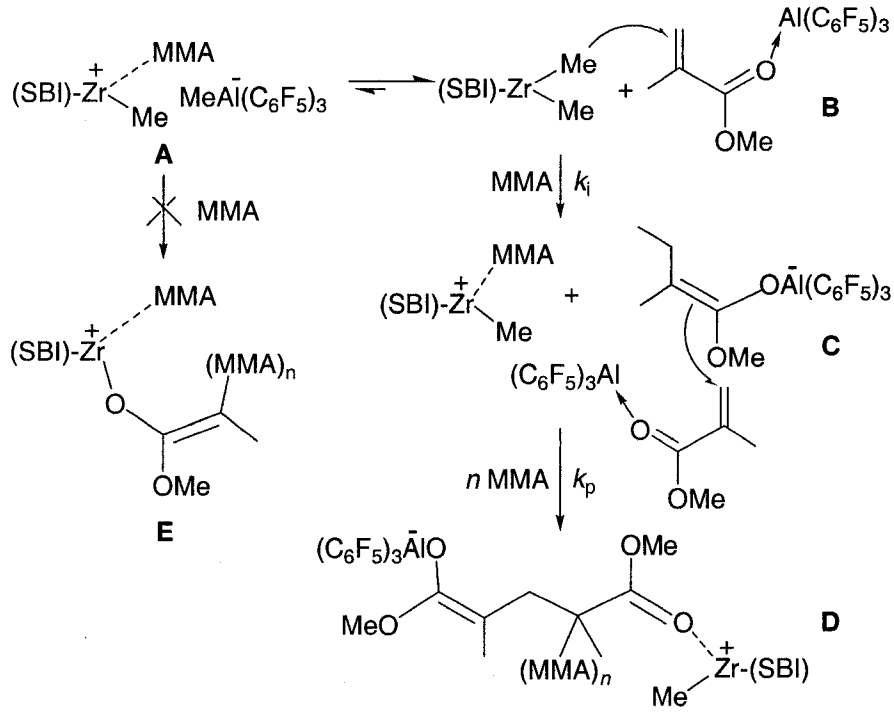

Scheme 15: Proposed mechanism for syndiospecific anionic MMA polymerization

The left hand pathway, showing monomer coordinated to the cationic Zr center, and initiation and propagation via intramolecular Michael addition is correct for the borate analog, but does not appear to be operative when the Al cocatalyst is employed. In this case, back transfer of methide generates free Lewis acid to which monomer coordinates, activating it to Michael addition. The neutral metallocene then functions as initiator, delivering methide anion to the β-carbon, generating an enolaluminate. Propagation ensues when another equivalent of monomer, activated by coordination to the Lewis acid, is then attacked by the enolate from the enolaluminate. The anionic polymer chain is then transferred back and forth between aluminum centers in a bimetallic mechanism that is consistent with the observations to date.

Striking evidence for the proposed mechanism was obtained by NMR studies employing the very convenient ^{19}F-NMR handle provided by the discrete perfluoroaryl activators employed in this study.

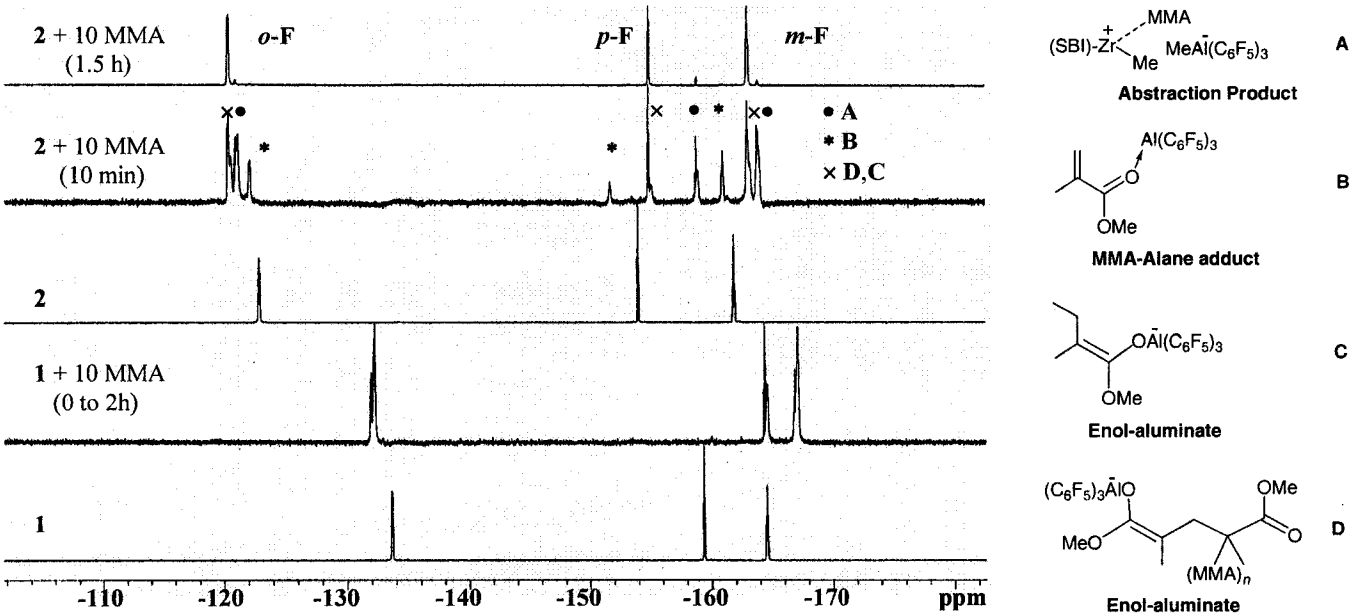

Figure 7: Fluorine NMR of aluminate and metallocenium borate polymerizations

1 = SBIZrMe+ ($MeB(C_6F_5)_3$)- ; 2 = SBIZrMe+ ($MeAl(C_6F_5)_3$)-

The lowest spectrum in figure 7 shows the metallocenium borate (o-, p-, and m- fluorine positions increasingly upfield), activated catalyst. The next spectrum up shows the same species in the presence of 10 equivalents monomer. The shifts in the three peaks, notably the para position, are due to the conversion from weakly-coordinated anion, to non-coordinated anion, as it is displaced from the coordination sphere of the Zr center by monomer as propagation ensues. This spectrum remains unchanged in the course of the oligomerization, a typical behavior for borate anions that gave rise to the term "spectator anion". The third spectrum from the bottom shows the metallocenium aluminate. Moving up to the fourth spectrum reveals very different behavior from the borane analog.

Addition of 10 equivalents monomer in the presence of the aluminate generates several different anionic species, as proposed. The methide abstraction product is observed ("A"; labeled with solid circles), but more importantly, so is the aforementioned, well-characterized MMA-$Al(C_6F_5)_3$ adduct ("B", labeled with stars), lending credence to the proposed mechanism. Broadened peaks ("C" and "D", labeled with X) have been assigned as enolaluminates, both monomeric (from methide initiation), and oligomeric (from enolate attack on activated monomer; various chain lengths). The top spectrum shows only one species present, assigned as oligomeric enolaluminate. Hence the behavior of the aluminate anion is not simply that of a "spectator", in sharp contrast to the well established borane activator. Several anionic species are present in solution, which appear to be enolaluminates. Observation of all of these species is consistent with the proposed anionic, bimetallic mechanism, and the previously detailed experimental evidence.

Given that enolaluminates appear to be active species in these systems, and numerous examples have shown that the cation is relatively unimportant, direct syntheses of simple enolaluminates were attempted. Reactions of a variety of alkyl enolates of lithium and potassium with the toluene adduct of $Al(C_6F_5)_3$ in a variety of solvents, and at temperatures ranging from -78°C to room temperature resulted in formation of aluminates which appeared to be discrete and clean via ^{19}F NMR. However, the proton spectra were very complicated, and the materials were not isolable in crystalline form. This may be taken to indicate that the species are oligomeric, or fluctional on a time scale not observed in the fluorine experiments. In any event, enolaluminates with simple

counterions do not appear to be discrete, single site species as was hoped. Attempts to isolate metallocenium enolaluminates will be discussed later.

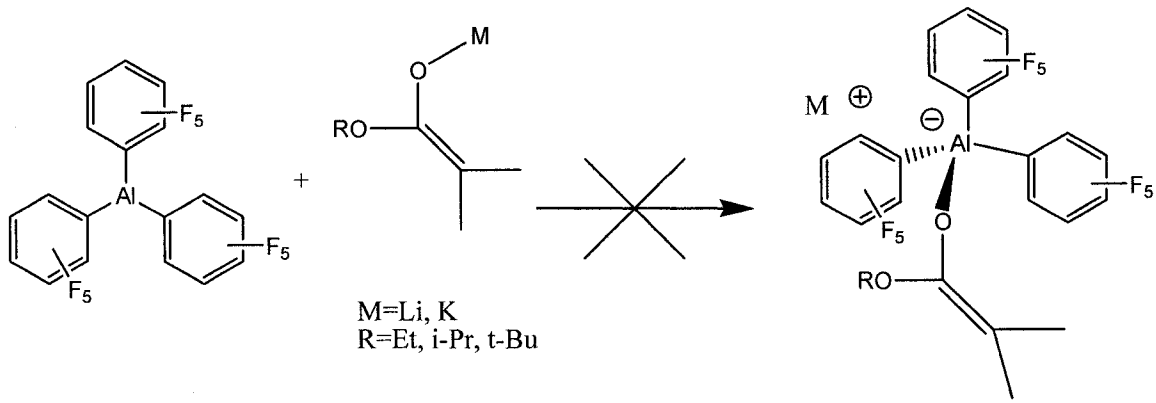

Scheme 16: Attempted direct synthesis of simple enolaluminates

Inoue *et al.* have reported[58] observation of aluminum enolates, and Gibson[59] has reported their synthesis under nickel catalysis. However, in both cases, the products are neutral aluminum enolates, unlike the anionic species discussed here, and the metal centers are stabilized by bulky, chelating ligand sets (aryl-substituted porphyrin derivatives, and chelating Schiff base complexes, respectively).

D. Stereo-diblock copolymers

The previous work highlights the fact that the commercially useful syndiotactic form of MMA can be formed by an anionic process catalyzed by tris(pentafluorphenyl)alane, wherein the cationic gegenion exhibits very little function in the process. This is a reversal from the traditional homogeneous Ziegler-Natta systems, wherein the anion is the "spectator" ion, and the cation is the active site. This raised the intriguing possibility of catalyst systems wherein both the (isospecific) cation, and the (syndiospecific) anion exhibit complementary reactivity to produce stereoblock copolymers. Given that mixtures of the two homopolymers form helical architectures

when blended under suitable conditions, it seemed likely that stereoblock copolymers wherein both forms were present in the same chain, would form novel, robust materials.

For this strategy to succeed, however, there must be a mechanism by which the anionic polymer chains can be transferred from one active site to the other. Having demonstrated the exceptional oxophilicity of $Al(C_6F_5)_3$, which prefers coordination to neutral, oxygen-containing MMA over anionic methide, it seemed more likely that the alane could be used to abstract isotactic chains from the cationic zirconocene, rather than relying on transfer of the syndiotactic blocks from the polymeric enolaluminate (which would require cleavage of anionic O-Al bond). Therefore, it seemed likely that if the cationic zirconocenium enolate could be converted to a neutral species, that the oxophilic alane would preferentially abstract the (isotactic) polymeric enolate moiety. In this fashion, isotactic blocks could be used as initiators for syndiospecific polymerization catalyzed by the alane.

E. Model compounds 1: Unbridged metallocene enolates

To test the feasibility of this strategy, metallocene monomethyl enolates were required as model compounds. Given that, until the present, ansa-zirconocene (mono- or di-) enolates have not been reported in the literature, and initial synthetic efforts in my hands were unsuccessful, we turned to the corresponding unbridged variants, some of which have been reported. It bears mentioning that these are not ideal model compounds. Their cations are syndiospecific, so pairing them with alane activators could only be expected to produce s-PMMA, and not block copolymers. In addition, the bis-Cp systems have been know to show divergent reactivity from the bridged metallocenes. However, in lieu of the desired ansa-metallocene enolates, they served their purpose to

show proof of concept. MMA is a methyl ester; therefore, the logical target would be zirconocene compounds of the enolates of α,β-unsaturated methyl esters. Unfortunately, there is precedent[60] for side reactions involving these species (illustrated in scheme 17) which would unnecessarily complicate model reactions.

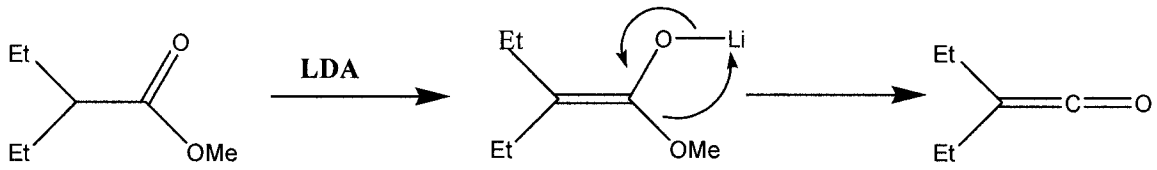

Scheme 17: Synthetic difficulties with Methyl ester enolates

Hocker had noted the absence of crystalline zirconocene monomethyl enolates in the literature, as all of the known compounds of this class were reported as oils. Whereas he was successful in producing such a compound, and characterizing it via x-ray crystallography, his product was not the intended one, nor is it a direct model suitable for use in our model studies. The problem lies in the facile reaction pathway shown in scheme 17. Treatment of the methyl ester compound with the sterically hindered strong base, lithium diisopropyl amide does indeed produce the desired lithium enolate. However, lithium methoxide is readily eliminated, to yield the ketene shown. As expected for these highly reactive intermediates, they went on to perform various side reactions which would make model studies with these species all but useless.

Presumably due to the difficulties noted above, Scott Collins had employed the corresponding t-butyl ester enolates in his studies, and produced the desired zirconocene monomethyl (t-butyl ester enolate) compound. Although these species have not yet been isolated in the crystalline state, but rather as oils, they have been successfully applied to model reactions, and so we sought to employ them in our system. Hence, lithio t-butyl isobutyrate was synthesized. However, low temperature NMR studies were performed to

probe the interaction of this species with the aluminum Lewis acid, and an incompatibility was observed, illustrated in scheme 18.

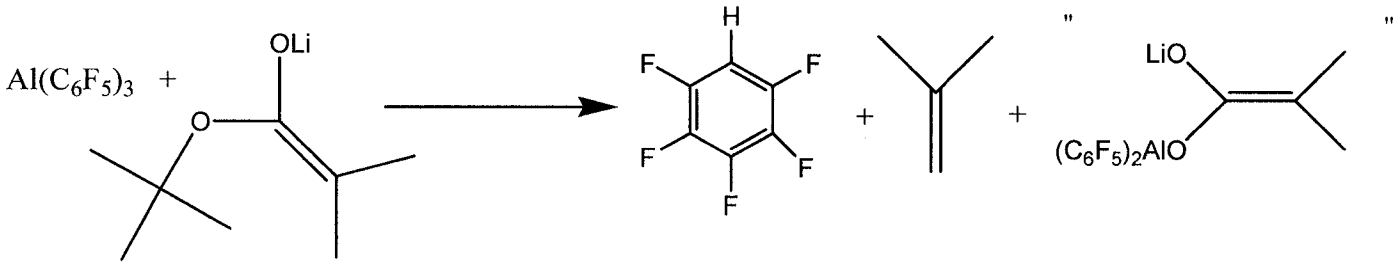

Scheme 18: Synthetic difficulties with t-butyl ester enolates

At temperatures above -40°C, Fluorine NMR clearly showed the generation of pentafluorobenzene, and the proton NMR revealed the presence of isobutylene. Presumably, protonolysis of the perfluoroaryl group occurred from a proton from the t-Butyl group, generating the fluorinated benzene product. Elimination of isobutylene would then be facile, and the extremely electrophilic and oxophilic Al cation would bond to the resultant anionic oxygen functionality. The aluminum product shown is based on mass balance, and was not directly observed; it may exist in several forms, and would presumably be a reactive intermediate which would participate in further side reactions. In any event, this observation precluded the use of t-Butyl esters in model studies involving the alane Lewis acid.

Hence, the next logical choice for model compounds involved the isopropyl ester enolates. Isopropyl isobutyrate is not commercially available, but was readily synthesized, as shown in scheme 16. Reaction of this species with LDA (generated in situ) generated the desired lithio i-propyl isobutyrate cleanly and in high yield. Alternatively, KHMDS was prepared and utilized to prepare the more highly reactive

potassium enolate species. $Cp_2ZrMeCl$ was then synthesized by literature procedures, and reacted with the enolate in a modification of Collins procedure.

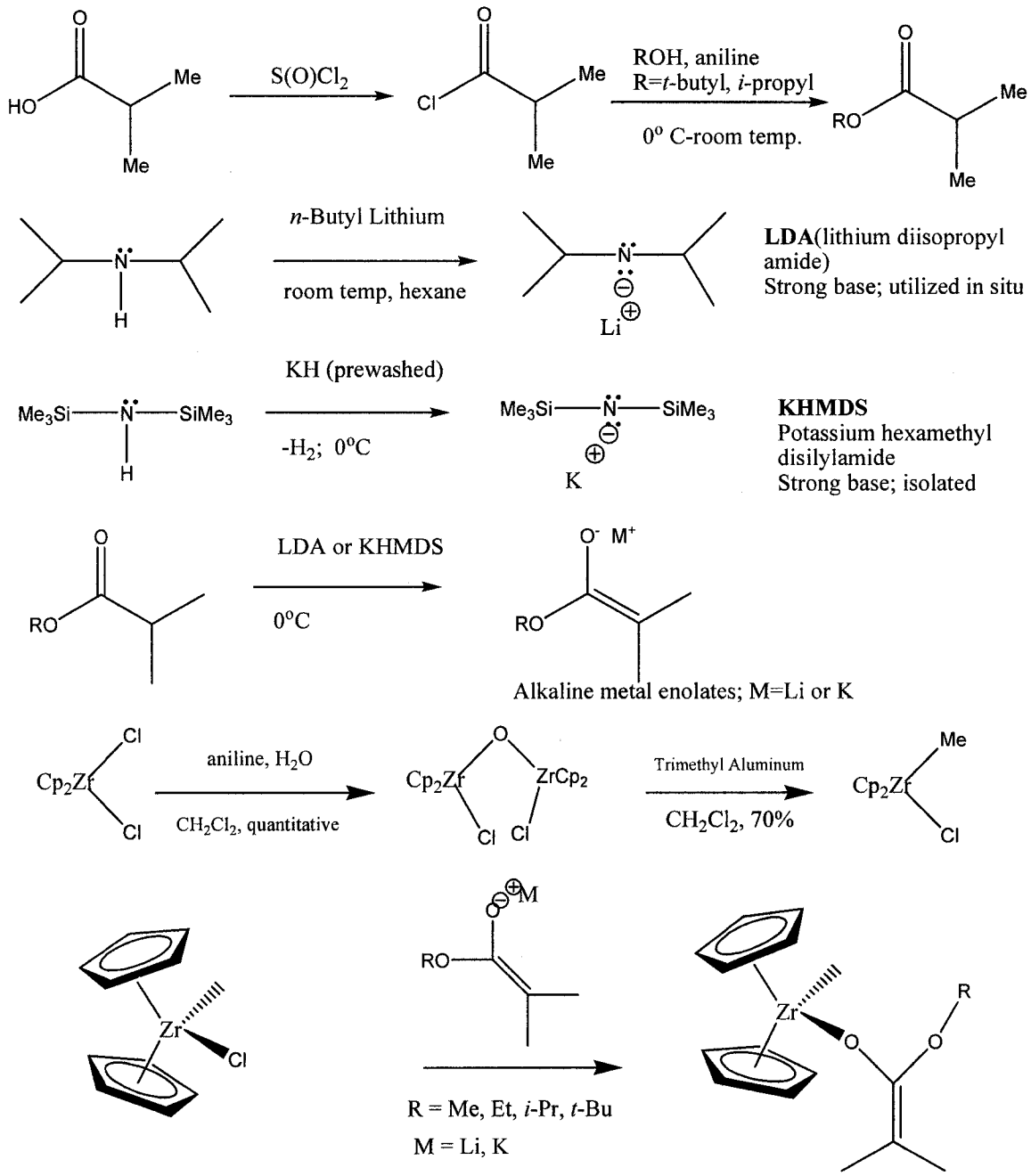

Scheme 19: Synthesis of unbridged zirconocene (monomethyl) enolates

With the monomethyl enolate model compound in hand, model studies were undertaken to probe the possibility of steroblock copolymers. Cationic zirconocenium

enolates have been demonstrated to be the propagating species in isospecific MMA polymerizations. We have demonstrated that $[(Me)Al(C_6F_5)_3]$- can transfer methide anion back to cationic zirconocenes, a reaction pathway which would generate a neutral monomethyl zirconocene with isotactic PMMA enolate functionality at the zirconium center. Hence these model compounds serve to mimic those neutral enolates directly. While it is expected that the borane abstraction agent would selectively remove methide anion, it was proposed that the oxophilic alane would selectively and directly abstract the enolate moiety, to generate an enolaluminate. This would provide evidence of a pathway by which isotactic blocks could initiate syndiospecific polymerization at aluminum.

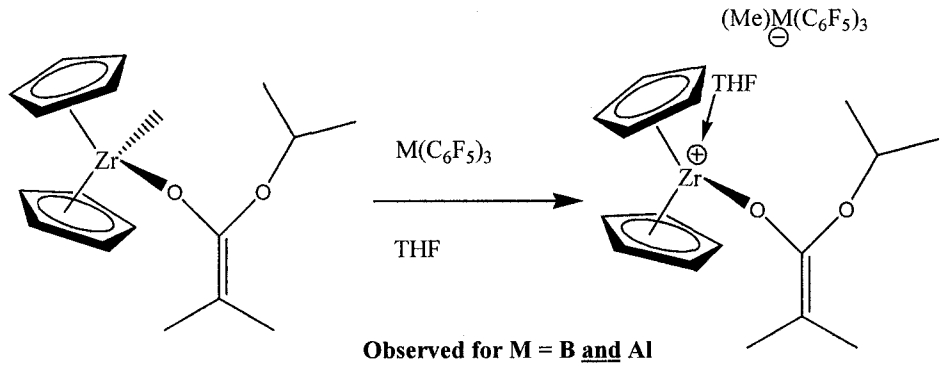

Scheme 20: Lewis acid abstraction

However, this was not observed. As expected, NMR studies in the presence of THF (to stabilize the cationic intermediates) revealed production of the weakly coordinating methyl borate anion. Surprisingly, the identical reaction pathway was observed for the alane, with the fluorine and proton NMR spectra clearly indicating the clean formation of methyl aluminate, and the enolate group remaining intact on the zirconium center.

This does not preclude the possibility of chain transfer, however, as an alternative pathway whereby the isotactic enolate chain could transfer to the aluminum center is feasible, as shown in scheme 21.

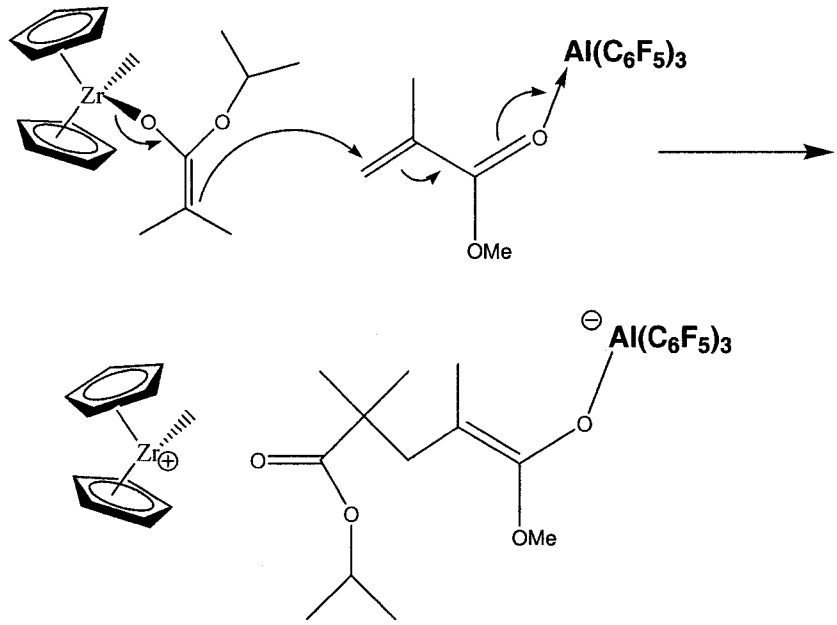

Scheme 21: Alternative mechanism for chain transfer

Although this pathway was not directly observed, it is reasonable, and expected to be much more favorable process, due to the driving force not only of the strong Al-O bond formation, but also the formation of a carbon-carbon bond. Therefore it seemed reasonable to propose that stereo(di)block copolymers could be produced by this mechanism, provided it was possible to convert the cationic zirconocenium borate to the neutral species and to transfer monomer to the alane to generate activated monomer, to which the enolate (isotactic chain in the actual polymerization) could transfer, as shown in scheme 22.

Model studies illustrated below demonstrated the practicality of this route.

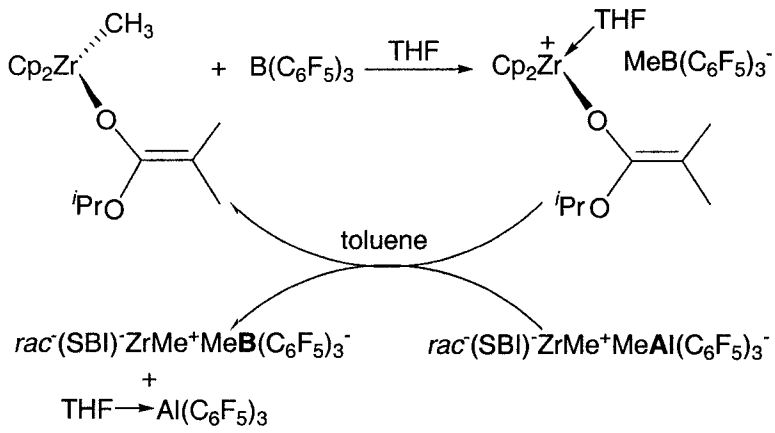

Scheme 22: Diblock model reactions

The upper reaction, generation of the THF adduct of metallocenium borate was shown in scheme 20. In this trial reaction, the coordinated THF is used as a crude model for MMA monomer. The direct experiment, employing actual monomer, was obviated based on the fact that rapid polymerization would obscure the results of the test. Hence, the oxygen functionality of THF, and its otherwise inert behavior under the reaction conditions allowed us to probe for transfer of heteroatom-containing species to aluminum. Next, a toluene solution of preformed ansa-zirconocenium (methyl)aluminate was added to the reaction mixture. As anticipated, methide was transferred to the cationic nonbridged zirconocene, generating a neutral species. In addition, the known THF adduct of the alane was formed as well. This experiment demonstrates the feasibility and compatibility of two of the three process required for production of diblock copolymers. First, isospecific metallocenium borates can be converted to neutral metallocene enolates. This opens the possibility of abstraction of the enolate group to an aluminum center to initiate syndiospecific propagation, producing the second block. Direct enolate transfer had not been observed, but this model reaction shows that the oxygen functionality is preferentially transferred to the aluminum center, not the ansa zirconocenium cation

which is also present. By analogy, this corresponds to production of the MMA-alane adduct, or activated monomer, to which enolate species can readily add via Michael addition. The latter had not been directly observed, but is operative between Al centers (in the syndiospecific homopolymerization), and so is reasonable to expect this transfer from the less oxophilic neutral ziroconium enolate species. Hence these reactions provided evidence for a reasonable route whereby isotactic polymeric enolates could initiate syndiospecific polymerization, generating diblock copolymers.

Efforts to demonstrate the final key step, enolate transfer to coordinated monomer were not conclusive, but did reveal interesting activity. Hence, the model compound $Cp_2Zr(Me)$(iPriButyrate) ("CpZipMe") was subjected to polymerization trials. In the absence of activator, it produced no PMMA in two hours at room temperature, as expected. Addition of 2 equivalents tris(pentafluorophenyl)aluminum, however, generated a highly active, syndiospecific polymerization system. Monomer was quantitatively consumed in 5 minutes at room temperature, producing syndio-enriched polymer (68.9% rr triads) with a very narrow molecular weight distribution of 1.16, possibly indicative of a living process[61]. Lowering the reaction temperature improved the percentage of syndiotacticity (77.7% rr triads), and lowered the PDI to 1.12. The higher degree of syndiotacticity in these systems may be attributed to the fact that the metallocene site here is itself syndiospecific, such that if reaction did take place at this site, the syndiotacticity would not be compromised, unlike the case with iso-specific ansa metallocenes.

These polymerization studies provide indirect evidence for the proposed key mechanistic step, that of enolate transfer from metallocene to coordinated monomer.

Whereas it cannot be directly demonstrated that the initiating group that begins the polymerization is the enolate, and not simply the methide anion, the former appears more likely. Substitution of Cp_2ZrMe_2 for the analogous monomethyl enolate shown here gave no activity at -78°C. Although this could conceivably be due to electronic differences between the two metallocenes, it seems to indicate that the enolate anion is in fact the initiating species, lending credence to the proposed (isotactic, polymeric) enolate transfer mechanism.

The polymerization strategy modeled and discussed above indeed proved to be effective[62], as illustrated in scheme 23.

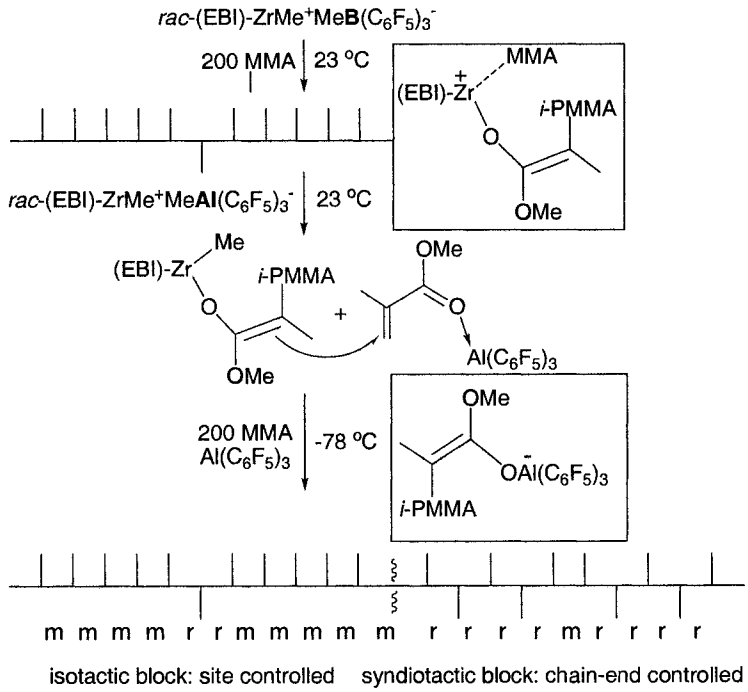

Scheme 23: Production of isotactic-*b*-syndiotactic stereoblock PMMA

The strategy is as follows. First, preformed ansa-metallocenium borate catalysts was added to 200 equivalents of monomer. This generated the isotactic block by the well known, enantiomorphic-site controlled propagation involving intramolecular Michael addition. After 45 minutes, monomer had been largely consumed, and the remaining

species was a cationic zirconocenium (i-PMMA-enolate). Addition of the ansa-metallocenium (methyl)aluminate at room temperature methylated the enolate species, generating neutral zirconocene (monomethyl) enolate as demonstrated in our model studies, and alane (either coordinated to remaining monomer, or as the free Lewis acid). Lowering the temperature to -78°C to enhance the syndiotacticity of the second block, followed by addition of another 200 equivalents of MMA in the presence of another equivalent of $Al(C_6F_5)_3$ (since the syndiospecific process requires 2 equivalents of Al to proceed) presumably led to isotactic chain transfer to activated monomer. This rapidly propagated via the syndiospecific mechanism, and monomer was quantitatively consumed after another hour at low temperature.

MMA Polymerization Results and Polymer Properties by Metallocene/Lewis Acid Hybrid Catalysts [a]

Run	initiator	T_p (°C)	t_p (h)	yield (%)	$10^4 M_n$ [b]	PDI_n [b]	T_g [c] (°C)	[rr] [d] (%)	[mr] [d] (%)	[mm] [d] (%)
1	*rac*-(EBI)$ZrMe_2$/B	23	2	100	2.97	1.18	55	1.2	2.8	96.0
2	*rac*-(SBI)$ZrMe_2$/B	23	2	80	2.84	1.12	55	3.1	6.5	90.4
3	*rac*-(EBI)$ZrMe_2$/Al	23	2	100	1.77	1.23	110	60.2	35.8	4.0
4	*rac*-(SBI)$ZrMe_2$/Al	23	2	85	2.88	1.19	111	60.6	35.1	4.3
5	(i) *rac*-(EBI)$ZrMe^+$(MeB)$^-$	23	0.75	100	5.43	1.61	87	45.7	7.9	46.4
	(ii) *rac*-(EBI)$ZrMe^+$(MeAl)$^-$	-78	1							
6	(i) *rac*-(SBI)$ZrMe^+$(MeB)$^-$	23	0.75	100	5.38	1.45	87	47.1	9.9	43.0
	(ii) *rac*-(SBI)$ZrMe^+$(MeAl)$^-$	-78	1							

[a] Polymerization conditions: 46.7 μmol initiator (I); mole ratio [MMA]/[I] = 200; 10 mL toluene; B = $B(C_6F_5)_3$; Al = $Al(C_6F_5)_3$. [b] Determined by GPC relative to PMMA (entries 1-4) or polystyrene (entries 5-6) standards. [c] Determined by DSC. [d] Determined by ^1H NMR spectroscopy.

Table 5: Diblock copolymerization results

Table 5 tabulates results shown schematically above. Both C2 symmetric ansa-zirconocene compounds from the SBI and the EBI ligand set were investigated, and exhibited similar performance, although the latter appears somewhat more reactive (runs 1 and 3 gave quantitative conversion, with 2 and 4 somewhat lower). For this reason, the

EBI ligand was used preferentially for further studies. Runs 1-4 are control reactions. 1 and 2 again demonstrate that borane activation of the metallocenes produces highly isotactic PMMA. Runs 3 and 4 illustrate again the reactivity with the analogous alane activator, and again, syndio-enriched polymer is formed. The main feature of note is the number average molecular weight (target = 20 kD), which ranges approximately from 18 kD to 30 kD. Runs 5 and 6 describe the reaction protocol depicted schematically in the previous scheme. The first key point to note is that the number average molecular weight is approximately doubled, to roughly 54 kD. This is significant, as it provides evidence that the product is not simply a mixture of homopolymers. If this was the case, and the isotactic chain was terminated, followed by syndiospecific propagation, these values should not increase over those shown in the homopolymerizations. The fact that the chain lengths have apparently doubled strongly suggests that, as intended, the isotactic blocks served as initiators for the syndiospecific enolaluminate polymerization, producing true stereo diblock copolymers. Next, the concentration of rr and mm triads are essentially identical, with a small degree of mr triads. Whereas the latter are typically interpreted as misinsertions, in this case, they also arise from the junctures between the stereoblocks. While this is the expected distribution of triads, it must be stressed that this does not prove the formation of block copolymers, as mixtures of the two homopolymers would give the same distribution. In both cases, the polydispersity indices are relatively low and monodisperse, indicating a well-defined process. The glass transition temperatures are roughly intermediate between the values for the homopolymers. Again, however, this does not necessarily indicate copolymer formation, as mixtures of the homopolymers would be expected to produce similar results. The strongest evidence that

these products are not simply mixtures of homopolymers derives from solvent fractionation studies. Both i- and s-PMMA are soluble in boiling isopropyl alcohol. However, soxhelet extraction of these polymeric products in refluxing isopropanol only removes negligible quantities of material, and NMR studies show the tacticity remains unchanged after the extraction. This is rather convincing evidence, although it does not completely rule out the possibility of some interaction between homopolymer chains (e.g. helical coils) which changes the solubility parameters of the blend.

F. Multi(stereo)block copolymers

The preceding work demonstrates that cationic zirconocenes and anionic aluminates may function complimentarily to produce diblock copolymers. However, diblock copolymers are typically much less robust than multiblock copolymers, so the latter are attractive targets. For instance, in the case of thermoplastic elastic copolymers consisting of "hard" (crystalline) and "soft" (amorphous) blocks, segregation of the two into largely separate domains is a relatively facile process, and as a result, diblocks of this type have very low resistance to shear stress. Multiblock variants, however, cannot segregate as readily, and therefore provide more sturdy materials. However, significant challenges make multiblock polymerizations a much more difficult synthetic process. Whereas the extreme oxophilicity of the aluminum Lewis acid makes it feasible to conceive of this species abstracting enolate functionality from zirconium (and indeed, this has been demonstrated), the reverse reaction appears unlikely. Hence, although we have used isotactic blocks to initiate syndiospecific polymerization, the possibility of a syndiotactic chain with enolate chain end transferring from the more oxophilic aluminum center to the less oxophilic Zr center seemed remote. To produce practical multiblock

copolymers the rates of enolate exchange between the two catalytic sites would need to be very closely matched, and somewhat slower than the propagation rate.

G. Model Compounds 2: Bridged metallocene enolates

To determine if this approach was feasible, efforts at model compound synthesis were redoubled. Based on Collins' successful route to non-bridged zirconocene bis-and monoenolates (the latter, unfortunately, as oils), efforts first began from the corresponding ansa zirconocene dichlorides, rac-EBIZrCl$_2$. The first difficulty came in the need for the monomethyl chloride intermediate for synthesis of the requisite monomethyl enolates. The route to the unbridged compound is not effective for the bridged relative. One literature reference mentions production of a related compound[63], rac-(EBTHI)Zr(Me)Cl, although no experimental details are given. Attempts to reproduce and modify this procedure yielded the desired product, although in disappointing yield. The major byproduct is the corresponding dichloride, resulting from double protonolysis. Later, I discovered that a metathesis reaction between the dimethyl and dichloride compounds produced the target intermediate in far better yield under milder conditions. Unfortunately, neither this compound nor the dichloride reacted as desired with lithium enolates or the more reactive potassium enolates. The latter have metal-oxygen bonds with significantly higher ionic character, and as such serve as sources of extremely nucleophilic enolate anions. The observation that even these enolates were not active for ligand substitution of the ansa-zirconocene chloride starting materials suggests that the latter are very sluggish to react. In fact, the preparation of rac-EBIZrCl$_2$ involves acidic aqueous workup, and the product is stable on the benchtop for

weeks, again suggesting a very stable and inert material poorly suited to ligand substitution due to the very strong transition metal-halide bonds.

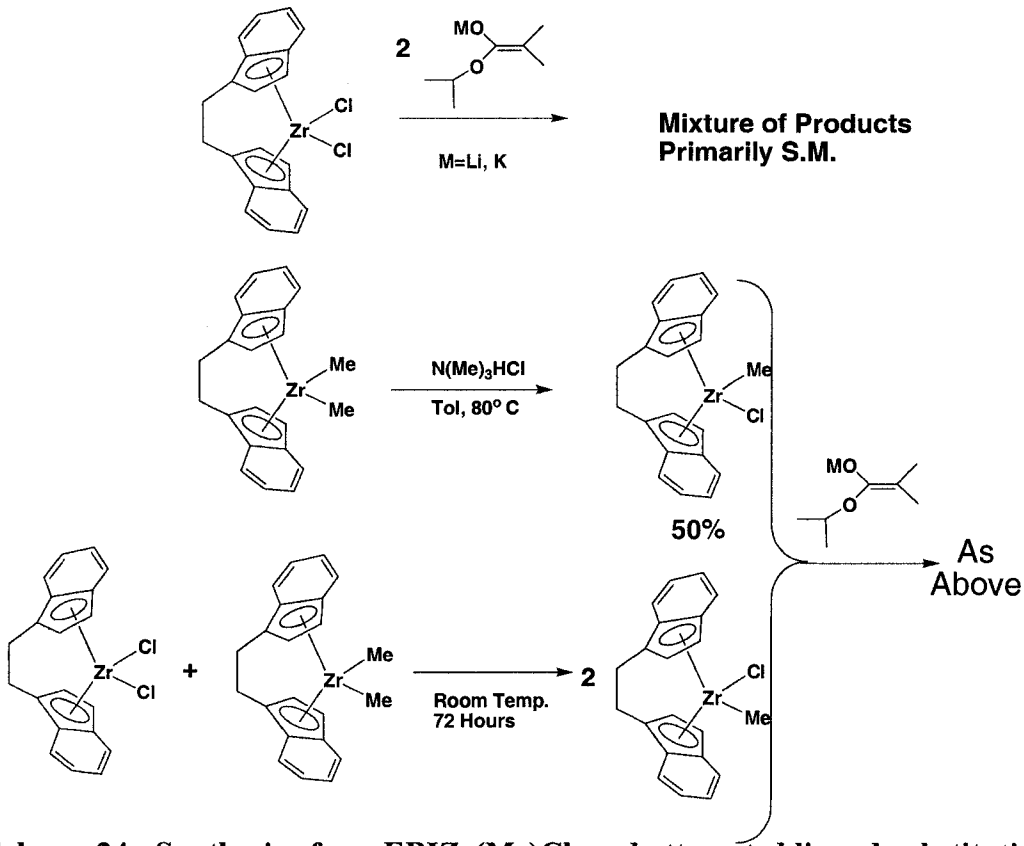

Scheme 24: Synthesis of rac-EBIZr(Me)Cl, and attempted ligand substitutions

Organic chemists have long exploited the reactivity of the "pseudo-halide" trifluoromethylsulfonate (triflate) anion, due to its exceptional aptitude as a leaving group, a result of its strongly electron withdrawing groups stabilizing the negative charge. In fact, an early example in simple S_N1 reactions revealed a rate acceleration of over 10^8 for the triflate compound relative to the chloride[64]. This has not escaped the attention of organometallic chemists, and Collins[65] even commented directly on the lability of the Zr-OTf bond, and its utility in ligand substitution reactions. He synthesized the related compound, (EBTHI)Zr$(OTf)_2$ and utilized the S-enantiomer to catalyze stereoselective Diels Alder reactions. Ironically, his research group does not seem to have investigated

these compounds as precursors to the ansa-metallocene enolates, as he expressed his inability, despite repeated attempts, to synthesize these very important model compounds[66], which are relevant both to his work and to ours. I sought to employ these triflates as intermediates for production of ansa-metallocene enolates.

Initial synthetic attempts employed the stable metallocene dichlorides as starting materials, as shown in scheme 25.

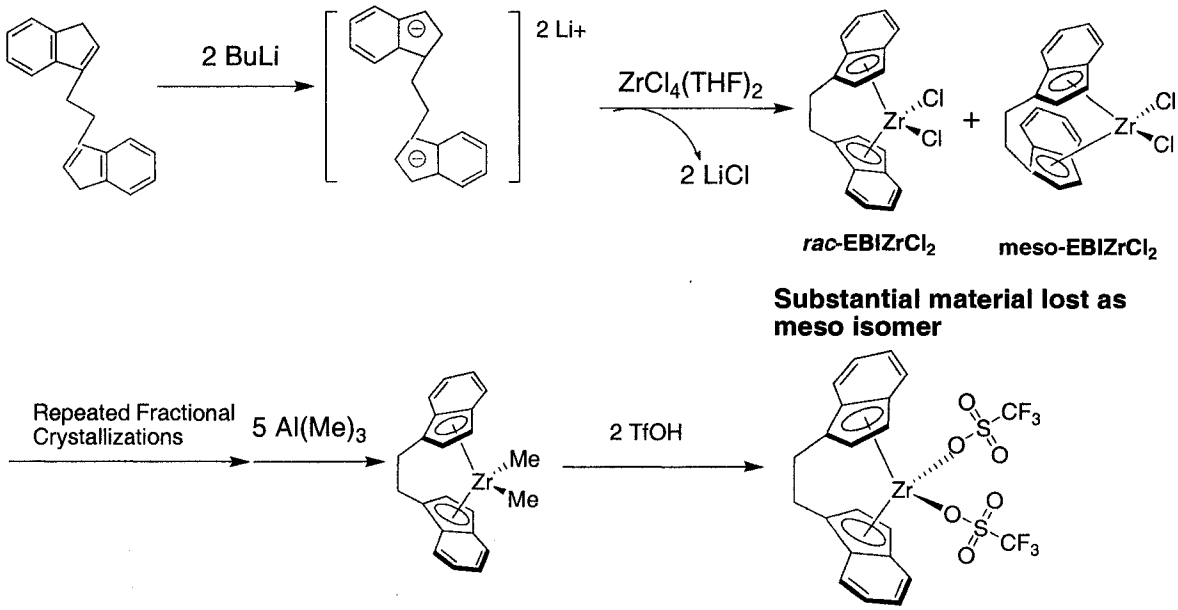

Scheme 25: Conventional route to triflate intermediates

Starting from the neutral ligand (available in moderate, yet highly variable yield), reaction with two equivalents of BuLi generates the dilithio salt, which was typically isolated and purified. $ZrCl_4$ itself is highly reactive, and generates complicated mixtures when reacted directly with the dianionic ligand, so it must be converted to the bis-THF adduct. Preparation of this material and reaction with the dianion of the ligand generates $EBIZrCl_2$, but in two forms. The first shown is the desired C_2 symmetric racemic form, shown on the left. However, this synthesis generates large concentrations of the unwanted meso form, shown on the right. While the latter is conceivably of interest for certain

applications, it is typically considered an unwanted byproduct which must be removed by several repeated fractional crystallizations in a time-consuming and tedious process. Once the racemic form is isolated, is must be methylated. Methyllithium is reported[67] to give mixtures of the rac and meso forms of the dimethyl product via an isomerization reaction. Given the multiple crystallizations required to remove this form from the dichloride, its subsequent regeneration and removal are certainly to be avoided. The milder methyl Grignard reagent avoids this complication, but complete removal of the magnesium salt byproducts is not always achieved, which complicates purification, isolation, and catalytic studies. Hence, trimethylaluminum is the methylating agent of choice. Unfortunately, this requires 5 equivalents of Al (= 15 equivalents methide) to drive the equilibrium to products. This process generates significant quantities of volatile, pyrophoric metal waste, and as such is not ideal. With the dimethyl ansa-zirconocene in hand, treatment with two equivalents of triflic acid generates the desired product in moderate yield. Complications here include difficulties and safety issues in handling this very strong, hygroscopic acid, and loss of material due to irreversible protonation of the indenyl ligand, resulting in lower yields than expected. Hence, the desired triflates can were synthesized in 5 steps from the neutral ligand using conventional methodology.

A significant improvement in the synthesis of ansa-metallocenes was developed by Jordan[68]. He revealed that the reagent $Zr(NMe_2)_4$ could be utilized both as a base to deprotonate the neutral ligand, and also as a metallating agent, removing a step from the conventional route. Furthermore, this process is selective for the desired racemic product, presumably through reversible deprotonation and complexation eventually

yielding the thermodynamically favored, desired isomer. The product here is rac-(EBI)Zr(NMe_2)$_2$, which may be converted to the dimethyl derivative via the same procedure used for the dichloride precursor. Hence this overall approach removes one step and numerous crystallizations from the synthesis of ansa metallocenes, making them significantly more accessible.

It occurred to me that the desired metallocene triflates might be directly prepared from (EBI)Zr(NMe_2)$_2$, thereby removing yet another step from the synthesis of the target ditriflate intermediates. Triflic acid is certainly strong enough to protonate the amino nitrogens, and dimethylamine is a sufficiently good leaving group, particularly since it is a gas, the removal of which would drive the equilibrium towards products. Indeed, it was shown that the treatment of (EBI)Zr(NMe_2)$_2$ with two equivalents TfOH at -78° cleanly generates the target compound directly, obviating the need for methylation, and the associated large quantities of metallic waste.

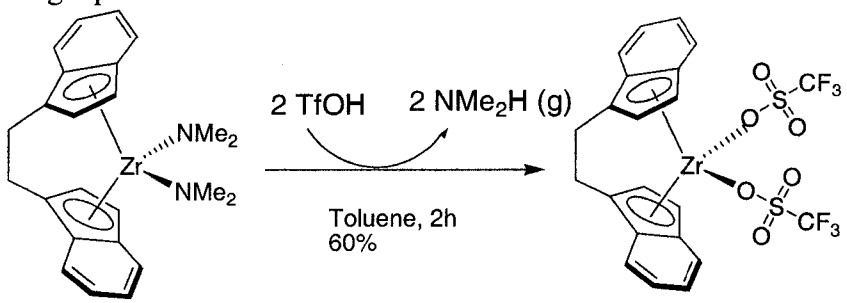

Scheme 26: Direct formation of ansa-zirconocene ditriflates

Scheme 27 illustrates the overall synthetic strategy, emphasizing efficiency, in an overall two-step procedure as opposed to the five step conventional approach shown earlier. Note that both the dimethyl and ditriflate can be produced in two steps from ligand.

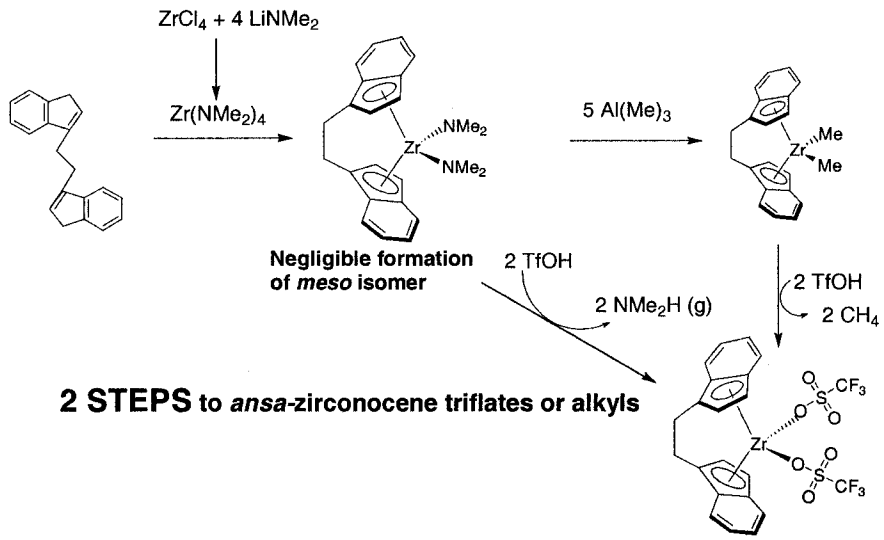

Scheme 27: Efficient, next-generation synthesis of metallocene triflates

Given that these materials proved to be worthwhile intermediates for production of enolate model compounds, further attention was paid to their synthesis. A very convenient route was discovered. *Ansa*-metallocene dichlorides are attractive starting materials, because, as mentioned, they are very stable and inert, and can be synthesized in multigram quantities. Hence a direct route from these stable materials to the highly reactive triflates would be desirable. Collins[69] had shown that a related material, S-(EBTHI)Ti$(Cl)_2$ could be converted to the ditriflate by a metathesis reaction with AgOTf. Interestingly, he synthesized the Zr analog via the more conventional route involving the protonolysis of the dimethyl derivative with two equivalents triflic acid, and does not comment on the reason for the divergent routes. Nevertheless, this route proved successful, and allows convenient preparation of the reactive ditriflate intermediates from the stable dichlorides in high yield. Ligand protonation problems are avoided, so yields in the triflation step are substantially higher by this route. Although this route involves more synthetic steps, it allows easy, relatively safe access to the desired targets.

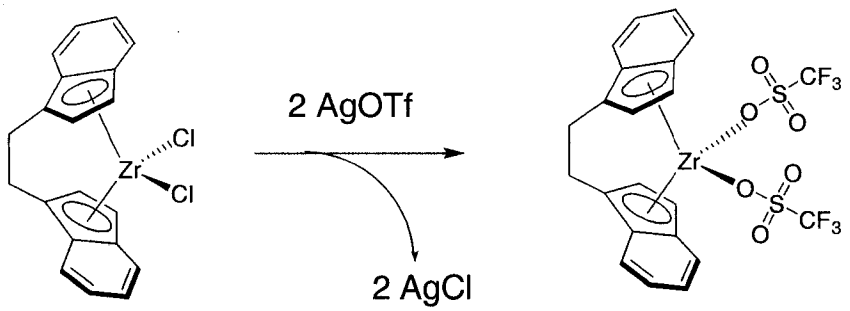

Scheme 28: Safe, facile route to reactive intermediates

With the ditriflate intermediate in hand, attention was focused on production of the monomethyl triflate, for use in formation of the monomethyl enolate, the main model compound of interest. One report in the literature[70] mentions preparation of a similar compound, S-(EBTHI)Zr(Me)(OTf); again, however, experimental details were lacking. The route employed by Buchwald was to treat the dimethyl derivative with one equivalent triflic acid at low temperatures. While this is a reasonable approach, the acid is very difficult to handle quantitatively, owing to its extremely hygroscopic and aggressive nature, and so this route seemed to be less than ideal. A more practical route was detailed[71] for the production of the analogous unbridged compound, $Cp_2Zr(Me)(OTf)$, which proved directly applicable to the ansa-derivatives of interest. Hence, as shown in scheme 29, metathesis of the dimethyl and ditriflate compounds rapidly produces rac-(EBI)Zr(Me)(OTf) in high yield. Given that both the dimethyl and ditriflate precursors are of interest for other reactions, this route allows one to prepare these useful materials, and simply mix them *in situ* to generate the metathesis product when it is desired.

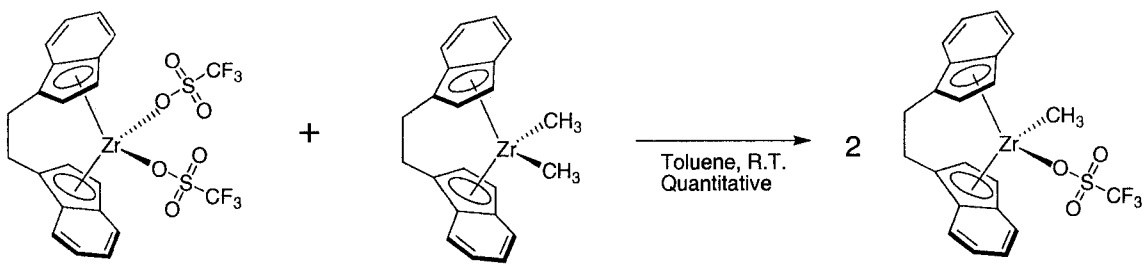

Scheme 29: Convenient synthesis of monomethyl intermediates

With both the di- and mono- triflate ansa metallocenes in hand, they were screened for reactivity in ligand substitution reactions to produce the corresponding enolates, and they functioned well in that regard. Treatment of the monomethyl compound with one equivalent of lithio isopropyl isobutyrate cleanly generates the desired target compound in high yield. The ditriflate forms the mono-substituted product fairly rapidly as well, but the second substitution is somewhat sluggish. Attempts to drive the equilibrium with excess enolate were frustrated by the difficulty in removing the residual excess from the product. Hence, the di-substituted product is only formed in modest yield. However, the fact that it is formed at all is significant in that previous workers have been unable to access these important model compounds. Single crystals have been grown, and the new compound characterized by x-ray crystallography[72]. The dienolate crystallizes in the monoclinic space group C2/*c* with C2 symmetry. The two *i*-Propyl *i*-Butyryl enolate ligands are symmetrically bonded to the distorted tetrahedral Zr center with a large Zr-O-C vector angle of $156.6(3)^0$ and a short Zr-O distance of 1.957(4) Å. These metric parameters are similar to known non-bridged zirconocene enolates.[73] The two isopropoxy ester groups are placed into the coordination sphere voids of the *rac*-ligand structure. Overall, the complex exhibits comprehensive steric shielding of the metal center.

The mono-methyl analog is prepared in sufficient purity to pass elemental analysis and appear pure via NMR; however, attempts to grow single crystals have not been successful. Hence both target compounds were produced, representing the first known chiral *ansa* metallocene mono- and di-enolates[74], allowing for more relevant model studies to be performed.

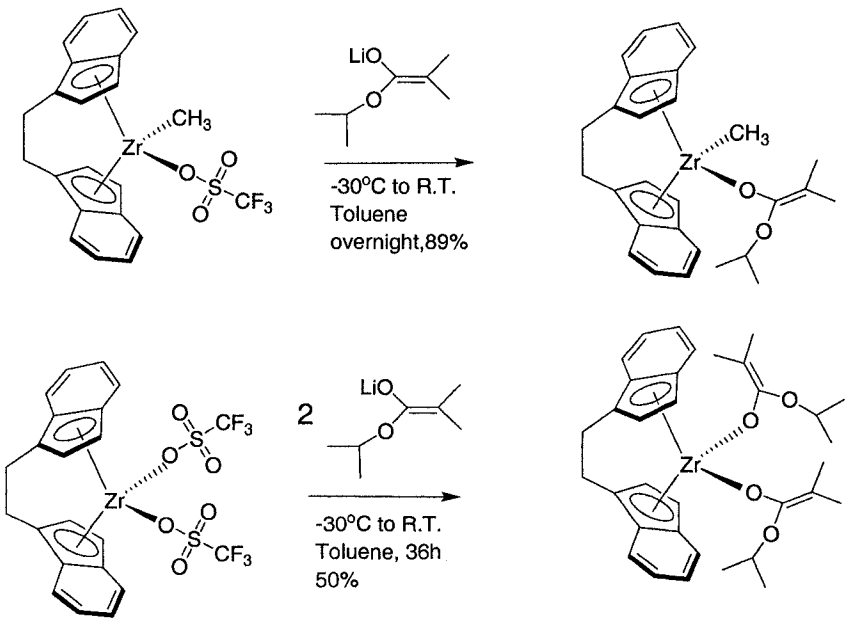

Scheme 30: Synthesis of ansa-metallocene mono-and di-enolates

Reactivity of the dienolate compound was first observed via NMR. Mixing with one equivalent $Al(C_6F_5)_3$ at room temperature led to virtually no change in the proton NMR spectrum of the reaction mixture versus that of the dienolate starting material. One minor species is present in addition to the unreacted starting material. Standing at room temperature for 24 hours did not lead to any noticeable change. In contrast, the fluorine NMR spectrum of the reaction was quite complex, indicating the presence of 4 different species. This is similar to the case observed when the Lewis acid is mixed directly with lithium enolates, which leads to speculation that the new species observed in the fluorine spectrum simply arise from the interaction of the Lewis acid with free lithium enolate contaminants, forming ill-defined oligomeric species. An alternate hypothesis is that, due to the great steric bulk around the Zr center, the abstractor is unable to interact directly with the carbonyl oxygen, but forms some small concentration of an adduct at the unsaturated α-carbon of the enolate. Trace quantities of this adduct might lead to abstraction; the enolate could then equilibrate between C-bound and O-bound forms,

giving rise to the many species observed in the fluorine spectrum. Given the high propensity of the alane for coordination to oxygen, this could explain the low level of abstraction apparently observed.

NMR-scale reactions of the monomethyl enolate proved far more interesting. Addition of C_6D_6 to a J-Young NMR tube containing the monomethyl enolate and the toluene adduct of $Al(C_6F_5)_3$ instantly generated a red solution, which rapidly faded to orange/yellow. This is commonly observed with the dimethyl derivative as well, and can be attributed to formation of the dicationic species (characteristically red), which then equilibrates rapidly with the dimethyl starting material to generate the monocationic zirconocenium aluminate. In this case, however, there are two possible forms of the monocation that can form; one arising from methide abstraction, and the other arising from enolate abstraction. The metal-methyl region of the proton NMR allows for the easiest diagnosis of chemical change, as the Zr-Me and bridging (abstracted) Al-Me peaks are known for the corresponding dimethyl derivative, and are distinct and well-resolved. The latter are broad, due to their bridging position, and further upfield, since the protons are more electron poor. The Zr-Me protons in the monomethyl enolate appear at -0.57 ppm in the neutral compound. Of course, the fluorine NMR is also helpful in providing a handle for observation of abstraction processes. ^1H Spectra run 15 minutes after mixing the reagents show two major methyl peaks, in a ratio of approximately 4:3, (~-0.7 and -0.6 ppm, respectively)and 3 minor peaks. Likewise, the fluorine spectrum shows two major sets of peaks corresponding to aluminates (no free alane is present), and three minor ones. After approximately 4 hours, the minor methyl peaks have decreased significantly in concentration, and the ratio of the two major peaks

present in the proton spectra has shifted to 4:1. At this point, the solution is yellow, with a faint green shade. Within 4.5 hours, the solution has changed to a very deep green shade, which persists for days in solution (this color was always observed in NMR experiments, but the product was yellow when a small-scale preparative reaction was performed; hence, the color may be concentration dependent, or due to some trace impurity). The fluorine spectrum shows one major product and trace quantities of other species, and this remains constant for >24 hours. After 13.5 hours, the minor peaks are negligible in concentration, and the ratio is approximately 20:3 by integration. After 14 hours, smaller methyl peak is nearly consumed, leaving relatively clean formation of one product in both the proton and fluorine spectra, which remain constant beyond 24 hours after mixing. The sharp resolution of this methyl peak indicates that it is attached to zirconium, as abstraction by the alane leads to a bridging intermediate which has a characteristic broad signal. Addition of a second equivalent of alane shifts the methyl peak downfield to ~-0.35 and broadens it substantially. This is consistent with formation of a dicationic species, analogous to that produced by the dimethyl zirconocene. The large shift in the methyl peak on addition of a second equivalent of Lewis acid, and its significant broadening both support the hypothesis that the major product (initially), is that arising from enolate abstraction by the alane. It is of course sterically less accessible, so methide abstraction is indeed observed, but eventually, through methide back-transfer mechanism, as has been shown for the dimethyl derivative, and enolate abstraction, the favored product is formed. The proposed equilibration implied by these NMR studies is shown in scheme 30.

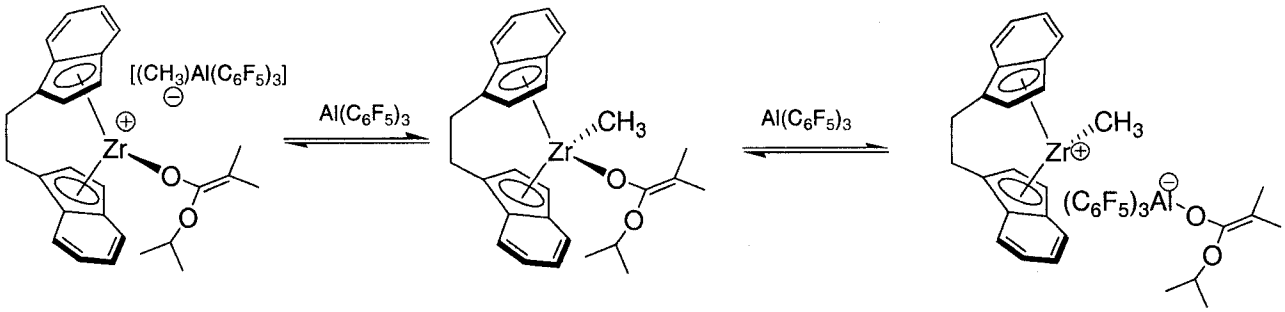

Scheme 30: Equilibration of monomethyl enolate metallocenes with $Al(C_6F_5)_3$

Presuming this interpretation is correct, it has significant implications for the production of multi(stereoblock)copolymers. The equilibration shown above involves enolate abstraction by the alane from the zirconium center, and subsequent back-transfer. The former process indicates that, in contrast to the unbridged variants, in the ansa metallocenes, the Lewis acid can directly abstract enolates from the transition metal center, allowing for isotactic blocks to directly transfer to syndiospecific sites. Even more surprising, the back transfer of the enolate moiety to the Zr cation suggests that syndiotactic chains can be transferred back to isospecific sites, providing a ready mechanism for formation of multiblock copolymers, as the growing enolate chains can apparently be transferred from site to site. The fact that the enolate abstraction product is thermodynamically more stable was expected, but does not preclude multiblock copolymers, because under polymerization conditions, there is rapid equilibration between the two abstraction products, allowing facile chain transfer. The stable product can be crystallized from toluene at -30°C in toluene or toluene/hexanes to yield clear yellow solid. Polymerization experiments, however, reveal that this material is not kinetically competent to be the active species.

Professor Chen was later able to isolate single crystals of this material and subject them to X-ray diffraction. The product is in fact a zirconocenium enolaluminate, but not the one proposed. The isolable species was conclusively identified as as a methyl

zirconocenium aluminate of *i*-butyrate. Elimination of propylene was observed via NMR, suggesting a pathway for the observed product, and a driving force for the reaction. Although it is unfortunate that the proposed intermediate has thus far eluded isolation, it must be noted that the isolated product almost certainly arises *from* the proposed intermediate (alternative mechanisms are difficult to propose). Hence, this result does not preclude the importance of the proposed ester enolaluminate under relevant polymerization conditions, which are far from equilibrium. It is well established that active catalytic species are seldom readily isolable, or stable.

Attempts to perform the analogous experiments with $B(C_6F_5)_3$ were frustrated by solubility issues. In deuterated benzene, the mixture turns red initially, as above, but an insoluble orange oil rapidly settles out of solution. The fluorine spectrum is complex, and no signal (other than solvent) is observed in the proton spectrum, as the product has precipitated out of solution. This is precedented in the dimethyl derivative; due to the weakly coordinating nature of the anion, the species is highly ionic, and hence not soluble in hydrocarbons. However, in the dimethyl case this can be remedied by switching to the more polar deuterated bromobenzene. This strategy was unsuccessful in this case. Hence it is clear that abstraction products are formed rapidly, generating ionic species that precipitate from solution. Given the lower oxophilicity of the borane, and the fast rate of this process, it seems likely that the product results from methide abstraction. If the product was that of enolate abstraction, it seems likely that the enolate functionality would bridge to the oxophilic zirconium center, generating a species with significantly less ionic character, which would thus be more soluble than the product that was observed. Professor Chen was later able to overcome this obstacle by utilizing deuterated

THF, which coordinates and stabilizes the intermediates, allowing isolation of cationic, chiral metallocenium ester enolates, elusive species that have long been proposed as propagating species.

Polymerization studies indicate that the enolate transfer demonstrated above can successfully be employed to produce multiblock copolymers. Hence, in a one-pot procedure, one equivalent of ansa-metallocene is mixed with one-half equivalent each of $B(C_6F_5)_3$ and $Al(C_6F_5)_3$ to generate both syndiospecific anions and isospecific cations in one hybrid catalyst system.

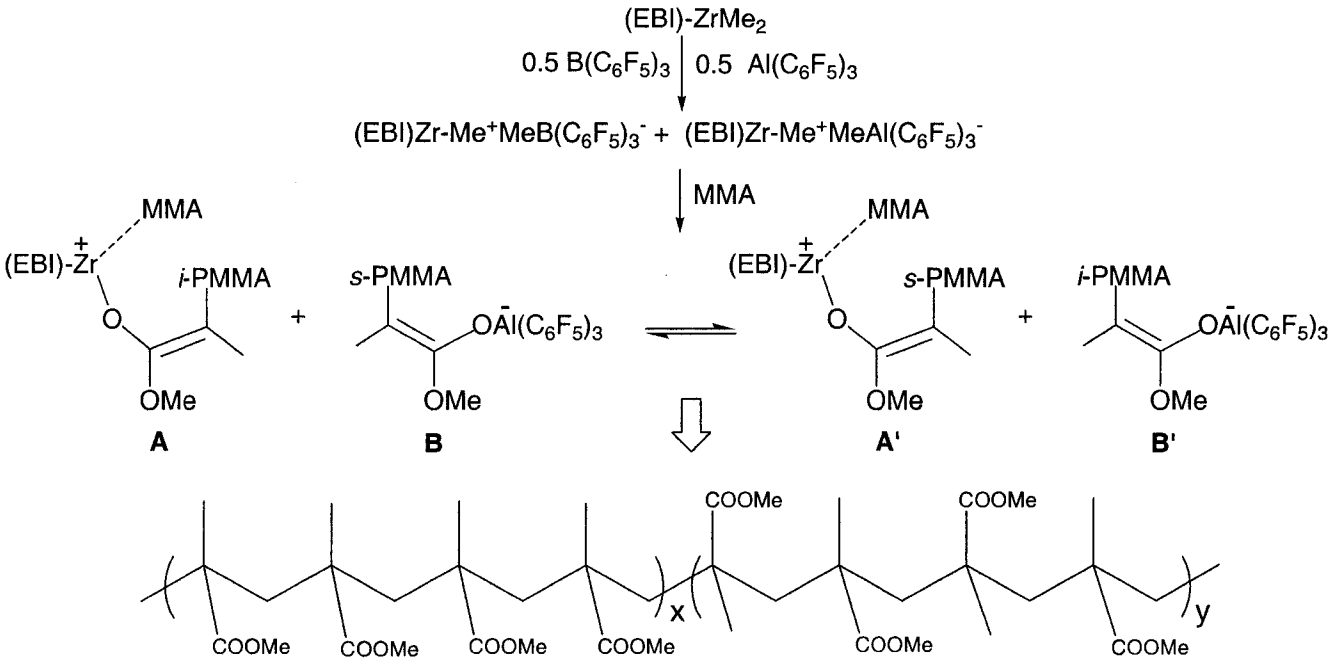

Scheme 31: Multi-stereoblock PMMA synthesis

PMMA produced under these conditions has a very narrow molecular weight distribution (PDI = 1.18). NMR studies of the tacticity show approximately 1:1 ratio of syndiotactic to isotactic triads (36.8% rr, 39.3% mm, 23.9% mr). The degree of mr triads is rather large; as mentioned in the connection with the diblock synthesis, these triads arise from chain transfer between the two different types of catalyst sites in copolymer synthesis, not

just from misinsertions. The ratio of syndiotactic to isotactic regions indicates that the rates of propagation for the cationic and anionic processes are nearly equal. The large percentage of mr triads indicates that chain transfer between sites is also very rapid, leading to production of rather short stereoblocks.

Further research by Chen[75] indicates that, as suggested above, block lengths are very short, and typically correspond to approximately 5 monomer units. As a result, glass transition temperatures for materials produced by this approach are very similar to that observed for atactic PMMA. Hence it appears that longer block lengths are required for the improved physical properties predicted for stereocomplexed stereoblock copolymers. Unfortunately, efforts to slow chain transfer by lowering the temperature result in predominantly s-PMMA (since the anionic process remains more active at low temperature), and dilution results primarily in i-PMMA (since the anionic process is bimetallic, so slows considerably when concentration is decreased).

XVI. Conclusions

Group IV metallocene precatalysts are conveniently activated with Lewis acids to generate species which polymerize the polar monomer, MMA. $B(C_6F_5)_3$ has been extensively employed in this regard, but these studies show that substitution of the more potent cocatalyst, $Al(C_6F_5)_3$ results in an anionic, bimetallic propagation involving enolaluminates. These species are relatively insensitive to cation, and thus allow access to the valuable syndiotactic form of PMMA, even in the absence of metallocenes. Given that metallocene cations are the active species when $B(C_6F_5)_3$ and metallocenes are

allowed to react, this suggested the possibility of generating stereoblock copolymers by exploiting both the reactivity of the conventional cationic metallocenium and enolaluminate anions. Initial attempts formed di-stereoblock copolymers by sequential formation of these two active species. More recent efforts indicate that both active species can be generated in situ, and that their rates of propagation are compatible, allowing production of stereoblock copolymers. The main challenge remaining in this area is to determine conditions which allow production of longer blocks before enolate chain switching occurs. Synthetic efforts at producing metallocene mono- and di-enolates for model compounds were successful when metallocene triflates were employed as intermediates, as opposed to the more conventional chlorides. Improved syntheses of these materials were developed. Useful model compounds, the ansa-zirconocene mono- and di-enolates are reported for the first time in this study. Model reactions using these species demonstrate the practicality of enolate chain transfer between the active cationic and anionic sites, providing support for the proposed mechanisms for production of di- and multi- stereoblock copolymers.

XVII. Experimental Section

Materials and Methods. All syntheses and manipulations of air- and moisture-sensitive materials were carried out in flamed Schlenk-type glassware on a dual-manifold Schlenk line or in an inert atmosphere (argon) glove box. NMR-scale reactions were conducted in

Teflon-valve-sealed sample J-Young tubes. Organic solvents were first saturated with nitrogen and then dried by passage through activated alumina and Q-5™ catalyst (Englehardt Chemicals Inc.) prior to use. Deuterated benzene and toluene were dried over sodium/potassium alloy and distilled and/or filtered prior to use. $CDCl_3$ was dried over activated Davison 4Å molecular sieves. Methyl methacrylate (MMA) monomer was degassed and dried over CaH_2 overnight, and then freshly vaccum-distilled before use. NMR spectra were recorded on either Varian Inova 300 (FT 300 MHz, ^1H; 75 MHz, ^{13}C; 282 MHz, ^{19}F) or Varian Inova 400 spectrometer. Chemical shifts for ^1H and ^{13}C spectra were referenced to internal solvent resonances and reported relative to tetramethylsilane. ^{19}F NMR spectra were referenced to external $CFCl_3$. In variable temperature NMR experiments, the probe temperature was calibrated using methanol (for $T < 20°C$) or ethylene glycol (for $T > 20°C$).

Tris(perfluorophenyl)borane $B(C_6F_5)_3$ was obtained as a research gift from Dow Chemical and Boulder Scientific Company and used without further purification for preparative reactions, or purified by recrystallization from hexane at -35°C for NMR-scale reactions. Trimethylaluminum (TMA) in toluene or hexanes, indene, MMA, *n*-BuLi in hexanes, *t*BuLi in heptane, MeMgBr in diethyl ether, methyl isobutyrate, diisopropylamine, Me_2SiCl_2, and $ZrCl_4$ were purchased from Aldrich Chemical Co. Tris(perfluorophenyl)alane ($Al(C_6F_5)_3$, as a toluene adduct) was prepared by exchange reaction between tris(perfluorophenyl)borane and trimethylaluminum as disclosed by Biagini, et al.[76] **Extra caution should be exercised when handling this material due to its thermal and shock sensitivity!**). *Rac*-dimethylsilane-bis(indenyl-1-yl)zirconium dichloride (SBI-$ZrCl_2$) was prepared according to literature procedures[77], and the

corresponding dimethyl complex was prepared from reaction of the dichloride with five equivalents of trimethyl aluminum in toluene at room temperature and purified by recrystallization from a mixture of toluene and hexane at -35°C. Cp_2ZrCl_2 was purchased from Strem and $Me_2C(Cp)(Flu)ZrCl_2$ was received from Boulder Scientific Company as a research gift. The corresponding dimethyl derivatives were prepared according to literature procedures[78]. *rac*-$Et(Ind)_2ZrCl_2$ was synthesized according to the literature procedure[79], and converted to the dimethyl derivative[80].

Preparation and characterization of *rac*-(SBI)$ZrMe^+MeM(C_6F_5)_3^-$ (M = B, Al) have been previously described in detail[81], and the analogous *rac*-(EBI)$ZrMe^+MeM(C_6F_5)_3^-$ was prepared in a similar manner. $Cp_2Zr(Me)Cl$ was prepared using a reported procedure[82]. Modified literature methods[83] were used to prepare *tert*-butyl isobutyrate and the lithium enolate of this ester (*tert*-butyl lithioisobutyrate). Other alkyl isobutyrates and the corresponding lithium enolates were synthesized in a similar manner. A general procedure of Collins[84] was followed to prepare methyl zirconocene alkylisobutyrates $Cp_2Zr(Me)O(OR)C{=}CMe_2$ (R = Me, Et, ^{i}Pr, *tert*-Bu).

***Rac*-(SBI)$ZrMe^+MeM(C_6F_5)_3^-$ (M = Al, 2; M = B, 1).** In situ generation of **2** was carried out in small vials in the glove box by mixing SBI-$ZrMe_2$ and $Al(C_6F_5)_3 \cdot 0.5$ toluene in a 1:1 ratio for 15 min at room temperature. The preparative isolation of **2** was carried out in the glove box by mixing SBI-$ZrMe_2$ (0.041 g, 0.10 mmol) and $Al(C_6F_5)_3 \cdot 0.5$ toluene (0.057 g, 0.1 mmol) in 5 mL of toluene and stirring at room temperature for 10 min. The solvent was removed under reduced pressure and the residue was washed

with 2 mL of cold hexane and dried in vacuo, affording quantitative yield of the clean product as an orange solid. ^{1}H NMR (C_6D_6, 23°C): δ 7.55 (d, J_{H-H} = 8.7 Hz, 1 H, Ind), 7.19 (d, J_{H-H} = 8.7 Hz, 1 H, Ind), 7.04 (m, 2 H, Ind), 6.93 (d, J_{H-H} = 8.7 Hz, 1 H, Ind), 6.75 (d, J_{H-H} = 8.7 Hz, 1 H, Ind), 6.65 (t, J_{H-H} = 7.5 Hz, 1 H, Ind), 6.53 (s br, 1 H, Ind), 6.44 (t, J_{H-H} = 7.5 Hz, 1 H, Ind), 6.36 (t, J_{H-H} = 7.5 Hz, 1 H, Ind), 5.61 (d, J_{H-H} = 3.2 Hz, 1 H, Ind), 5.06 (d, J_{H-H} = 3.2 Hz, 1 H, Ind), 0.36 (s, 3 H, $SiMe_2$), 0.26 (s, 3 H, $SiMe_2$), -0.71 (s, 3 H, Zr-Me), -0.96 (s br, 3 H, Al-μ-Me). ^{19}F NMR (C_6D_6, 23°C): δ -122.87 (d, $^3J_{F-F}$ = 15.3 Hz, 6 F, *o*-F), -153.93 (t, $^3J_{F-F}$ = 17.2 Hz, 3 F, *p*-F), -161.83 (t, $^3J_{F-F}$ = 18.3 Hz, 6 F, *m*-F). **1** was generated in the same manner as described in the above reaction but using $B(C_6F_5)_3$. ^{1}H NMR (C_6D_6, 23°C): δ 7.50 (d, J_{H-H} = 8.7 Hz, 1 H, Ind), 7.05 (m, 2 H, Ind), 6.90 (d, J_{H-H} = 8.7 Hz, 1 H, Ind), 6.72-6.58 (m, 4 H, Ind), 6.29 (m, 1 H, Ind), 6.21 (d, J_{H-H} = 3.2 Hz, 1 H, Ind), 5.67 (d, J_{H-H} = 3.2 Hz, 1 H, Ind), 4.99 (d, J_{H-H} = 3.2 Hz, 1 H, Ind), 0.36 (s, 3 H, $SiMe_2$), 0.22 (s, 3 H, $SiMe_2$), -0.45 (s br, 3 H, B-μ-Me), -0.51 (s, 3 H, Zr-Me). ^{19}F NMR (C_6D_6, 23°C): δ -133.55 (d, $^3J_{F-F}$ = 21.2 Hz, 6 F, *o*-F), -159.32 (t, $^3J_{F-F}$ = 21.4 Hz, 3 F, *p*-F), -164.45 (t, $^3J_{F-F}$ = 19.5 Hz, 6 F, *m*-F).

$Al(C_6F_5)_3$·MMA. ^{1}H NMR (C_6D_6, 23°C): δ 5.80 (s br), 4.92 (d) (2 H, CH_2=), 3.05 (s, 3 H, OCH_3), 1.22 (s, 3 H, CH_3). ^{19}F NMR (C_6D_6, 23°C): δ -123.38 (dd, 6 F, *o*-F), -151.60 (t, 3 F, *p*-F), -160.83 (tt, 6 F, *m*-F). ^{19}F NMR (C_7D_8, -40°C): δ -123.50 (d, 6 F, *o*-F), -151.04 (t, 3 F, *p*-F), -160.45 (t, 6 F, *m*-F).

$B(C_6F_5)_3$·MMA. ^{1}H NMR (C_6D_6, 23°C): δ 5.99 (s br), 5.09 (d) (2 H, CH_2=), 3.30 (s, 3 H, OCH_3), 1.70 (s, 3 H, CH_3). ^{19}F NMR (C_6D_6, 23°C): δ -129.39 (s br, 6 F, *o*-F), -142.94 (s br, 3 F, *p*-F), -160.32 (br s, 6 F, *m*-F).

[(SBI)ZrMe(MMA)]$^+$[MeAl(C$_6$F$_5$)$_3$]$^-$. ^{1}H NMR (C$_7$D$_8$, -40°C): δ 6.11 (s br), 5.11 (s br) (2 H, CH$_2$=), 3.27 (s, 3 H, OCH$_3$), 1.77 (s, 3 H, CH$_3$), 0.55, 0.41 (s, 6 H, SiMe$_2$), -0.72 (s br, 3 H, Zr-Me), -0.82 (s br, 3 H, Al-Me). Peaks for indenyl moieties are similar to those in **2** and not listed here. ^{19}F NMR (C$_7$D$_8$, -40°C): δ -121.22 (s br, 6 F, *o*-F), -158.11 (t, 3 F, *p*-F), -163.39 (t, 6 F, *m*-F).

Free Aluminate Anion MeAl(C$_6$F$_5$)$_3^-$. ^{19}F NMR (C$_6$D$_6$, 23°C): δ -121.16 (d, 6 F, *o*-F), -158.91 (t, 3 F, *p*-F), -163.92 (t, 6 F, *m*-F). **Free Borate Anion MeB(C$_6$F$_5$)$_3^-$.** ^{19}F NMR (C$_6$D$_6$, 23°C): δ -131.99 (d, 6 F, *o*-F), -164.36 (t, 3 F, *p*-F), -166.91 (t, 6 F, *m*-F). ^{19}F NMR (C$_7$D$_8$, -40°C): δ -132.15 (d, 6 F, *o*-F), -163.89 (s br, 3 F, *p*-F), -166.56 (s br, 6 F, *m*-F).

Chiral zirconocenium cations paired with both the methyl borate and methyl aluminate anions, *rac*-(EBI)ZrMe$^+$ [MeB(C$_6$F$_5$)$_3^-$]$_{0.5}$ [MeAl(C$_6$F$_5$)$_3^-$]$_{0.5}$ and *rac*-(SBI)ZrMe$^+$ [MeB(C$_6$F$_5$)$_3^-$]$_{0.5}$ [MeAl(C$_6$F$_5$)$_3^-$]$_{0.5}$ were cleanly generated from reactions of the corresponding dimethyl zirconocenes (*rac*-(EBI)ZrMe$_2$ and *rac*-(SBI)ZrMe$_2$) with a 1:1 mixture of Lewis acids M(C$_6$F$_5$)$_3$ (M = B, Al; Zr/B/Al = 1: 0.5: 0.5). NMR spectra are simply a sum of two individual ion pairs (i.e., *rac*-(EBI)ZrMe$^+$MeM(C$_6$F$_5$)$_3^-$ or *rac*-(SBI)ZrMe$^+$ MeM(C$_6$F$_5$)$_3^-$).

For spectroscopic data of **Al(C$_6$F$_5$)$_3$·THF**, see Belgardt, T.; Storre, J.; Roesky, H. W.; Noltemeyer, M.; Schmidt, H.-G. *Inorg. Chem.* **1995**, *34*, 3821-3822. We independently isolated the adduct Al(C$_6$F$_5$)$_3$·THF and found the chemical shifts are slightly different from the reported values. ^{1}H NMR (C$_6$D$_6$, 23°C): δ 3.43 (m, 4H), 1.05 (m, 4H). ^{19}F NMR

(C_6D_6, 23°C): δ -123.13 (d, 6F, *o*-F), -151.23 (t, 3F, *p*-F), -160.81 (tt, 6F, *m*-F). ^{19}F NMR (THF-d_8, 23°C): δ -119.84 (d, 6F, *o*-F), -151.14 (t, 3 F, *p*-F), -159.71 (tt, 6F, *m*-F).

Polymerization Procedures and Polymer Characterizations.

Homopolymerizations

MMA polymerizations were performed in 50 mL Schlenk tubes with a septum and an external temperature-controlled bath on a Schlenk line or a glove box. In a typical procedure, **1** (46.7 μmol), isolated or generated in situ by mixing 1:1 molar ratio of *rac*-(SBI)-$ZrMe_2$ and $B(C_6F_5)_3$ in toluene for 10 min at room temperature, was loaded into the tube in a glove box and toluene was added (10 mL total volume). The tube was removed from the box and put on the Schlenk line. MMA (1.00 mL, 0.936 g, 9.35 mmol) was added through the septum via syringe. A typical color change observed during the polymerization using **1** was from orange (before adding MMA, the toluene solution of **1**) to cloudily yellow (immediately after addition of MMA, formation of less soluble MMA-separated ion pair) to orange (after further stirring, formation of cationic zirconocene enolates). On the other hand, the color change observed during the polymerization using **2** was different, which was from orange yellow (before adding MMA, the toluene solution of **2**) to cloudy yellow (immediately after addition of MMA, formation of less soluble MMA-separated ion pair) to yellow (solution, after further stirring for formation of anionic aluminum enolates). Heat was involved in both types of polymerizations. The polymerization reaction was stirred for 2 h (for 23°C runs) or 4 h (for 0°C runs) and quenched by adding 2 mL of acidified methanol. The polymer product was precipitated

into 50 mL methanol, filtered, washed with methanol, and dried in vacuo at 40°C to a constant weight.

Di-stereoblock copolymers

In a typical stereoblock polymerization procedure, *rac*-(SBI)ZrMe$^+$ MeB$(C_6F_5)_3^-$ (23.35 μmol), isolated or generated in situ by mixing 1:1 molar ratio of *rac*-(SBI)$ZrMe_2$ and $B(C_6F_5)_3$ in toluene for 10 min at room temperature, was loaded into the tube in the glove box and toluene was added (10 mL total volume). The tube was removed out of the box and attached onto the high vacuum line. After the external bath temperature was stabilized to 23 °C, MMA (0.50 mL, 4.67 mmol) was quickly injected through the septum via gas-tight syringe. The solution mixture gradually turned to be more viscous and color changed from orange yellow to orange red. After stirring for 45 min, a solution of *rac*-(SBI)ZrMe$^+$MeAl$(C_6F_5)_3^-$ (23.35 μmol), isolated or generated in situ by mixing 1:1 molar ratio of *rac*-(SBI)$ZrMe_2$ and $Al(C_6F_5)_3$ in 2 mL toluene in the glove box, was injected via gas-tight syringe. The mixture was stirred at this temperature for additional 10 min during which time the color changed to yellow. This clear yellow solution was then cooled down to –78 °C and the second portion of MMA (0.50 mL, 4.67 mmol) mixed with $Al(C_6F_5)_3$ (0.093 mmol) was quickly injected via gas-tight syringe. The reaction mixture was stirred for additional 1 h and quenched by adding 2 mL of acidified methanol. The polymer product was precipitated into 50 mL methanol, filtered, washed with methanol, and dried in a vacuum oven at 50 °C overnight to a constant weight.

Multi-stereoblock copolymers

All ion pairs were generated in situ for polymerization studies. In a typical procedure, a metallocene complex (or a complex mixture in a desired ratio) and an activator M(C6F5)3 (M = B, Al) (or a 1:1 activator mixture) in a 1:1 complex/activator ratio were loaded into the flask in a glovebox. Toluene was added (10 mL total volume) and the mixture was stirred for 10 min. For polymerizations carried out on the Schlenk line, the flask was then removed from the box and put on the Schlenk line. After a desired temperature was reached, MMA (1.00 mL, 9.35 mmol) was quickly added through the septum via a gastight syringe. The polymerization was quenched by adding 2 mL of acidified methanol after the measured time interval. The polymer product was precipitated into 50 mL methanol, filtered, washed with methanol, and dried in a vacuum oven at 50 °C overnight to a constant weight.

Polymer Characterization

Glass transition temperatures of polymers were measured by differential scanning calorimetry (DSC 2920, TA Instruments, Inc.). Samples were first heated from room temperature to 180 °C. After being held at this temperature for 4 min, the samples were cooled to –20 °C at 10/min and were then heated to 160°C at 10/min after being held at –20°C for 4 min. Gel permeation chromatography (GPC) analyses of polymer samples were carried out at room temperature using THF as elutant on a Waters 150CV instrument and calibrated using mono-dispersed PMMA standards at a flow rate of 1.0 mL/min. Number-average molecular weights and polydispersities of PMMA were given relative to PMMA standards. ^{1}H and ^{13}C spectra for the analysis of PMMA

microstructures were recorded in $CDCl_3$ and analyzed according to the literature (Bovey, F. A.; Mirau, P. A. *NMR of Polymers*; Academic Press: San Diego, 1996).

XVIII. References

[1] a)Ziegler, K.; Holzkamp, E.; Breil, H.; Martin, H. *Angew. Chem.*, **1955,** *67,* 541.
b) For recent reviews, see: Wilke, G. *Angew. Chem. Int. Ed.*, **2003**, *42*, 5000-5008
Bohm, L. L. *Angew. Chem. Int. Ed.*, **2003**, *42*, 5010-5030
[2]Stevens, M.P., "Polymer Chemistry," 3rd edition, Oxford Press: New York, 1999; pp. 234-244.
[3] Odian, G., "Principles of Polymerization," 3rd edition; Wiley: New York, 1991; p. 632.
[4] Natta, G.; Pino, P.; Corradini, P.; Danusso, F.; Mantica, E.; Mazzanti, G.; Moraglio, G. *J. Am. Chem. Soc.*, **1955**, *77*, 1708-1710.
[5] Odian, G., "Principles of Polymerization," 3rd edition; Wiley: New York, 1991; pp. 29-33
[6] Stevens, M.P., "Polymer Chemistry," 3rd edition, Oxford Press: New York, 1999; pp. 78-79
[7] Natta, G.; Pino, P.; Mazzanti, G.; Giannini, U. *J. Am. Chem. Soc.*, **1957**, *79,* 2975-6.
[8] Breslow, D.S.; Newburg, N.R. *J. Am. Chem. Soc.*, **1957**, *79,* 5072-3.
[9] Sinn, H.; Kaminsky, W.; Vollmer, H.-J.; Woldt, R. *Angew. Chem. Int. Ed.*, **1980**, *19*, 390-392.
[10] Harlan, C.J.; Bott, S.G.; Barron, A.R. *J. Am. Chem. Soc.*, **1995,** *117*, 6465-6474.
[11] Sishta, C.; Hathorn, R.M.; Marks, T.J. *J. Am. Chem. Soc.*, **1992**, *114*, 1112-4.
[12] Yang, X.; Stern, C.L.; Marks, T.J. *J. Am. Chem. Soc.*, **1991**, *113*, 3623-5.
[13] Massey, A.G.; Park, A.J. *J. Organomet. Chem.*, **1964**, *2*, 245-50.
[14] For recent reviews, see: (a) Chum, P. S.; Kruper, W. J.; Guest, M. J. *Adv. Mater.* **2000**, *12*, 1759-1767. (b) Gladysz, J. A.; Ed. *Chem. Rev.* **2000**, *100*, 1167-1682. (c) Marks, T. J.; Stevens, J. C.; Eds. *Top. Catal.* **1999**, *7*, 1-208. (d) Britovsek, G. J. P.; Gibson, V. C.; Wass, D. F. *Angew. Chem., Int. Ed. Engl.* **1999**, *38*, 428-447. (e) Jordan, R. F. Ed. *J. Mol. Catal.* **1998**, *128*, 1-337. (f) McKnight, A. L.; Waymouth, R. M. *Chem. Rev.* **1998**, *98*, 2587-2598. (g) Piers, W. E. *Chem. Eur. J.* **1998**, *4*, 13-18. (h) Kaminsky, W.; Arndt, M. *Adv. Polym. Sci.* **1997**, *127*, 144-187. (i) Bochmann, M. *J. Chem. Soc., Dalton Trans.* **1996**, 255-270. (j) Brintzinger, H.-H.; Fischer, D.; Mülhaupt, R.; Rieger, B.; Waymouth, R. M. *Angew. Chem., Int. Ed. Engl.* **1995**, *34*, 1143-1170.
[15] Stevens, M.P., "Polymer Chemistry," 3rd edition, Oxford Press: New York, 1999; pp. 247-8.
[16] For a comprehensive review of activation processes, see: Chen, E. Y.-X.; Marks, T.J. *Chem. Rev.*, **2000**, *100*, 1391-1434.
[17] Lin, Z.; Le Marechal, J.-F.; Sabat, M.; Marks, T.J. *J. Am. Chem. Soc.*, **1987**, *109*, 4127-9.
[18] Hlatky, G.G.; Upton, D.J.; Turner, H.W. PCT Int. Appl. WO 91/09882 1991.
[19] Chien, J.C.W.; Tsai, W.-M.; Rausch, M.D. *J. Am. Chem. Soc.*, **1991**, *113*, 8570-1.
[20] Kaminsky, W.; Kulper, K.; Brintzinger, H.H.; Wild, W.P. *Angew. Chem. Int. Ed. Engl.*, **1985**, *24*, 507.
[21] Herrmann, W.A.; Rohrmann, J.; Herdtweck, E.; Spaleck, W.; Winter, A. *Angew. Chem. Int. Ed. Engl.*, **1989**, *28*, 1511-2.
[22] Chen, E. Y.-X.; Marks, T.J. *Chem. Rev.*, **2000**, *100*, 1391-1434.
[23] Chen, Y.-X.; Yang, S.; Stern, C.L.; Marks, T.J. *J. Am. Chem. Soc.*, **1996**, *118*, 12451-2.
[24] Li, L.; Marks, T.J. *Organometallics*, **1998**, *17*, 3996-4003
[25] Chen, Y.-X.; Metz, M.V.; Li, L.; Stern, C.L.; Marks, T.J. *J. Am. Chem. Soc.*, **1998**, *120*, 6287-6305.
[26] Elschenbroich, C.; Salzer, A. "Organometallics: A Concise Introduction," 2nd edition; VCH: Weinheim, 1992; pp. 84-86.
[27] Siedle, A.R.; Newmark, R.A.; Lamanna, W.M.; Schroepfer, J.N. *Polyhedron,* **1990**, *9,* 301-8.
[28] Bochmann, M.; Sarsfield, M.J. *Organometallics,* **1998**, *17*, 5908-5912.
[29] Pohlmann, J.L.; Brinckman, F.E. *Z. Naturforsch. B.: Anorg. Chem. Org. Chem.* **1965**, *20B*, 5-11.
[30] Belgardt, T.; Storre, J.; Roesky, H.W.; Noltemeyer, M.; Schmidt, H.-G. *Inorg. Chem.*, **1995**, *34*, 3821-2.

[31] Biagini, P.; Lugli, G.; Abis, L.; Andreussi, P. U.S. Pat. 5.602,269, 1997 (Enichem)
[32] Hair, G.S.; Cowley, A. H.; Jones, R.A.; Mcurnett, B.G.; Voigt, A. *J. Am. Chem. Soc.* **1999**, *121*, 4922-3.
[33] Olah, G.A.; Lin, H.C.; Mo, Y.K. *J. Am. Chem. Soc.* **1972**, *94*, 3667.
[34] Rathore, R.; Hecht, J.; Kochi, J. *J. Am. Chem. Soc.*, **1998**, *120*, 13278-13279.
[35] Chakraborty, D.; Chen, E.Y.-X. *Macromolecules*, **2002**, *35*, 13-15.
[36] Chakrabory, D.; Chen, E.Y.-X. *Inorg. Chem. Commun.*, **2002**, *15*, 698-701.
[37] Lee, C.H.; Lee, S.J.; Park, J.W.; Kin, K.H.; Lee, B.Y.; Oh, J.S. *J. Mol. Catal. A:Chem,* **1998**, *132*, 231-239.
[38] This is established by comparing $\Delta\square$ ($\square_{adduct}$ - $\square_{MMA}$) for CH_3O and CH_3 groups of the following adducts: $B(C_6F_5)_3$•MMA (-0.04, -0.09), (SBI)$ZrMe^+$•MMA (-0.13, -0.02), $Al(C_6F_5)_3$•MMA (-0.29, -0.57), suggesting the highest degree of activation by the alane in this series.
[39] Chen, E.Y.-X.; Kruper, W.J.; Roof, G.; Wilson, D.R. *J. Am. Chem. Soc.*, **2001**, *123*, 745-746.
[40] Benedek, I.; Simionescu, C.; Asandei, N.; Ungurenasu, C. *Eur. Polym. J.* **1969**, *5,* 449.
[41] Yasuda, H.; Yamamoto, H.; Yokota, K.; Miyake, S.; Nakamura, A. *J. Am. Chem. Soc.*, **1992**, *114*, 4908-4910.
[42] Collins, S.; Ward, D.G. *J. Am. Chem. Soc.*, **1992**, *114*, 5460-5462.
[43] Collins, S.; Ward, D. G.; Suddaby, K.H. *Macromolecules*, **1994**, *27*, 7222-7224.
[44] a) Sogah, D. Y.; Hertler, W. R.; Webster, O. W.; Cohen, G. M. *Macromolecules* **1987**, *20*, 1473-1488.
b) Webster, O. W.; Hertler, W. R.; Sogah, D. Y.; Farnham, W. B.; RajanBabu, T. V. *J. Am. Chem. Soc.* **1983**, *105*, 5706-5708.
[45] Bovey, F.A.; Tiers, G.V.D. *J. Polym. Sci.* **1960,** *44,* 173-182.
[46] Fox, T.G.; Garrett, B.S.; Goode, W.E.; Gratch, S.; Kincaid, J.F. Spell, A.; Stroupe, J.D. *J. Am. Chem. Soc.*, **1958**, *80*, 1768.
[47] Liquori, A.M.; Anzuino, G.; Coiro, V.M.; D'Alagni, De Santis, P.; Savino, M. *Nature,* **1965,** *206*, 358-362.
[48] Yang, X.; Stern, C.L.; Marks, T.J. *J. Am. Chem. Soc.*, **1994**, *116*, 10015-10031.
[49] Soga, K.; Deng, H.; Yano, T.; Shiono, T. *Macromolecules,* **1994**, *27*, 7938-7940.
[50] Cameron, P.A.; Gibson, V.C.; Graham, A.J. *Macromolecules*, **2000**, *33*, 4329-4335.
[51] Chen, Y.-X.; Metz, M.V.; Li, L.; Stern, C.L.; Marks, T.J. *J. Am. Chem. Soc.,* **1998**, *120*, 6287-6305.
[52] a) Ewen, J.A. *J. Am. Chem. Soc.*, **1984**, *106*, 6355-6364.
b) Ewen, J.A. *J. Mol. Catal. A: Chem.,* **1998**, *128*, 103-109.
[53] Cameron, P.A.; Gibson, V.C.; Graham, A.J. *Macromolecules*, **2000**, *33*, 4329-4335.
[54] Elschenbroich, C.; Salzer, A. "Organometallics: A Concise Introduction," 2nd edition; VCH: Weinheim, 1992; p. 20.
[55] Bovey, F.A.; Tiers, G.V.D. *J. Polym. Sci.* **1960,** *44,* 173-182.
[56] Spaether, W.; Klass, K.; Erker, G.; Zippel, F.; Frohlich, R. *Chem. Eur. J.*, **1998**, *4*, 1411-1417.
[57] Bolig, A.D.; Chen, E.Y.-X. *J. Am. Chem. Soc.*, **2001**, *123*, 7943-7944.
[58] Kuroki, M.; Aida, T.; Inoue, S. *J. Am. Chem. Soc.*, **1987**, *109*, 4737-4738.
[59] Cameron, P.A.; Gibson, V.C.; Irvine, D.J. *Angew. Chem. Int. Ed.* **2000**, *39*, 2141-2141.
[60] Engler, U.; Stuhldreier, T.; Keul, H.; Hocker, H. *Organometallics*, **2000**, *19,* 5231-5234.
[61] Webster, O.W. *Science,* **1991**, *251*, 887-893.
[62] Bolig, A.D.; Chen, E.Y.-X. *J. Am. Chem. Soc.*, **2002**, *124*, 5612-5613.
[63] Sweeney, Z.K.; Salsman, J.L.; Andersen, R.A.; Bergman, R.G. *Angew. Chem. Int. Ed.* **2000**, *39*, 2339-2343.
[64] Noyce, D.S.; Virgilio, J.A. *J. Org. Chem.,* **1972**, *37*, 2643-2647.
[65] Jaquith, J.B.; Guan, J.; Wang, S.; Collins, S. *Organometallics*, **1995**, *14*, 1079-1081.
[66] Nguyen, H.; Jarvis, A.P.; Lesley, M.J.G.; Kelly, N.J.; Collins, S. *Macromolecules*, **2000**, *33*, 1508-1510.
[67] Diamond, G.M.; Jordan, R.F.; Petersen, J.L. *J. Am .Chem. Soc.*, **1996**, *118*, 8024-8033.
[68] Diamond, G.M.; Jordan, R.F.; Petersen, J.L. *J. Am .Chem. Soc.*, **1996**, *118*, 8024-8033.
[69] Jaquith, J.B.; Guan, J.; Wang, S.; Collins, S. *Organometallics*, **1995**, *14*, 1079-1081.
[70] Grossman, R.B.; Davis, W.M.; Buchwald, S.L. *J. Am. Chem. Soc.,* **1991**, *113*, 2321-2322.
[71] Luinstra, G.A. *J. Organomet. Chem.,* **1996**, *517*, 209-215.

[72] See appendix for full crystallographic data tables.

[73] a) Stuhldreier, T.; Keul, H.; Hocker, H.; Englert, U. *Organometallics*, **2000**, *19*, 5231-5234
b) Gambarotta, S.; Strologo, S.; Floriani, C.; Chiesi-Villa, A.; Guastini, C. *Inorg. Chem.* **1985**, *24*, 654-660.

[74] Bolig, A.D.; Chen, E.Y.-X. *J. Am. Chem. Soc.*, **2004**, *126*, 4897-4906.

[75] Chen, E.Y.-X.; Cooney, M.J. *J. Am. Chem. Soc.*, **2003**, *125*, 7150-7151.

[76] Biagini, P.; Lugli, G.; Abis, L.; Andreussi, P. U.S. Pat. 5,602269, 1997.

[77] a) Herrmann, W. A.; Rohrmann, J.; Herdtweck, E.; Spaleck, W.; Winter, A. *Angew. Chem., Int. Ed. Engl.* **1989**, *28*, 1511-1512
b) Christopher, J. N.; Diamond, G. M.; Jordan, R. F.; Petersen, J. L. *Organometallics* **1996**, *15*, 4038-4044.

[78] a) Samuel, E.; Rausch, M. D. *J. Am. Chem. Soc.* **1973**, *95*, 6263-6267.
b) Razavi, A.; Thewalt, U. *J. Organomet. Chem.* **1993**, *445*, 111-114.

[79] Collins, S.; Kuntz, B.A.; Taylor, N.J.; Ward, D.G. *J. Organometallic Chem.*, **1988**, *342*, 21-29.

[80] Bochmann, M.; Lancaster, S. J. *Organometallics* **1993**, *12*, 633-640.

[81] Chen, E. Y.-X.; Kruper, W. J.; Roof, G.; Wilson, D. R. *J. Am. Chem. Soc.* **2001**, *123*, 745-746.

[82] Wailes, P. C.; Weigold, H.; Bell, A. P. *J. Organomet. Chem.* **1971**, *33*, 181-189.

[83] Kim, Y.-J.; Bernstein, M. P.; Galiano Roth, A. S.; Romesberg, F. E.; Williard, P. G.; Fuller, D. J.; Harrison, A. T.; Collum, D. B. *J. Org. Chem.* **1991**, *56*, 4435-4439.

[84] Li, Y.; Ward, D. G.; Reddy, S. S.; Collins, S. *Macromolecules* **1997**, *30*, 1875-1883.

XIX. Appendix A

Crystallographic Data

Table 1. Crystal data and structure refinement for ec17.

Identification code	ec17 (A. Bolig)	
Empirical formula	C34 H42 O4 Zr	
Formula weight	605.90	
Temperature	173(2) K	
Wavelength	0.71073 Å	
Crystal system	Monoclinic	
Space group	C2/c	
Unit cell dimensions	a = 21.52(2) Å	α= 90°.
	b = 11.188(11) Å	β= 98.308(17)°.
	c = 13.016(12) Å	γ = 90°.
Volume	3101(5) $Å^3$	
Z	4	
Density (calculated)	1.298 Mg/m^3	
Absorption coefficient	0.389 mm^{-1}	
F(000)	1272	
Crystal size	0.40 x 0.30 x 0.30 mm^3	
Theta range for data collection	1.91 to 23.38°.	
Index ranges	-24<=h<=23, -12<=k<=12, -14<=l<=14	
Reflections collected	9255	
Independent reflections	2259 [R(int) = 0.1084]	
Completeness to theta = 23.38°	99.6 %	
Absorption correction	SADABS	
Refinement method	Full-matrix least-squares on F^2	
Data / restraints / parameters	2259 / 0 / 178	
Goodness-of-fit on F^2	1.133	
Final R indices [I>2sigma(I)]	R1 = 0.0721, wR2 = 0.1659	
R indices (all data)	R1 = 0.0857, wR2 = 0.1741	
Extinction coefficient	0.0001(4)	
Largest diff. peak and hole	0.955 and -1.016 $e.Å^{-3}$	

Table 2. Atomic coordinates (x 10^4) and equivalent isotropic displacement parameters ($Å^2$x 10^3) for ec17. U(eq) is defined as one third of the trace of the orthogonalized U^{ij} tensor.

	x	y	z	U(eq)
Zr(1)	5000	2090(1)	2500	38(1)
O(1)	5691(2)	3244(4)	2692(3)	57(1)
O(2)	6367(2)	4135(4)	1762(3)	67(1)
C(1)	5233(3)	1991(5)	653(4)	56(2)
C(2)	5505(4)	987(6)	1177(4)	62(2)
C(3)	5036(4)	220(5)	1425(4)	63(2)
C(4)	5137(5)	-953(5)	1996(5)	83(3)
C(5)	5564(4)	739(6)	3973(4)	61(2)
C(6)	6183(5)	365(8)	3976(6)	85(3)
C(7)	6640(5)	1057(10)	4472(7)	100(3)
C(8)	6523(4)	2135(9)	4961(7)	97(3)
C(9)	5939(4)	2544(7)	4970(5)	72(2)
C(10)	5429(4)	1837(5)	4482(5)	58(2)
C(11)	6001(3)	4262(5)	2527(4)	46(1)
C(12)	5948(3)	5250(5)	3039(5)	53(2)
C(13)	6314(5)	6355(7)	2816(7)	100(3)
C(14)	5506(3)	5402(6)	3794(5)	70(2)
C(15)	6869(3)	3290(9)	1967(6)	85(3)
C(16)	7404(4)	3854(12)	2705(7)	133(4)
C(17)	7061(5)	2963(13)	941(8)	156(6)

Table 3. Bond lengths [Å] and angles [°] for ec17.

Zr(1)-O(1)	1.957(4)
Zr(1)-O(1)#1	1.957(4)
Zr(1)-C(2)	2.493(6)
Zr(1)-C(2)#1	2.493(6)
Zr(1)-C(3)	2.524(6)
Zr(1)-C(3)#1	2.524(6)
Zr(1)-C(1)#1	2.528(6)
Zr(1)-C(1)	2.528(6)
Zr(1)-C(5)#1	2.600(6)
Zr(1)-C(5)	2.600(6)
Zr(1)-C(10)	2.627(6)
Zr(1)-C(10)#1	2.627(6)
O(1)-C(11)	1.352(7)
O(2)-C(11)	1.363(7)
O(2)-C(15)	1.432(8)
C(1)-C(2)	1.398(9)
C(1)-C(10)#1	1.422(10)
C(2)-C(3)	1.398(10)
C(3)-C(5)#1	1.441(10)
C(3)-C(4)	1.508(9)
C(4)-C(4)#1	1.514(14)
C(5)-C(6)	1.397(11)
C(5)-C(3)#1	1.441(10)
C(5)-C(10)	1.444(9)
C(6)-C(7)	1.342(13)
C(7)-C(8)	1.403(13)
C(8)-C(9)	1.341(11)
C(9)-C(10)	1.424(10)
C(10)-C(1)#1	1.422(10)
C(11)-C(12)	1.305(8)
C(12)-C(14)	1.472(10)
C(12)-C(13)	1.517(9)
C(15)-C(17)	1.499(11)
C(15)-C(16)	1.525(12)

O(1)-Zr(1)-O(1)#1	97.4(3)
O(1)-Zr(1)-C(2)	90.9(2)
O(1)#1-Zr(1)-C(2)	129.6(2)
O(1)-Zr(1)-C(2)#1	129.6(2)
O(1)#1-Zr(1)-C(2)#1	90.9(2)
C(2)-Zr(1)-C(2)#1	120.6(3)
O(1)-Zr(1)-C(3)	122.3(2)
O(1)#1-Zr(1)-C(3)	124.0(2)
C(2)-Zr(1)-C(3)	32.3(2)
C(2)#1-Zr(1)-C(3)	91.4(2)
O(1)-Zr(1)-C(3)#1	124.0(2)
O(1)#1-Zr(1)-C(3)#1	122.3(2)
C(2)-Zr(1)-C(3)#1	91.4(2)
C(2)#1-Zr(1)-C(3)#1	32.3(2)
C(3)-Zr(1)-C(3)#1	68.0(3)
O(1)-Zr(1)-C(1)#1	99.14(19)
O(1)#1-Zr(1)-C(1)#1	84.20(19)
C(2)-Zr(1)-C(1)#1	143.3(2)
C(2)#1-Zr(1)-C(1)#1	32.32(19)
C(3)-Zr(1)-C(1)#1	121.1(2)
C(3)#1-Zr(1)-C(1)#1	53.9(2)
O(1)-Zr(1)-C(1)	84.20(19)
O(1)#1-Zr(1)-C(1)	99.14(19)
C(2)-Zr(1)-C(1)	32.32(19)
C(2)#1-Zr(1)-C(1)	143.3(2)
C(3)-Zr(1)-C(1)	53.9(2)
C(3)#1-Zr(1)-C(1)	121.1(2)
C(1)#1-Zr(1)-C(1)	175.0(3)
O(1)-Zr(1)-C(5)#1	137.93(19)
O(1)#1-Zr(1)-C(5)#1	91.4(2)
C(2)-Zr(1)-C(5)#1	53.6(3)
C(2)#1-Zr(1)-C(5)#1	91.1(2)
C(3)-Zr(1)-C(5)#1	32.6(2)
C(3)#1-Zr(1)-C(5)#1	83.0(2)
C(1)#1-Zr(1)-C(5)#1	122.7(2)

C(1)-Zr(1)-C(5)#1	53.8(2)
O(1)-Zr(1)-C(5)	91.4(2)
O(1)#1-Zr(1)-C(5)	137.93(19)
C(2)-Zr(1)-C(5)	91.1(2)
C(2)#1-Zr(1)-C(5)	53.6(3)
C(3)-Zr(1)-C(5)	83.0(2)
C(3)#1-Zr(1)-C(5)	32.6(2)
C(1)#1-Zr(1)-C(5)	53.8(2)
C(1)-Zr(1)-C(5)	122.7(2)
C(5)#1-Zr(1)-C(5)	108.9(3)
O(1)-Zr(1)-C(10)	78.03(19)
O(1)#1-Zr(1)-C(10)	110.45(19)
C(2)-Zr(1)-C(10)	119.9(2)
C(2)#1-Zr(1)-C(10)	52.7(2)
C(3)-Zr(1)-C(10)	114.9(2)
C(3)#1-Zr(1)-C(10)	53.2(2)
C(1)#1-Zr(1)-C(10)	32.0(2)
C(1)-Zr(1)-C(10)	147.0(2)
C(5)#1-Zr(1)-C(10)	136.2(2)
C(5)-Zr(1)-C(10)	32.07(19)
O(1)-Zr(1)-C(10)#1	110.45(19)
O(1)#1-Zr(1)-C(10)#1	78.03(19)
C(2)-Zr(1)-C(10)#1	52.7(2)
C(2)#1-Zr(1)-C(10)#1	119.9(2)
C(3)-Zr(1)-C(10)#1	53.2(2)
C(3)#1-Zr(1)-C(10)#1	114.9(2)
C(1)#1-Zr(1)-C(10)#1	147.0(2)
C(1)-Zr(1)-C(10)#1	32.0(2)
C(5)#1-Zr(1)-C(10)#1	32.07(19)
C(5)-Zr(1)-C(10)#1	136.2(2)
C(10)-Zr(1)-C(10)#1	167.6(3)
C(11)-O(1)-Zr(1)	156.6(4)
C(11)-O(2)-C(15)	115.6(5)
C(2)-C(1)-C(10)#1	107.7(6)
C(2)-C(1)-Zr(1)	72.5(3)
C(10)#1-C(1)-Zr(1)	77.8(3)

C(1)-C(2)-C(3)	109.9(7)
C(1)-C(2)-Zr(1)	75.2(4)
C(3)-C(2)-Zr(1)	75.1(3)
C(2)-C(3)-C(5)#1	107.9(6)
C(2)-C(3)-C(4)	126.2(8)
C(5)#1-C(3)-C(4)	125.8(7)
C(2)-C(3)-Zr(1)	72.6(3)
C(5)#1-C(3)-Zr(1)	76.6(3)
C(4)-C(3)-Zr(1)	117.5(4)
C(3)-C(4)-C(4)#1	112.4(5)
C(6)-C(5)-C(3)#1	133.2(7)
C(6)-C(5)-C(10)	120.5(7)
C(3)#1-C(5)-C(10)	106.3(6)
C(6)-C(5)-Zr(1)	121.3(5)
C(3)#1-C(5)-Zr(1)	70.8(3)
C(10)-C(5)-Zr(1)	75.0(3)
C(7)-C(6)-C(5)	117.4(8)
C(6)-C(7)-C(8)	123.2(9)
C(9)-C(8)-C(7)	121.8(8)
C(8)-C(9)-C(10)	118.0(8)
C(1)#1-C(10)-C(9)	132.9(6)
C(1)#1-C(10)-C(5)	108.0(6)
C(9)-C(10)-C(5)	119.0(7)
C(1)#1-C(10)-Zr(1)	70.2(3)
C(9)-C(10)-Zr(1)	121.1(4)
C(5)-C(10)-Zr(1)	72.9(3)
C(12)-C(11)-O(1)	123.4(5)
C(12)-C(11)-O(2)	124.3(6)
O(1)-C(11)-O(2)	112.3(5)
C(11)-C(12)-C(14)	123.5(6)
C(11)-C(12)-C(13)	120.4(7)
C(14)-C(12)-C(13)	115.9(6)
O(2)-C(15)-C(17)	107.0(7)
O(2)-C(15)-C(16)	109.0(7)
C(17)-C(15)-C(16)	112.4(7)

Symmetry transformations used to generate equivalent atoms:

#1 -x+1,y,-z+1/2

Table 4. Anisotropic displacement parameters ($Å^2 x\ 10^3$) for ec17. The anisotropic displacement factor exponent takes the form: $-2\pi^2[\ h^2\ a^{*2}U^{11} + ... + 2\ h\ k\ a^*\ b^*\ U^{12}\ ]$

	U^{11}	U^{22}	U^{33}	U^{23}	U^{13}	U^{12}
Zr(1)	56(1)	35(1)	27(1)	0	18(1)	0
O(1)	74(3)	56(2)	49(3)	-12(2)	35(2)	-17(2)
O(2)	47(3)	114(4)	42(2)	14(2)	15(2)	11(2)
C(1)	85(5)	57(4)	27(3)	6(3)	19(3)	-3(4)
C(2)	102(5)	60(4)	31(3)	-7(3)	31(3)	14(4)
C(3)	129(7)	40(3)	24(3)	-9(2)	23(4)	-6(4)
C(4)	161(8)	43(4)	51(4)	-3(3)	36(5)	2(4)
C(5)	98(6)	56(4)	32(3)	8(3)	17(3)	20(4)
C(6)	123(8)	87(6)	49(4)	15(4)	21(5)	42(6)
C(7)	91(7)	140(8)	70(6)	12(6)	7(5)	43(7)
C(8)	79(6)	136(8)	68(6)	4(5)	-11(4)	4(6)
C(9)	81(6)	88(5)	43(4)	-4(4)	-2(4)	-1(4)
C(10)	89(5)	54(4)	32(3)	4(3)	17(3)	3(3)
C(11)	33(3)	67(4)	41(3)	-1(3)	10(2)	0(3)
C(12)	44(4)	47(4)	64(4)	-1(3)	-3(3)	-6(3)
C(13)	121(7)	75(5)	96(6)	11(5)	-9(5)	-38(5)
C(14)	67(5)	62(4)	80(5)	-30(4)	5(4)	10(3)
C(15)	58(5)	150(7)	51(4)	-1(4)	23(4)	44(5)
C(16)	58(5)	266(13)	71(6)	-30(7)	-6(4)	52(7)
C(17)	77(6)	318(18)	76(6)	-55(8)	22(5)	57(8)

Table 5. Hydrogen coordinates (x 10^4) and isotropic displacement parameters ($Å^2$x 10^3) for ec17.

	x	y	z	U(eq)
H(1A)	5463	2612	304	67
H(2A)	5962	780	1250	75
H(4A)	5593	-1119	2145	100
H(4B)	4940	-1602	1545	100
H(6A)	6278	-353	3640	102
H(7A)	7064	806	4493	121
H(8A)	6868	2588	5294	116
H(9A)	5866	3283	5292	86
H(13A)	6593	6160	2308	149
H(13B)	6565	6634	3460	149
H(13C)	6022	6986	2537	149
H(14A)	5295	4641	3882	105
H(14B)	5193	6008	3539	105
H(14C)	5736	5657	4462	105
H(15A)	6716	2560	2296	102
H(16A)	7256	4053	3362	200
H(16B)	7545	4583	2391	200
H(16C)	7754	3288	2835	200
H(17A)	6704	2605	495	234
H(17B)	7408	2388	1050	234
H(17C)	7198	3683	608	234

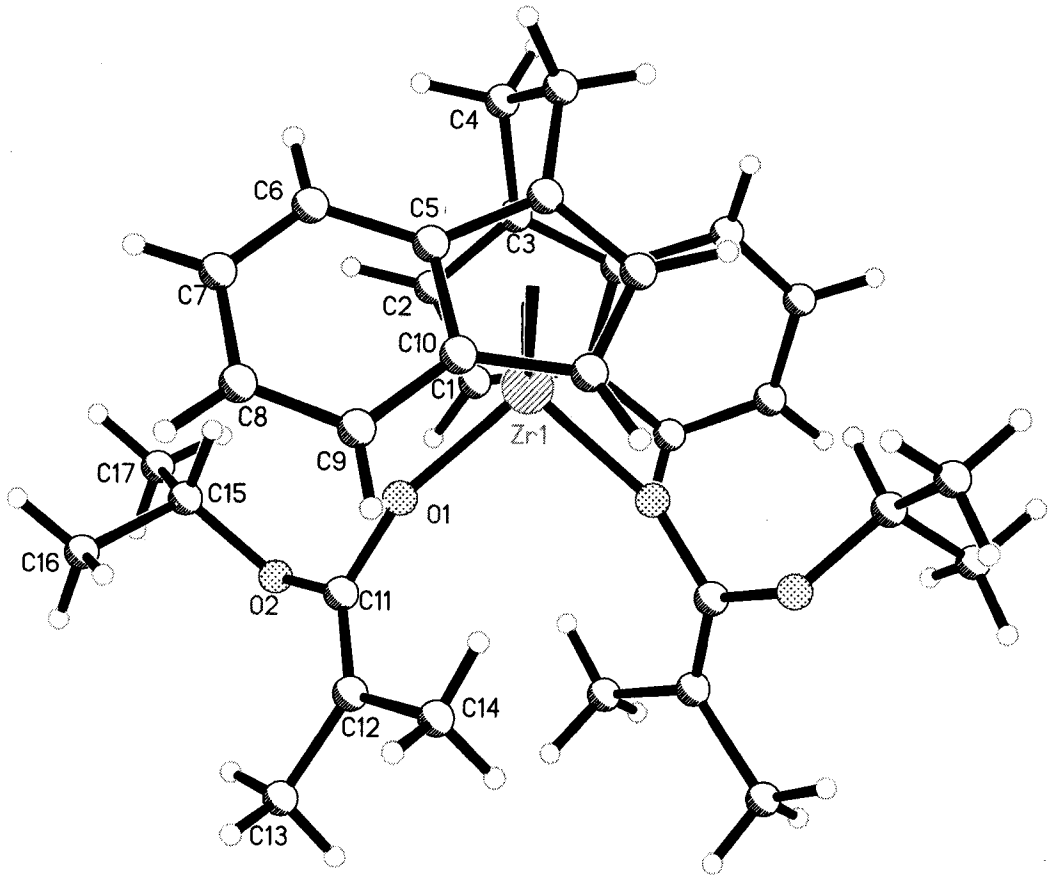

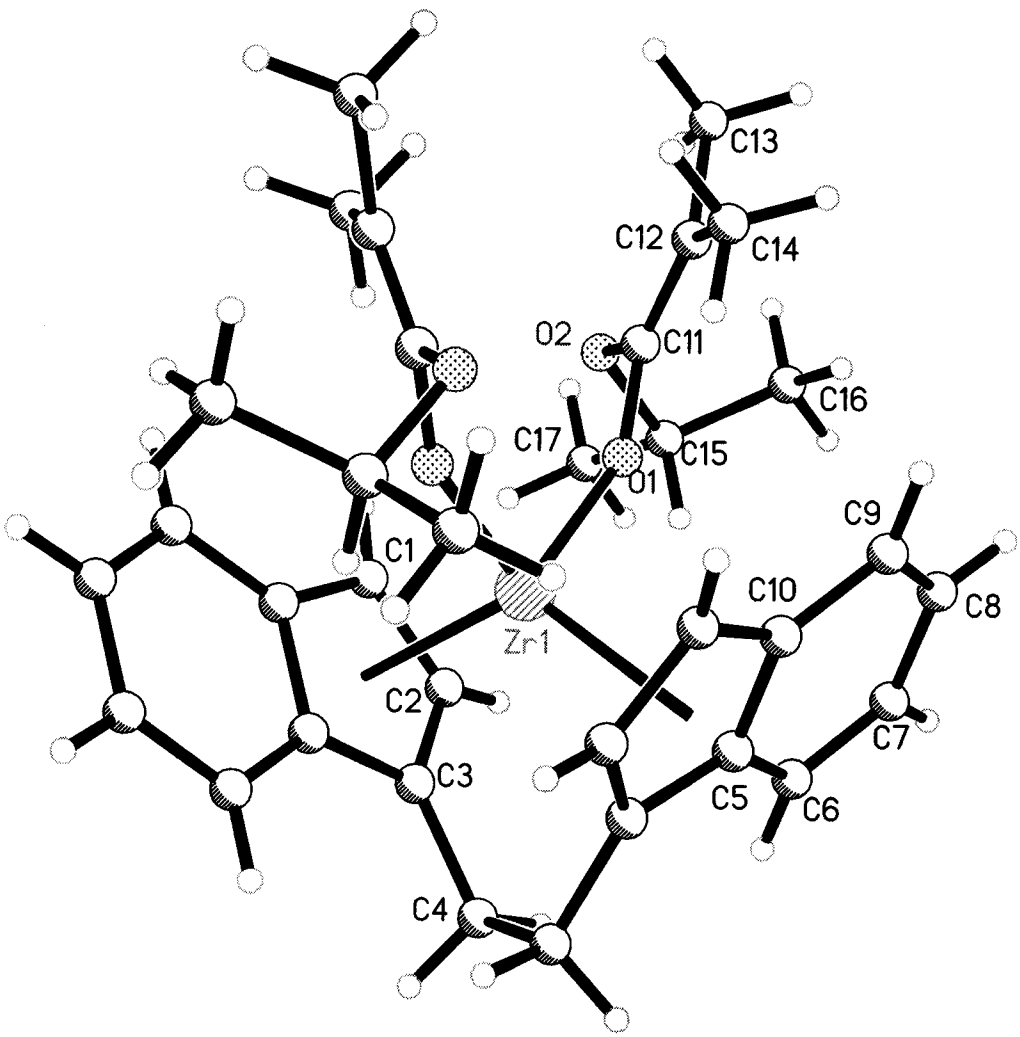

Chapter 2

Introduction

I. Supramolecular Chemistry

Although humans have employed natural and synthetic polymers for centuries, it was not until the introduction of the theory of macromolecules by Staudinger[1] in the 1920's (recognized by a Nobel Prize in 1953) that an appreciation developed for the idea that their properties arise from well-known intermolecular forces acting between high molecular weight units. This concept opened up a new realm of chemistry which continues to develop, producing novel materials with useful, often unexpected, properties[2], such as those discussed in the previous chapter.

In the ensuing decades, an appreciation of the exquisite complexity of biopolymers (e.g. polypeptides, DNA and RNA) and their bonding and conformations in three dimensions[3] was developed. This inspired a dramatic increase in the complexity of synthetic targets for chemists. Attaining these goals requires the chemist to look beyond simply the order of covalent attachment of subunits (1^0 structure), to the spatial arrangement of the backbone and sidechains of the subunits (2^0 and 3^0 structures), and ultimately to the non-covalent interactions which hold different subunits (not covalently bound) in specific orientations with respect to one another (4^0 structure). Subtle effects such as hydrogen bonding and Coulombic forces are exploited to control the overall three dimensional structures. Attempts to apply these principles to synthetic systems are currently of great interest. Thus, the demonstration of the existence of polymeric constructs caused a quantum shift in chemistry in the previous century; the study of

natural analogs has informed and improved this field, requiring understanding of intermolecular forces. In both biological and synthetic systems it has been shown that the non-covalent interactions of distinct molecular entities are crucial to the observed properties.

Similarly, the concept of supramolecular chemistry, recognized by a Nobel Prize in 1987[4] has more recently caused a dramatic shift in the targets of interest to synthetic chemists. This field is broadly defined by Lehn (ref. 4c) as "the chemistry beyond the molecule, bearing on the organized entities of higher complexity that result from the association of two or more chemical species held together by intermolecular forces." One relevant, very attractive goal for modern chemists is the construction of photochemical molecular devices (PMD's)[5], which can utilize photons to generate chemical[6] or electrical energy[7]. Whereas natural PMD's such as photosynthetic systems employ complex membranes to affect spatial control over reaction centers, a current approach is to utilize the tools of supramolecular chemistry to confront this massive synthetic challenge. In order to approach this long-term goal, then, it is necessary to first create "monomer" subunits that have certain desirable properties (e.g. redox properties, absorbance, and excited state lifetime), establish their physical properties and then develop strategies for assembling these into well-defined 3-dimensional arrays.

Interestingly, however, only a very few "privileged" moieties such as metal polypyridyls[8] and metal carboxylates[9] have been extensively explored in this area. Unfortunately, despite several decades of intense effort, few devices of real practical utility have been developed. In fact, it is widely accepted that the goal of rational engineering of useful crystalline arrays of transition metals is far from generally

achieved. Indeed, two recent editors of *Nature* have decried this situation, one proclaiming, "it remains one of the continuing scandals in the physical sciences that it remains impossible to predict crystalline architecture from a knowledge of chemical composition."[10] Clearly, a better understanding of the physical properties and crystalline packing motifs of potential subunits should contribute knowledge to improve this disparity. Further, many scientists believe that advances in this basic science will likely not come from continuing to follow the same "usual suspects."[11] Therefore, there is substantial driving force for the investigation of new ligand types and bonding modes. The discrete molecular properties of new ligands and complexes must be thoroughly investigated before they can be incorporated in supramolecular architectures. Towards this goal, investigations of metal complexes of dioxocyclams have been ongoing in the Hegedus labs. It is proposed that the subunits discussed herein may eventually be useful for construction of supramolecular arrays, though it must be stressed that the current state of the art involves the study of the subunits themselves.

The goal of the present work is to covalently bind polypyridyl species (widely utilized in coordination chemistry both to link together supramolecular arrays, and as a photosensitizer) with capped dioxocyclams. The latter are relatively unexploited ligands for transition metals with potential applications to catalysis[12] and useful electrochemical properties.[13] Although terpyridine coordination has been extensively investigated, the number of substituted variants, particulary those containing chiral centers, remains very small.[14] Coordination of metals to the two bound ligand classes will generate organometallic subunits with potential applications to the formation of rationally

designed supramolecular arrays for use in photochemistry and catalysis. In short, the well-known coordination chemistry of terpy ligands will be coupled to less-studied metallo-dioxocyclams to generate novel bimetallic complexes.

As mentioned, progress in supramolecular chemistry has been relatively slow. It is proposed that the application of previously unexplored functional groups (e.g. dioxocyclams) may lead to unexpected advances. The present work will primarily be concerned with synthesis and characterization of the subunits, which is crucial before the properties of their self-assembled arrays can be approached. Indeed, although supramolecular chemistry was initially concerned primarily with weak interactions between individual molecules, the focus has recently shifted towards developing more complex covalently assembled units which can be utilized as "building blocks" for more varied and useful supramolecular arrays.[15]

II. Dioxocyclam Background

The Hegedus group has performed extensive research into the synthetic utility of the photochemistry of chromium Fischer carbene complexes. Particularly noteworthy is the mild synthesis of β-lactams[16] and a wide variety of their analogs which are of interest as antibiotics. This methodology was later directly applied to the production of azapenams[17] from the photolysis of carbenes with imidazolines. These heterocycles were produced as BOC-protected amines. Reductive deprotection under acidic conditions neatly cleaved the strained β-lactam ring, generating caprolactams. This serendipitous discovery suggested a further experiment: treatment of the azapenams with a catalytic amount of acid in the absence of hydrogen gas. This reaction affords a smooth

dimerization to a bis-imine which is readily reduced to allow access to functionalized dioxocyclams, (scheme 1) fourteen membered tetra-aza macrocycles.

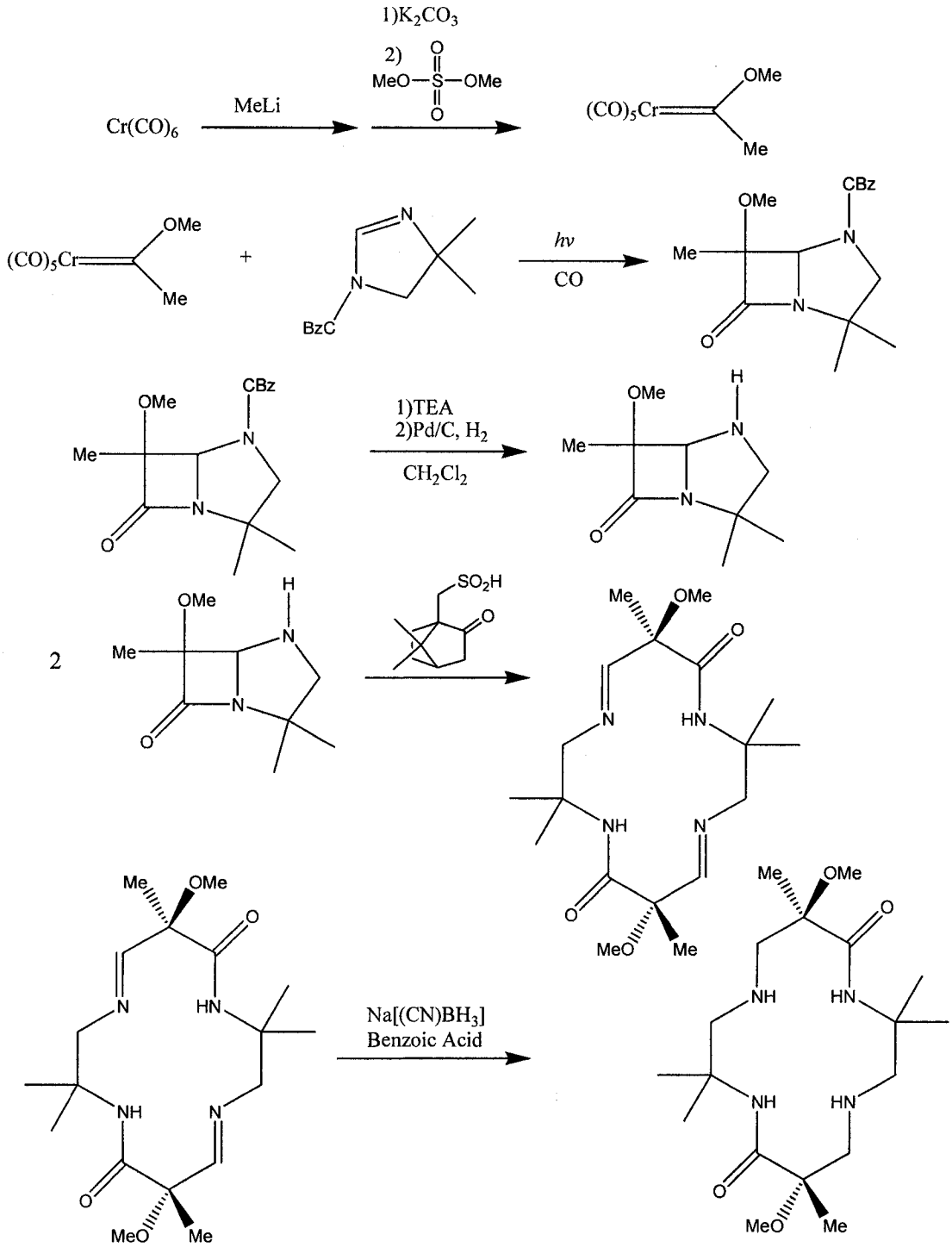

Scheme 1: Synthesis of *trans*-Me/OMe dioxocyclam, 1.

Elegant studies[18] later revealed that dimerization to the bis-imine produces both C_2- (R,R and S,S at the quaternary centers) and C_S- (R,S) symmetric products. However, the latter (illustrated in scheme 1) is more crystalline, so simply allowing the dimerization reaction to equilibrate under acidic conditions for several days affords the centrosymmetric isomer in high (>80%) yield. Crossover experiments appear to demonstrate that, in acid, the dimer is in equilibrium with the monomer, possibly via a postulated 7-membered imine. Interestingly, metal complexes of these two isomers have dramatically different properties.[19] Notably, the Cu(II) complex of the C_2 dioxocyclam has reversible oxidation chemistry, whereas the C_S complex only shows irreversible oxidation (but reversible reduction[20]). Because of their greater stability and higher yield, the C_S symmetric ligands will be of interest to the following studies. A further advantage is the smaller number of possible isomers produced on capping with bis-electrophiles.

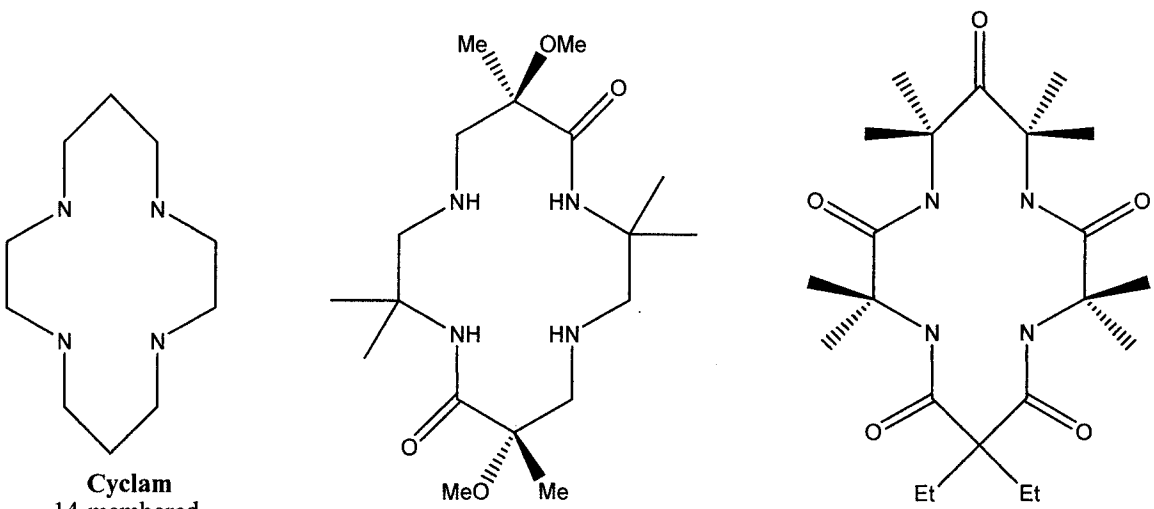

Cyclam
14-membered-
Tetra-amine

5,12-dioxocyclam
14-membered
Bis-amine
Bis-amide

TAML Ligand
14-membered
Tetra-amide

Figure1: Related tetra-aza macrocycles

These ligands bear an obvious similarity to their better-studies relatives, the cyclams, which are, likewise, 14-membered tetra-aza macrocycles, but with all four nitrogens as amines. Cyclams have been extensively studied, particularly in their complexes with first row transition metals[21] such as Cu and Ni. Further, they complex some second row transition metals including Pd,[22] and main group elements such as Al.[23] Cyclams, the related cyclens (12-membered tetra-amine macrocycles), and their fully N-substituted derivatives selectively bind some heavy metals, lanthanides, and actinides, and even anions in some cases[24]. Such extreme versatility and selectivity has led to many useful applications. Catalytic applications of these complexes include olefin epoxidation,[25] cleavage of DNA[26] and catalytic oxidations[27].

It is interesting to note that although classical coordination chemistry has studied monodentate amine complexes for well over a century, the chelate effect was postulated just over 50 years ago.[28] Appreciation of the further enhanced binding proffered by macrocycles was not developed for approximately another quarter century,[29] and three-dimensional macropolycycles such as the capped cyclams discussed later represent a relatively recent advance.

The two amide nitrogen functionalities in dioxocyclams are expected to alter the binding specificities and potential applications of interest here relative to the tetra-amines. Deprotonated amides are expected to exhibit a higher ligand field strength relative to neutral amines[30], and they can potentially ligate metals via N- or O-coordination[31], so should exhibit a rich diversity of complexation patterns. In addition, they are expected to stabilize metals in high oxidation states.[32] Their potential as ligands has been relatively unexploited, with the exceptions of the work of Kimura, Hegedus, and

more recently, Guilard. Their binding properties are generally intermediate between the aforementioned cyclams (tetra-amine macrocycles), and cyclic tetra-amide macrocycles. A few examples of the latter are known, including biological and synthetic oligopeptides[33] (polyamides), and the TAML ligands of Collins[34]. Iron complexes of TAML ligands are extremely robust oxidation catalysts. Their extreme oxidative stability has rendered them commercially useful for paper pulp bleaching, obviating the need for chlorine bleaches and their toxic dioxin byproducts.

Therefore, both tetra-amine and tetra-amide heterocycles have demonstrated interesting properties and applications. Accordingly, the Hegedus group has expended considerable effort in exploring the properties of dioxocyclams and their metal complexes, which should combine the useful properties of their more well-known relatives. Indeed, Kimura has directly compared[35] the redox properties of cyclams to mono-, di-, tri-, and tetra- oxocyclams, revealing trends which suggest that synthetic access to all members of this ligand series would be useful. Notably, however, this work only addressed 5,7-dioxocyclams, not the 5,12-substituted variants generated via the Hegedus methodology.

One potential advantage of the mixed amine-amide dioxocyclams is that the two types of nitrogen atoms exhibit very different reactivities. As such, they can be considered "autodiprotected"[36] variants on the cyclam skeleton. Selective functionalization of the ring nitrogens is an attractive goal, and this represents a successful approach. Thus, Guilard has prepared (unsubstituted) dioxocyclams, selectively capped them with bis-electrophiles across the amine nitrogens[37]. However, the amides were then reduced to yield the corresponding *trans*-capped cyclam, so the

mixed amine/amide systems were merely protected intermediates. The Hegedus group has, on the other hand, investigated the synthesis and properties of these less well-known capped dioxocyclams in their own right [38] by the reaction of bis-electrophiles selectively with the nucleophilic secondary amines, as shown in scheme 2.

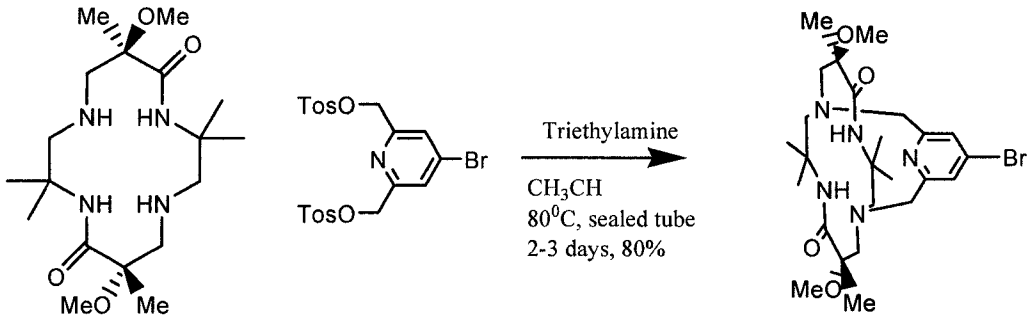

Scheme 2: Selective "capping" of a dioxocyclam to yield ligand 2.

Hence, capping with a pyridine-based bis-electrophile produces a 5-coordinate, approximately square pyramidal pocket into which copper can be readily inserted. Alternatively, a pyrazine-capped dioxocyclam[39] affords an additional exocyclic binding site which can be exploited for coordination to building blocks such as metal pthalocyanines for production of arrays.[40]

Pyridine and pyrazine, however, have dramatically different electronic properties; as such, it would be beneficial to have access to 4-substituted pyridyl capping reagents. Similar to the pyrazine group, these would allow an exocyclic site for elaboration of arrays, but would allow for fine-tuning of electronic, steric, and binding properties. Towards this end, a variety of capping reagents and their capped-dioxocyclam products were synthesized recently. *Para*-substituents on the pyridine cap included EWG's (NO_2, NO, CN) and EDG's (amine and protected amine)[41]. Furthermore, the great utility of the 4-bromo capped dioxocyclam (**2**, scheme 2) was discovered. This advanced intermediate

can undergo palladium-catalyzed cross-coupling reactions to afford 4-functionalized capped dioxocyclams in high yield. This versatility in the late stage of the synthesis allows facile access to a wide variety of building blocks. This illustrates the ability to generate relatively complex building blocks and tailor them directly in late-stage, high-yielding reactions.

In spite of the many known metal complexes of cyclic tetra-amines and tetra-amides, metallations of substituted dioxocyclams have proven relatively synthetically challenging. Thus far, most examples have involved late first-row transition metals (Cu, Ni, Co). For example, although the related carboxylate-substituted cyclens bind Gd^{3+} tightly (the complexes are used clinically as magnetic resonance contrast agents)[42], similarly functionalized dioxocyclams apparently only bind this lanthanide very weakly, and not via the amide groups[43]

Ni(II) dioxocyclams were known to catalyze the epoxidation of olefins[44]; when the Hegedus group developed methodology for producing dioxocyclams with chirality incorporated into the backbone[45], these became very attractive targets. More recently, the nickel complexes of dioxocyclams substituted with quinoxaline groups for DNA binding were synthesized and investigated for their ability to bind and cleave the phosphodiester backbone of DNA. Although the expected binding was not observed, this is an interesting application of supramolecular chemistry, wherein specific binding modes are exploited to bring functional groups into close proximity, after which useful reactions may proceed.

Copper-dioxocyclam complexes have been studies in somewhat more detail by Kimura,[46] Hegedus,[47] and recently, Guilard and Kadish[48]. Cupration is relatively facile,

and the products have been extensively characterized by x-ray crystallography, electrochemistry, and SQUID. Although previous studies in our group did not identify useful electrochemical properties, studies reported herein and recent work by Kadish[48] show that there is potentially useful redox chemistry in these complexes.

Efforts were next focused on production of cobalt-dioxocyclam complexes. Surprisingly, a wide variety of cobalt salts combined with a selection of bases in several solvents at various temperatures completely failed to produce the desired species. Previous cupration chemistry had proceeded very efficiently (although giving surprising products[49]) under irradiation in a commercial microwave oven. Application of this protocol with cobaltous acetate hydrate finally yielded cobalt macrocyclic compounds, both capped and uncapped[50] in moderate yield. Lengthy application of reflux conditions utilizing the same reagents yield no reaction whatsoever. It is unclear why such forcing conditions are required with cobalt, though it should be noted that attempts to form complexes with Fe, Ru, and Zn all have yet to produce the desired results; dioxocyclams are quite selective in their metal binding properties.

III. Polypyridine Coordination Chemistry Background

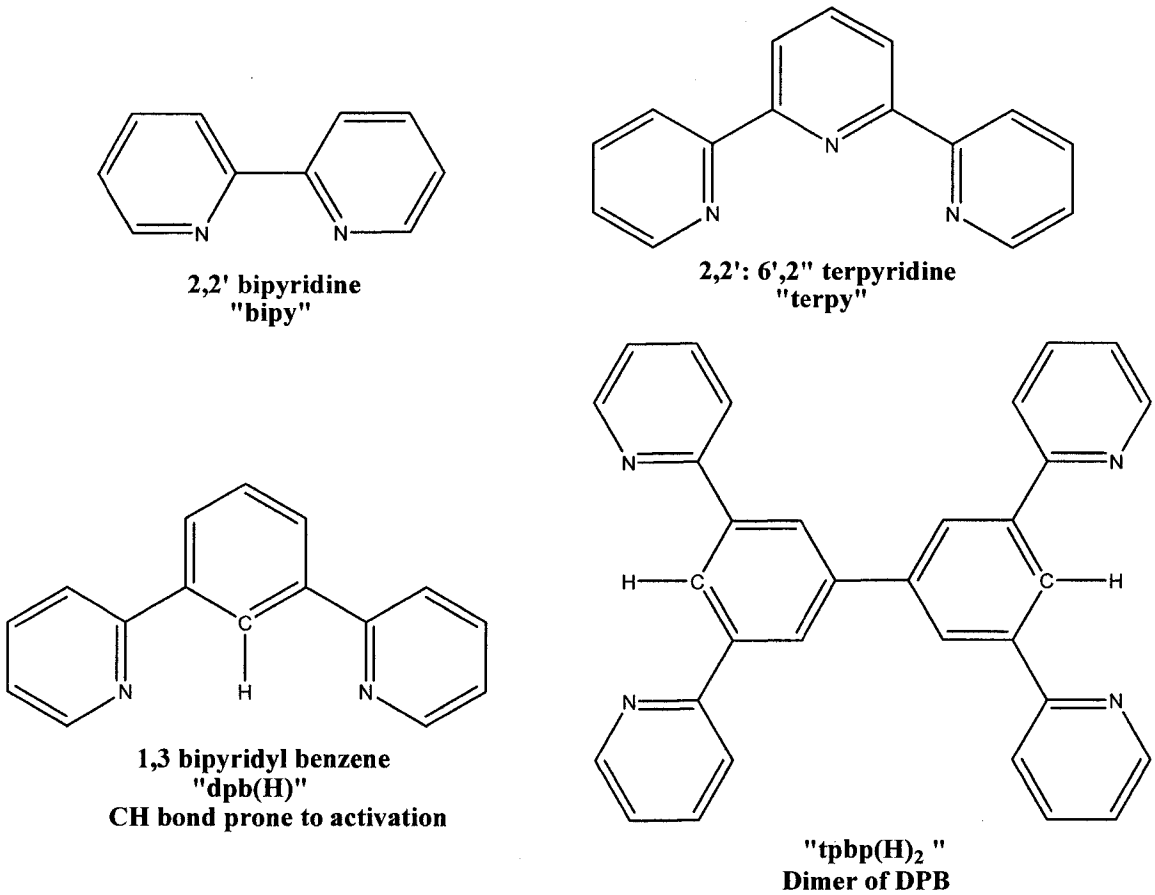

Figure 2: Representative polypyridyl ligands.

The prototypical ligand in this class is 2,2'-bipyridine (see figure 2), and the best known complexes are those of "bipy" with ruthenium.[51] The first bipy iron complex was isolated well over a century ago by Blau[52], and related species have had a rich history since their inception. The high affinity of transition metals for nitrogen, and the chelating nature of this ligand combine to generate very stable complexes. In the area of applications to photochemistry, $Ru(bpy)_3$ is well renowned for its relatively long-lived excited state. This unique feature has led to the useful devices employing $Ru(bpy)_3$ as a photosensitizer; in fact, this has been the most-studied candidate for current attempts at artificial photosynthesis[53]. Efforts have been ongoing and perhaps most notable in the

area of solar energy harvesting and conversion.[54] However impressive the excited state characteristics might be of these coordination compounds, a significant challenge lies in the substitution chemistry. Although symmetric substitution at the 4,4' positions can be achieved in many cases, mono-substitution is problematic. Such a substitution pattern disturbs the symmetry of the metal tris(bipy) complex, and in many cases introduces geometrical isomerism.[55]

In order to address this shortcoming, several research groups have more recently directed their attention to the related ligand, 2,2':6',2"-terpyridine ("terpy", or "tpy"),[56] shown in figure 2. This ligand was first described in 1931[57] and has similarly found applications in analytical chemistry (as a colorimetric indicator of iron in solution)[58]and as a chelating agent for several transition metals.[59] This tri-imino ligand chelates transition metals in a 2:1 fashion. Furthermore, 4'-substituted analogs are readily available. Homoleptic bis(terpy) complexes of these ligands are not generally isomeric, simplifying synthesis, analysis, and isolation relative to the tris(bipy) case.

Both bipy and terpy moieties have been incorporated into polymers and oligomers to generate metallosupramolecular polymers[60] by coordination to Ru, although the bidentate versions have seen much more attention. The relatively slow development of metallo-terpy polymers, arrays, and devices compared to bipy analogs has been ascribed to the more difficult syntheses involved, and to another, more fundamental issue. Although luminescent due to MLCT (metal to ligand charge transfer) at low temperatures, it has been clearly demonstrated[61] that the lifetime of the excited state of photoexcited Ru complexes of terpy is several orders of magnitude smaller (250 ps at room temperature) than the analogous tris-bipy complexes, limiting the potential utility of

devices incorporating this photosensitizer. Despite several efforts, no satisfying explanation has been forthcoming regarding this fundamental difference[62]. However, it was proposed[63] that substitution of conjugated aromatic species should increase the excited state lifetime. Several groups investigated this possibility, but it was not until the combined efforts of Constable and Tocher were published in 1992[64] that a systematic study of 6 different substituted substituted terpys and their 21 possible heteroleptic and homoleptic Ru complexes allowed direct evaluation of the theory. Gratifyingly, groups as simple as tolyl were shown to markedly enhance the excited state lifetime, and other groups have gone on to further exploit conjugated substituents on tpy as "excited state storage elements".[65] Further, it has been demonstrated that multiple conjugated Ru(tpy) systems exhibit even more dramatically extended lifetimes[66], which bodes well for their incorporation into supramolecular arrays. However, the results were still less than impressive compared to $Ru(bipy)_3$, which in turn pales in comparison to natural photosystems which have excited state lifetimes at least six orders of magnitude greater yet[67].

Hence there exists a strong driving force for the preparation of more effective ligands for stabilizing metals in their excited states, and for electronic bridging between metal centers. The latter goal has seen intense research since the pioneering work of Creutz and Taube[68] involving pyrazine-bridged mixed-oxidation state $Ru^{II/III}$ systems. These mixed valence systems are important for furthering our fundamental understanding of electron transfer reactions, biochemical modeling and biomimicry (especially Cu, Fe, and Mn), and their potential applications in molecular electronics and as such continue to excite further studies[69]. Although several bridging ligands afford large coupling between

metal centers at short range, few show significant delocalization over more than 5 atoms[70].

One particularly fruitful avenue of research in bridging ligands has been the cyclometallating dipyridylbenzene (dpb(H), figure 2) ligands developed by Collin and Sauvage[71]. The initial goal was to develop a terpy analog with a stronger ligand field. Towards this end, a tricyclic ligand differing from terpy only in the replacement of the central ring nitrogen with a carbon, was developed. Asymmetric variants were also explored, wherein the carbon substitution for nitrogen was not on the central ring[72]. Although they outperformed tpy ligands, they were inferior to the symmetric variant discussed here. Cyclometallated complexes with Ru were prepared in reasonable yield. A most interesting serendipitous discovery then ocurred, wherein excess $AgBF_4$ apparently reacted with Ru-dpb complexes to form C-C coupled complexes of the ligand $tpbp(H)_2$ (figure 2), with the central phenyl rings of each dpb coupled *para* to the cyclometallated positions. Although the mechanism of this reaction remains a mystery, its synthetic utility does not. The resultant bis-cyclometallating bridging ligand allows for extremely high coupling of metal centers. Studies of the mixed-valent bis-Ru and bis-Os complexes thereof revealed substantial evidence of significant charge delocalization[73]. This strong coupling of metal centers bodes very well for the application of this ligand class to useful supramolecular arrays. Several years later, these researchers were able to produce a related ligand with 3 phenylene units inserted between the dpb functionalities. Charge transfer was observed between the two mixed valent Ru centers, corresponding to charge transfer over 24 Å, claimed to be the longest distance ever recorded.[74] In addition, the excited state lifetimes are dramatically enhanced relative to the tpy analog.[75]

Thus the dpb analogs have key advantages as ligands for use in photosensitizers in arrays; notably, their ability to stabilize and hence extend the lifetime of the excited state, and their ability to highly couple metal centers when utilized as a bridge. Two other significant advantages should be mentioned. First, the covalent organometallic bond produced by cyclometallation eliminates ligand scrambling. For heteroleptic terpy complexes, this is a major issue.[76] Although in some cases it is possible to optimize the synthesis to minimize the homoleptic byproducts, they always form to some extent under the conditions required for complexation (and in potential applications), and their separation is difficult in the cases where it is possible. Cyclometallation obviates this possibility, and allows isolation of heteroleptic Ru complexes with ease. Interestingly, however, homoleptic Ru(dpb) complexes are not found in the literature. It is believed that attempts to form such complexes result in reduction of the Ru and subsequent decomposition. The dpb-type ligands provide yet another benefit in their anionic nature. As a result, complexes of dpb require one less counteranion relative to their tpy analogs. This is of practical import for the project at hand, which involves substituting these ligands and their complexes with extensive organic frameworks. The combination of highly polar $Ru(tpy)_2^{2+}$ cations with large, relatively non-polar organic functionalities produces materials with properties similar to phase-transfer catalysts that are consequently relatively difficult to isolate and purify; the less ionic dpb variants mitigate this issue.

IV. Objectives

Building on these developments, the present work has several goals. The first is to investigate the metal coordination-based linkage of capped dioxocyclams via covalently bound polypyridyl moieties. Second, the ability to coordinate metals into the macrocyclic dioxocyclam cavities will be investigated. The very selective binding properties of dioxocyclams lends them to the production of heterobimetallic species, since the polypyridyl functionalities coordinate much more readily. Next, the goal will be to construct species containing metallo dioxocyclams covalently bound to metallo polypyridine groups. Attempts to probe for coupling of the two metal centers will be described. Lastly, potential strategies for linking these subunits into larger arrays will be explored.

V. Results and Discussion

Terpyridine capped Dioxocyclam (3)

The work presented here began initially to test the complexation properties of the difunctional ligand **3** shown below, first reported by Dr. Jory Wendling and the Hegedus group in 2003,[77] referred to as "cyctpy." As previously mentioned, the 4-Br pyridyl-capped dioxocyclam **2** represents a versatile advanced intermediate for further functionalization[78]. Indeed, in the original disclosure, this molecule was subjected successfully functionalized via Stille, Sonogashira, and Buchwald-Hartwig reactions.

Williams[79] had recently synthesized the terpy boron ester **4** (scheme 3), and demonstrated that it was a useful intermediate for Suzuki coupling reactions with aryl

bromides. Although that work described coupling conditions, Wendling employed different methodology[80] utilizing Ag_2O as a cocatalyst, which afforded the desired product in moderate yield. However, he employed very large Pd(tetrakis(triphenylphosphine)) catalyst loadings (25 mol%), whereas Williams had been successful with 6% Pd. It was noted in the dissertation that the product could not be obtained completely free from an impurity of triphenylphosphine. (NMR experiments have since shown that the major impurity is actually the oxide of triphenylphosphine, presumably from interaction with the large excess of the silver oxidant.) Indeed, the coupling product and the phosphine co-elute and co-crystallize under a number of conditions explored by Dr. Wendling. Since each Pd center is coordinated by 4 triphenylphosphine ligands, 25 mol % "tetrakis" can conceivably contribute 1 full stoichiometric equivalent of phosphine as a troublesome impurity in the coupling product. Hence, I investigated lower catalyst loadings down to 6% with no adverse effects on the yield. Moderately lower yields were observed at 3% loading, but the decrease in [phosphine oxide] contamination simplified purification. The chromatographic purification may be somewhat improved over that reported by following the procedure optimized for the dipyridyl cyclam derivative described in the experimental section. Unfortunately, a minimum of two consecutive column separations are still required to isolate pure material. However, given that the goal of the present work is to study the complexation behavior of these new ligands, the complete removal of competing ligands such as phosphines is critical.

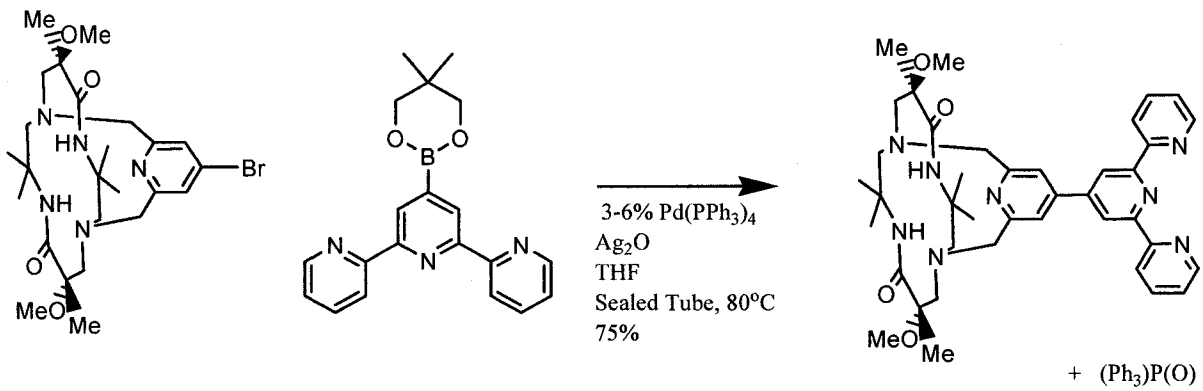

2 **4** **3**

Scheme 3: Synthesis of terpyridine-capped dioxocyclam 3.

$[Ru^{II}$(terpy-dioxocyclam)$_2](PF_6)_2$ (5)

Once pure **3** was in hand, complexation studies began. Given the diversity of groups actively investigating ruthenium polypyridyl coordination chemistry, a number of synthetic routes are available. Virtually all begin with the commercially available $RuCl_3$ (xH_2O). The Meyer group[81] has shown that the direct ligand exchange reaction of this ill-defined species allows clean formation of Ru(terpy)Cl_3 in nearly quantitative yield. Others have since shown[82] that substituted terpy derivatives form analogous complexes. These intermediates could then be selectively reacted with other ligands. Interestingly, the first complexes investigated were with triphenylphosphine, which rapidly coordinates to the metal center. This underscores the importance of removing this triphenylphosphine oxide impurities from the above ligand, as this could conceivably form triphenylphosphine *in situ*, under reducing conditions. Meyer also gave a general procedure for ligand exchanges; unfortunately, the solvent is listed incorrectly in the experimental section as $CHCl_3$. Terpy-capped dioxocyclam **3** did not react in this solvent (though it does in MeOH, which is discussed in the text of the paper). Hence, I adapted

the more detailed procedure of Constable[83] with gratifying results as shown in scheme 4. Meyer employed triethylamine as a reductant, whereas Constable uses the more expensive N-ethyl morpholine (others use ascorbates). TEA is effective in my experience, and thus was used throughout in lieu of more exotic reductants.

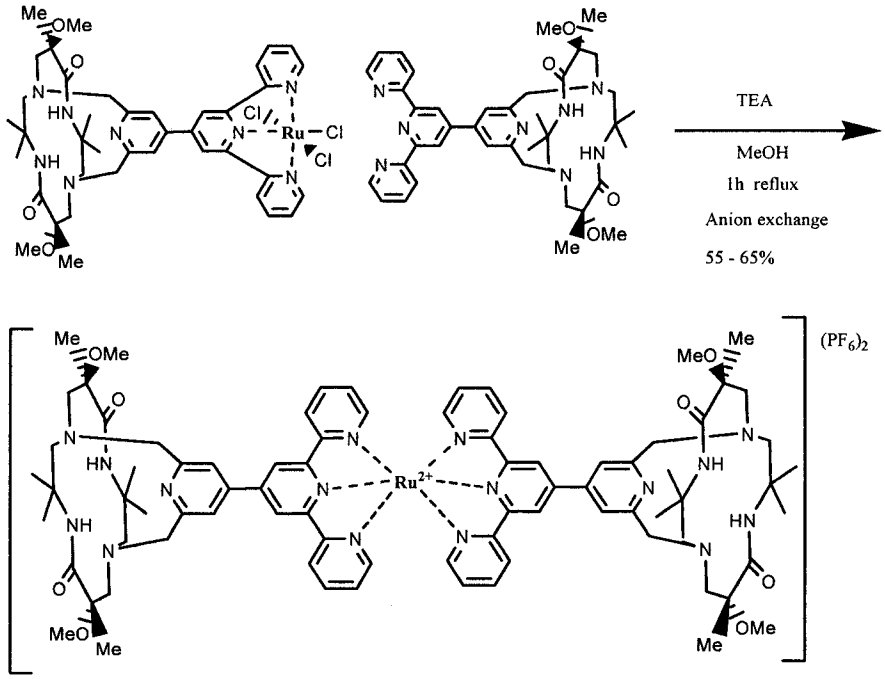

Scheme 4: Early Synthesis of 5

Thus, the initial attempts at formation of **5** were based on a two-step methodology shown above. However, $RuCl_3$(terpy) is less than ideal as an intermediate, as it is paramagnetic, and has fairly poor solubility, such that isolation and characterization are cumbersome. Indeed, for homoleptic complexes such as the one shown here, there seems to be no advantage to isolating this compound. Realizing this, Constable later published[84] 1-pot methodology for homoleptic Ru(terpy) complexes. This was simpler and higher yielding relative to the previous methodology for my purposes, and became the method of choice. Thus, 2 equivalents of the desired ligand are reacted directly with commercial ruthenium trichloride trihydrate at high temperature. This methodology was

first developed for terpy ligands substituted with groups bearing chirality, much like the current systems of study. Instead of refluxing methanol for 1h, the reaction is subjected to ethylene glycol (with no additional reductant required) at 140^0 C for 3h. This suggests that more forcing conditions are required for highly substituted terpys. As we shall see, such conditions are unfortunately not practical for heteroleptic complexes due to ligand scrambling. Although this methodology is very satisfactory, the solvent is perhaps not optimized, as it is very difficult to completely precipitate the product in the presence of this coordinating solvent, so yields are not ideal (though still better than the two-step methodology).

Constable reported that substituted Ru(terpy) complexes could be purified by chromatography over silica gel utilizing acetonitrile/ sat'd. aqueous KNO_3 as an eluant. Such attempts were generally disastrous with these dioxocyclam products, so initial purification was limited. To begin with, the dioxocyclam functionality and the highly ionic nature of the product slow elution drastically. Further, in the presence of water and anionic impurities (such as KNO_3), ion exchange of the product occurs. Chromatographic properties can vary drastically between two species such as the one shown above, and its variant differing only by counterion. Often, the product will stubbornly stick to the column; when isolated, it shows very different behavior on TLC analysis from the starting complex. In most cases, simply repeating the anion exchange procedure to regenerate the PF_6 salt is effective. However, it must be noted that the complex shown here has amphiphillic properties, given on one hand its highly polar ionic nature in the metallic region, and the extensive, organic soluble, heavily substituted dioxocyclam region. This greatly complicates purification, although the present work

shows that satisfactory separations may be achieved by chromatography over neutral alumina.

$[Co^{II}(terpy\text{-}dioxocyclam)_2](PF_6)_2$ (6)

In order to explore the diversity of polypyridine coordination possible with these ligands, the cobalt analog of the bis(dioxocyclam) complex **5** shown above was investigated. Co(terpy) complexes are very rare; in contrast to the ubiquitous Ru(terpy)'s, only a handful of examples appear in the literature. Constable[85] is one of the rare few who have studied these complexes. Unlike the Ru complexes, in no case has it proven possible to isolate heteroleptic Co(terpy) species. This is attributed to rapid ligand exchange at the labile d^7 Co(II) center, which yields statistical mixtures of products which have not been possible to separate. Another consequence of this labile metal center is that the initial reaction is very facile. Thus, coordination is generally complete after 1h at room temperature (vs. 3h at 140^0C for Ru). When this methodology was applied to dioxocyclam substituted terpyridine **2** as shown in scheme 5, formation of the complex was observed (deep red color forms instantaneously on dissolution of solids). Stirring for 1h followed by anion exchange yielded approximately a quantitative amount of crude material (purity unknown). However, chromatography over neutral alumina resulted in only 50-55% recovery, suggesting decomposition. NMR is not a feasible technique for characterization of this paramagnetic complex. Mass spectral investigation ((+)E.S.) shows formation of product, though substantially more free ligand vs. complex is seen. In contrast, under identical conditions, the Ru complex produces

very little free ligand. Thus, the Co complex is much more fragile than the Ru relative (although electrospray ionization methods are admittedly somewhat less than gentle). The material appears to be light sensitive as well; attempts to crystallize the product resulted in precipitation of an unidentified decomposition product. The UV-vis analysis of this material reveals absorptivity more than an order of magnitude smaller than the analogous Ru complex; this is likely due in part to decomposition such that the actual concentration of desired product analyzed was much smaller than anticipated.

Thus, although it appears to be facile to form Co(II) complexes of terpyridine-capped dioxocyclams, the resultant products are rather unstable. Given the potentially interesting electrochemistry described later, these complexes may warrant further research; however, they have several disadvantages relative to their Ru analogs.

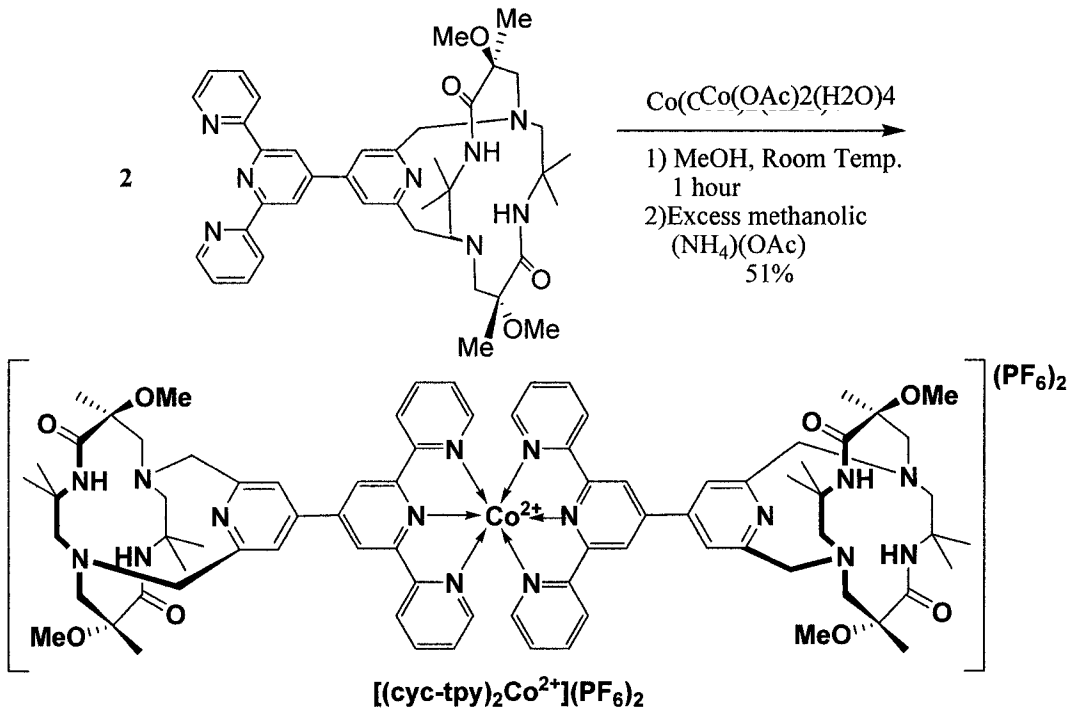

Scheme 5: Synthesis of cobalt-coordinated polypyridine dioxocyclam

$[Ru^{II}$(terpy-dioxocyclam)(terpy)$](PF_6)_2$ (7)

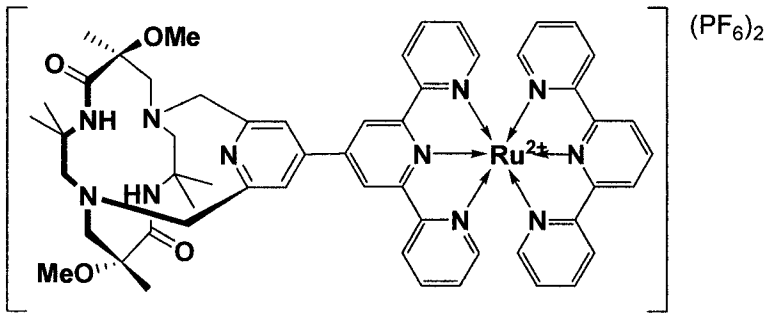

Figure 3: Heteroleptic terpyridine complex 7

Once initial success was achieved with the homoleptic terpy complexes, attention was turned to the more complex heteroleptic variants. These require the two-step methodology[86] first employed (see discussion above) in this project. Thus, Ru(terpy)Cl_3 was synthesized and isolated, then reacted with (dioxocyclam-terpy) in a second step in the presence of methanolic triethylamine as a reductant. Conversely, Ru(dioxocyclam-terpy)Cl_3 could be synthesized, and reacted with terpy with little effect on the yield. As Constable notes, however, the heteroleptic products are always contaminated with some homoleptic byproducts which cannot be removed by recrystallization. Further, in general (with very simply substituted terpy), 1h at reflux in methanol gave the best proportion of the desired products. Unfortunately, as discussed above, highly substituted terpys are more sluggish to react, and require much more forcing conditions to form in high yield (140^0C for 3h!). Thus, this reaction must strike a delicate balance in that considerable thermal energy is required to form the desired products, but ligand scrambling is apparently facile under those conditions. Mass spectral evidence clearly shows that the desired product is formed as the major product in 1h at reflux in methanol. However, the homoleptic byproducts (compound **5** and Ru(terpy)$_2$) are clearly present as well. While it

has proven possible to completely remove $Ru(terpy)_2$, the substituted impurity **5** generally co-elutes with the desired product. The material may be enriched in the heteroleptic product, but has not yet been isolated in pure form, so in-depth characterization has not been performed. Furthermore, Constable clearly showed in his 1992 paper that the chemical shifts of the terpy ligands are not appreciably shifted by substituents on the other tridentate ligand. Hence, a 1:1 mixture of homoleptic products would appear identical to the heteroleptic product in NMR (and possibly other) experiments. This greatly complicates the characterization and hence purification of these materials.

It seems feasible that reaction conditions could be optimized to allow access to reasonably pure heteroleptic products such as those shown here. However, they would be prone to interconversion at high temperatures, limiting their utility. Fortunately, a subtle variation in the ligand design completely obviates this problem, as will be seen in the next section. For that reason, these systems have not been pursued further.

Dipyridylbenzene-capped Dioxocyclam (cyc-dpb(H)) (8)

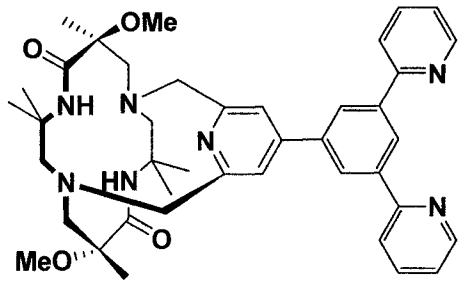

Cyc-dpb(H)
8

Figure4: DPB-capped dioxocyclam

As discussed in the introduction section, cyclometallating dipyridylbenzene (dpb) ligands have been shown to have several advantages over terpy, and are well suited for

bridging metal centers when coupled to other suitable ligands. Further, they produce cyclometallated complexes which negate the problem of ligand scrambling that is associated with terpy ligands. In order to follow similar methodology to generate this bifunctional ligand to that employed above, the dipyridyl benzene boron ester (dpb(B(OR)$_2$) **9** was required. This should be directly accessible from the corresponding bromide **10** (dpbBr). Considerable effort was invested in attempts to follow a literature procedure[87] towards this target. The methodology reported therein does not generate the products claimed and is flawed in several regards. Fortunately, Collin had earlier[88] published a route to dpbBr via Negishi cross coupling methodology which proved effective, shown in scheme 6 below.

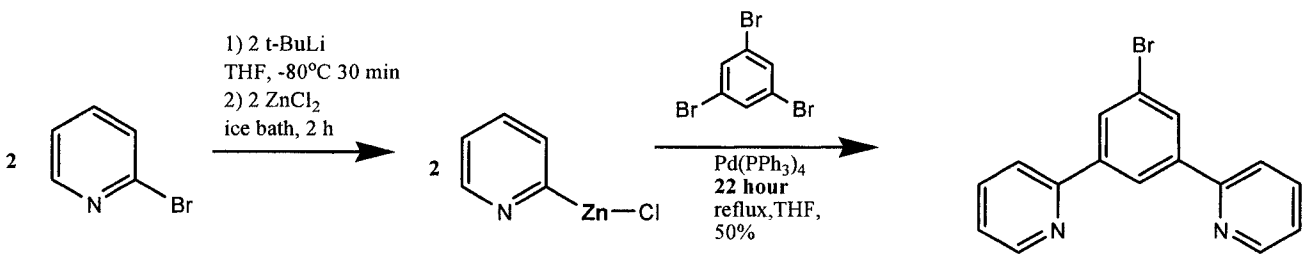

Scheme 6: Collin's Synthesis of dpbBr, 10.

It should be noted that this reaction is higher yielding, faster, and more convenient than the reaction to produce the corresponding terpy-Br intermediate, making this dioxocyclam-dpb target even more attractive. Miyaura's elegant Pd-catalyzed methodology[89] was again employed to cleanly generate the bis(neopentylglycolato) heterocycle from the bromide, shown in scheme 7. No further purification was required after Celite filtration.

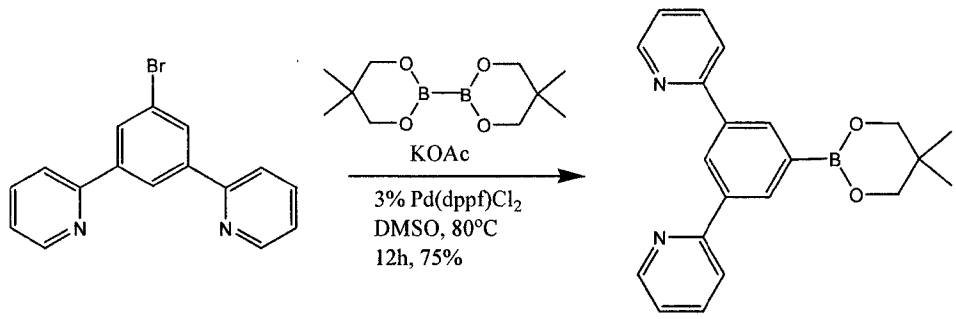

Scheme 7: Borylation to generate dpb boronic ester 9.

The Suzuki cross-coupling between bromopyridyl-capped dioxocyclam **3** and boron diester **9** was again efficient and clean, yielding dpb-capped dioxocyclam **8** in 79% yield. As discussed above, lower Pd catalyst loading obviate much of the purification by decreasing the source of the primary impurity. This results in higher recovery and hence somewhat better yields relative to the terpy variant.

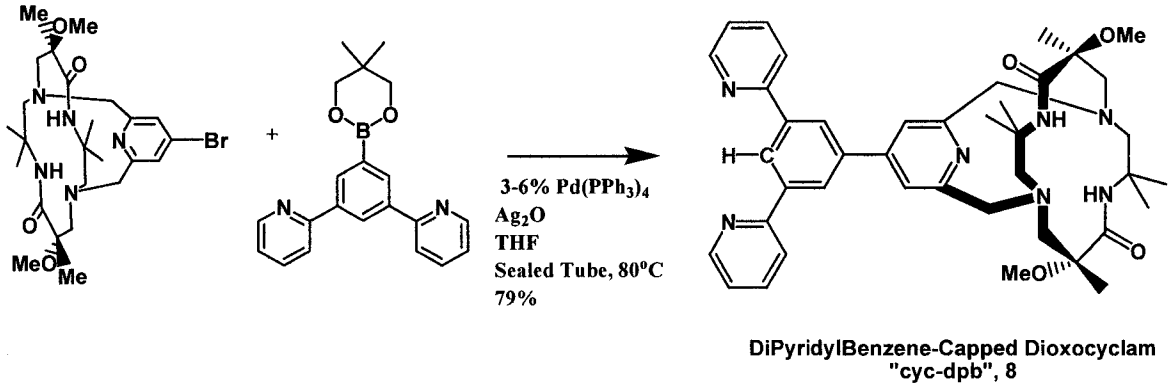

Scheme 8: Suzuki Coupling to generate dpb-dioxocyclam 8.

[Ru^{II}(cyc-dpb)(terpy)](PF$_6$) ("CDRTP") (11)

With this new bifunctional ligand in hand, cyclometallation studies began. Slight modification of Collin's procedure[90] afforded organometallic complex **11** in good yield in a straightforward manner as shown in scheme 9.

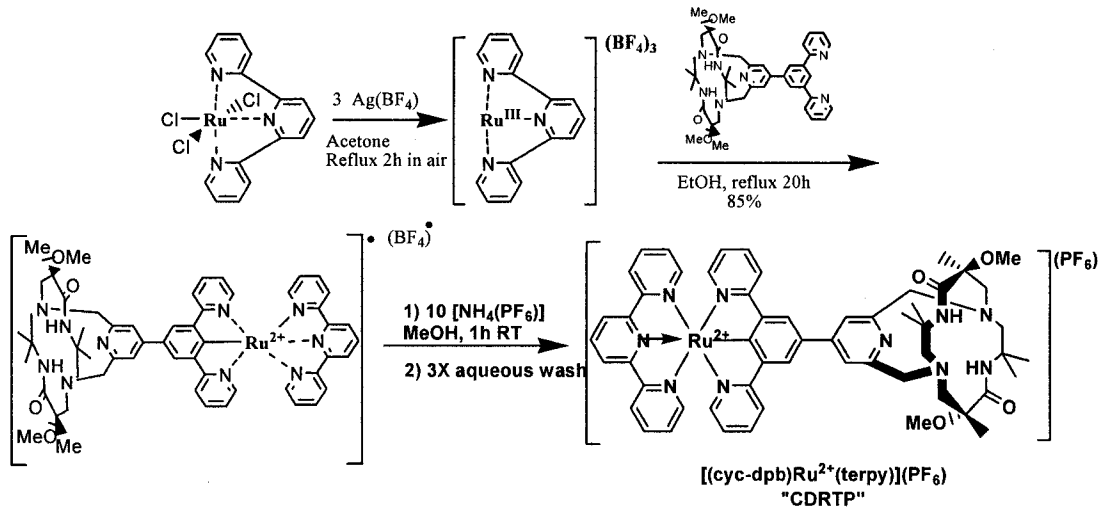

Scheme 9: Synthesis of CDRTP, 11.

Thus, $Ru(terpy)Cl_3$ was dehalogenated with silver tetrafluoroborate to form $Ru(terpy)(BF_4)_3$. The borate counterions are relatively loosely coordinated, and thus this likely exists as an acetone solvate. It is much more reactive than the trichloride, but is stable enough to handle on the benchtop. Addition of the ligand **8** in degassed absolute ethanol and refluxing overnight yields the desired product **11** as shown. This conversion requires reduction of the Ru(III), coordination to the chelating dpb ligand, and insertion into the aromatic C-H bond. Chromatography of the BF_4 salt, followed by anion exchange afforded the hexafluorophosphate salt in good yield (76% isolated)

The extra stability afforded by this cyclometallation is that the strong carbon-metal σ-bond, in addition to the chelate effect, removes the problem of ligand scrambling observed with terpy ligands. Of course, the terpy ligand in this complex may become dissociated under extreme conditions; but since the dpb ligand should remain bound to the metal center, a free terpy could only exchange places with another terpy, rendering no net change in the bulk properties of the solid. Bis-cyclometallated dpb Ru compounds are not found in the literature, and attempts to form them in my hands resulted in

reduction and subsequent decomposition, likely a result of increased electron density at the metal center relative to nitrogen donors.

This material is a robust, stable, deep red solid. Given its utility as a building block, it was synthesized repeatedly on moderate scale, and crystallization was attempted repeatedly. Identification of crystals suitable for diffraction was difficult because the compound and its solutions are very intensely colored. Eventually, layering of ether onto a saturated acetone solution of the compound afforded large blocky crystals that appeared well-formed. However, several attempts were made before a crystal was found with acceptable diffraction. This problem was well-precedented. Sauvage, who first synthesized dpbH[91], was only able to obtain a crystal structure of one of its complexes with difficulty. He noted that the crystalline compound is unstable due to loss of acetone from the lattice, which breaks the crystals when removed from solution. In his case, low temperatures were sufficient to retard this decomposition. Compound **11** indeed proved to be an acetone adduct in the crystalline state, containing one equivalent acetone and another, highly disordered solvent. In fact, NMR studies (see experimental section) revealed that all diamagnetic Ru complexes studied herein occlude acetone when dissolved in that solvent.

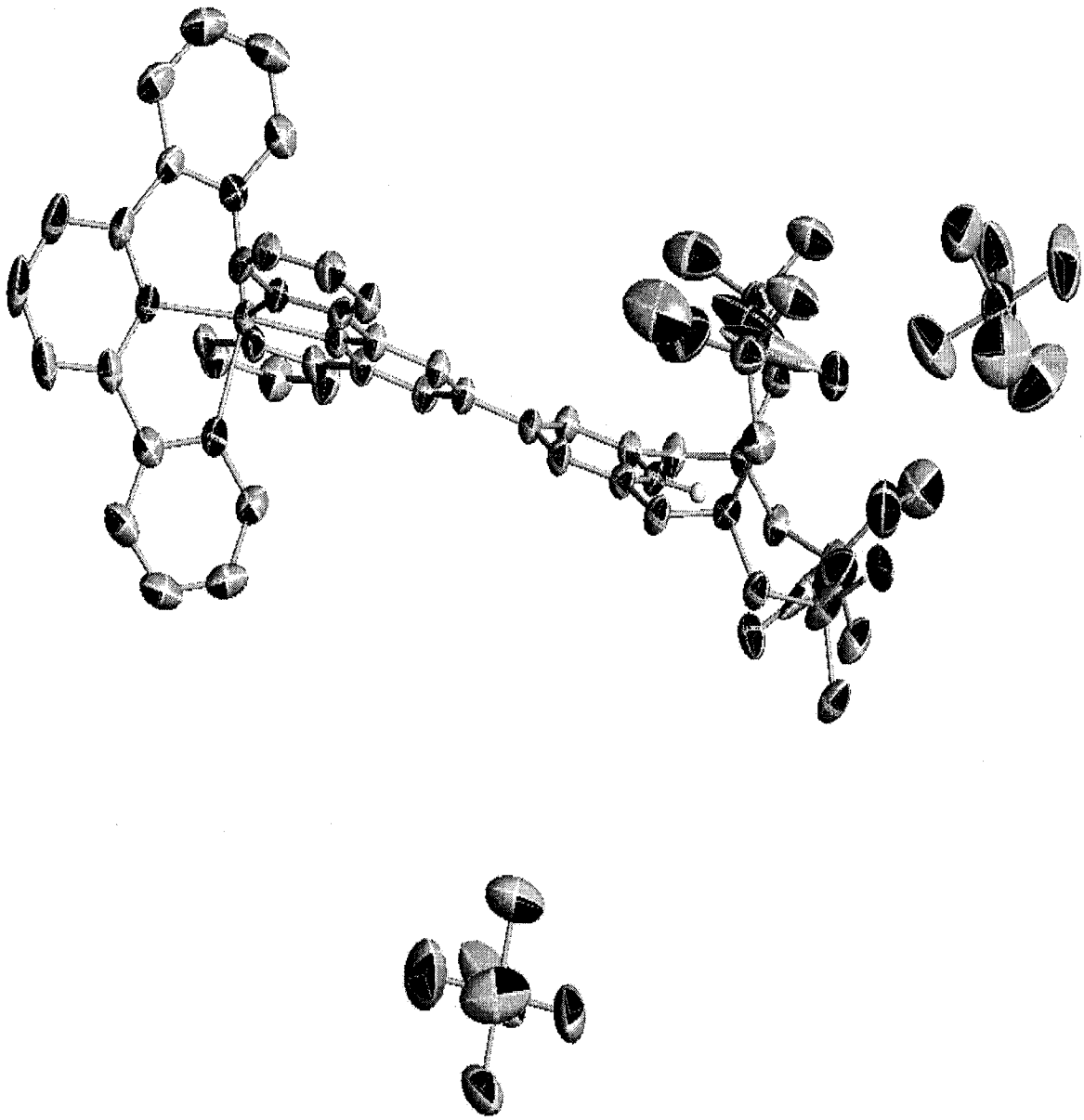

Figure 5: Thermal Ellipsoid Plot of [11(HPF_6)].

The compound **11** crystallized in the monoclinic space group P2(1)/c, with distorted octahedral coordination around the ruthenium center as seen in figure 5. The cyclometallated ligand exhibits a 1.947 Å Ru(1) – C(1) bond length, typical of dpb compounds.[92] The structure clearly shows one equivalent of coordinated acetone, and another, highly disordered solvent molecule, (common with cyclometallated ruthenium complexes). One major facet stands out clearly from the atom map: the crystallized

product contains two PF_6 counterions per Ru center. Closer examination allowed actual location of a proton on the pyridine nitrogen in the cyclam cavity, with an N(10) – H(10) bond length of 0.934 Å. This configuration appears to be extensively stabilized by hydrogen bonding involving primarily the two dioxocyclam amine nitrogens N(6) and N(7), with interatomic distance of 2.266Å and 2.237Å, respectively. These are consistent with the shortest of weak hydrogen bonds (H---B = 2.2 – 3.2 Å).[93] Further, both amide nitrogens, N(9) and N(8) may have very weak hydrogen bonding to the pyridinium proton, with H---B distances of 2.922Å and 3.197Å, respectively. The significant weakening of the second amide nitrogen interaction is due the associated amide carbonyl oxygen, O(2), having a H----B distance of 2.639Å to the proton, providing further stabilization. Although this was not observed with the second amide carbonyl group, both amide groups were somewhat disordered, perhaps as a result of isomerization of the hydrogen bonding interactions. It is clear, however, that the dioxocyclam cavity provides numerous hydrogen bonding interactions that stabilize the protonated pyridinium. Indeed, capped cyclams have been referred to as "proton sponges."[94] Although dioxocyclams are less basic, the presence of five basic sites constrained in close proximity yields relatively high affinities for protons. Alcock and Busch have identified this characteristic in cyclam systems and discovered that constrained cyclams only complex Li, Ni, and Cu effectively in protic solvents. However, in rigorously aprotic conditions, they react with Cr, Mn, Fe, Co, Ni, Cu, and Zn, often in unusual and variable oxidation states. Thus, the protonation of this capped dioxocyclam should be a facile process, and perhaps explains the reluctance that capped dioxocyclams exhibits towards metal complexation. However, it is not clear that this crystal represents the bulk state of

the product (unfortunately, insufficient quantities were obtained in this crystallization, so further analysis was not obtained on this particular batch). ^{1}H NMR does not reveal this proton in any of the other isolated material, crystalline or not, though the signal may be broad and thus not observed. Further, the primary peak in the MS is for (M-PF_6) (M=non-protonated, mono-phosphate salt). ($M + H^+$) is much smaller by comparison. If the bulk product were protonated, this peak ($M + H^+$) should arise simply and abundantly by loss of PF_6. The observed major peak would require loss of H^+ and 2 PF_6 anions from the protonated product observed in the crystal structure. Hence, it is proposed that, either under anion exchange and isolation conditions (involving aqueous NH_4PF_6), or on standing (with residual quantities of the ammonium hexafluorophosphate present), a small portion of the complex becomes protonated. This salt is more crystalline than the bulk, and thus was isolated. It is not proposed that the major isolated material is present in this form. Crystallographic data tables are contained in the appendix at the end of this chapter.

[Co^{III}(CN)(cyc-dpb)(terpy) Ru^{II}] ("RuCo") (12)

Thus high-yielding metallation of the polypyridyl functionality of this bifunctional ligand was established. The next objective was to coordinate a metal in the dioxocyclam cavity of the molecule. Investigations have been ongoing in this regard for some time, pioneered largely by Angela Reiff[95] and Dr. Eva Garcia-Frutos for simply capped dioxocyclams without appended polypyridine functionality. Finally, after screening a large number of cobalt salts in a variety of conditions, it was discovered that microwave irradiation of capped cyclams in the presence of an excess of $Co(OAc)_2 \cdot 4(H_2O)$ and Hunig's base in methanol allowed formation of the cobalt-dioxocyclams in moderate

yield. Interestingly, other cobalt sources were not effective, and simple heating in a variety of solvents for weeks on end yielded no conversion to product. Given the use of a hydrated cobalt starting material and methanol which was not rigorously dried, the "proton sponge" effect described above may be an issue here.

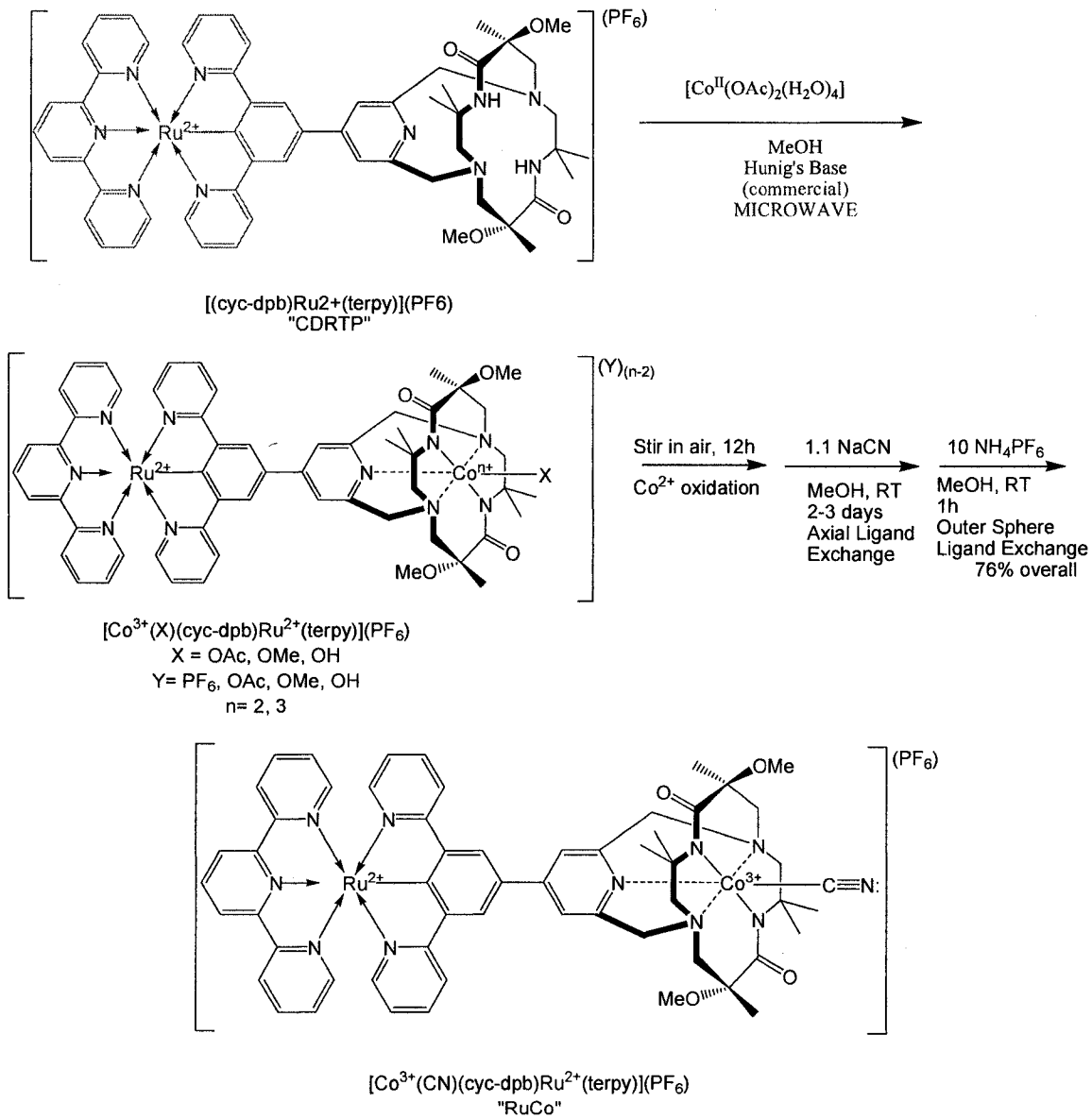

Scheme 10: Synthesis of RuCo(CN)heterobimetallic compound 12.

This microwave methodology translated directly to the cyclometallated Ru product **11**, yielding the desired product **12**, shown in scheme 10. Given the inhomogeneous field

employed in the household microwave ovens utilized in this synthesis, results were somewhat unpredictable. On the whole, however, the sample was exposed to intense temperatures and pressures, which occasionally resulted in minor explosions. However, it was even possible in this event to recover unreacted, undecomposed starting material. This is a testament to the robust nature of the Ru(cyclam-dpb) building block, and bodes well for its integration into useful arrays. Although this synthetic route is somewhat cumbersome and variable, it is exceptional in that it allows access to hetero-bimetallic polypyridyl/dioxocyclam building blocks for further investigation. As with other capped dioxocyclams, no conversion was observed after refluxing the same starting materials for over two weeks. The product from microwave reactions is isolated as a mixture of hydroxide, methoxide, and acetate ions axially coordinated to the Co, but is readily converted to the discrete Co(III)cyano complex by stirring in air overnight, then reacting with 1.1 equivalents sodium cyanide at room temperature in methanol. Finally, anion exchange with NH_4PF_6 in methanol for 2 hours, followed by washing with deionized water and collection on a centrifuge yields the product shown in the figure below in overall 76% yield. Mass spectral evidence clearly shows the product **12**, which has further been characterized by NMR, IR, and UV-vis techniques. The cyano group further offers the capability of bridging metal centers, which may be exploited for the production of arrays.

Positive electrospray mass spec demonstrated the presence of the $(M - (PF_6)^-)$ ion (calculated *m/z* 1122.32; found 1122.4), and the isotopic distribution clearly shows that both cobalt and ruthenium are incorporated in the product. The proton NMR spectrum reveals the absence of both amide protons, consistent with deprotonation and

complexation of cobalt A dramatic shift in the amide stretching frequency is observed in the FTIR spectrum (1652 to 1569 cm^{-1}), typical for deprotonated, metal-complexed dioxocyclam amides.

$[Cu^{II}(cyc\text{-}dpb)(terpy)Ru^{II}](PF_6)$ (13)

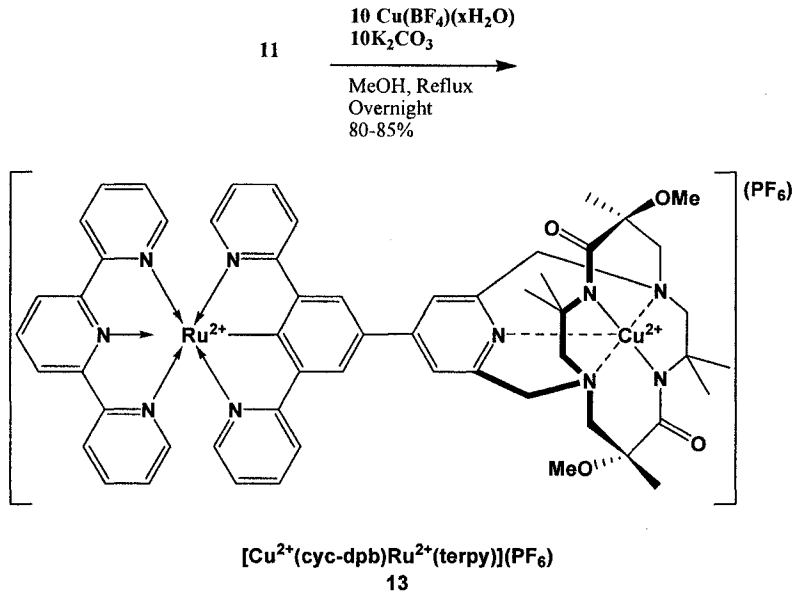

Scheme 11: Synthesis of Copper/Ruthenium bimetallic product 13.

To allow access to a multitude of building blocks, it became important to investigate other metals which could coordinate the macrocyclic portion of the molecule. Towards this end, organometallic intermediate **11** was subjected to cupration conditions previously investigated in the Hegedus group[96]. Thus, simply refluxing the cyclometallated starting material overnight in methanol with an excess of copper (II) tetrafluoroborate and potassium carbonate afforded copper complex **13** in high yield (90-97%) after anion exchange and column chromatography as illustrated in scheme 11. The resultant hetero-bimetallic product is robust and stable. The synthesis is gratifyingly

simple and straightforward relative to the cobalt variant described above. Initially, however, this target was considered less interesting than the mixed cobalt/ruthenium species, due to the known reversible redox properties of cobalt. In practice, as will be seen shortly, these are not operative in this ligand environment. Further, capped copper dioxocyclams exhibit interesting reversible redox chemistry to be discussed in the section covering electrochemistry. Thus, these species may prove interesting and useful in spite of the fact that capped copper dioxocyclams were previously thought to only show irreversible oxidations. One fixed design limitation, though, is the fact that copper will not assume an octahedral coordination sphere. As a result, coordination of axial ligands to promote further elaboration of metallo-polymers or arrays is not likely, unlike with the cobalt analog.

[(cyclam-dpb)Ru^{II}(cyclam-terpy)](PF$_6$) ("(CD)R(CT)P") (14)

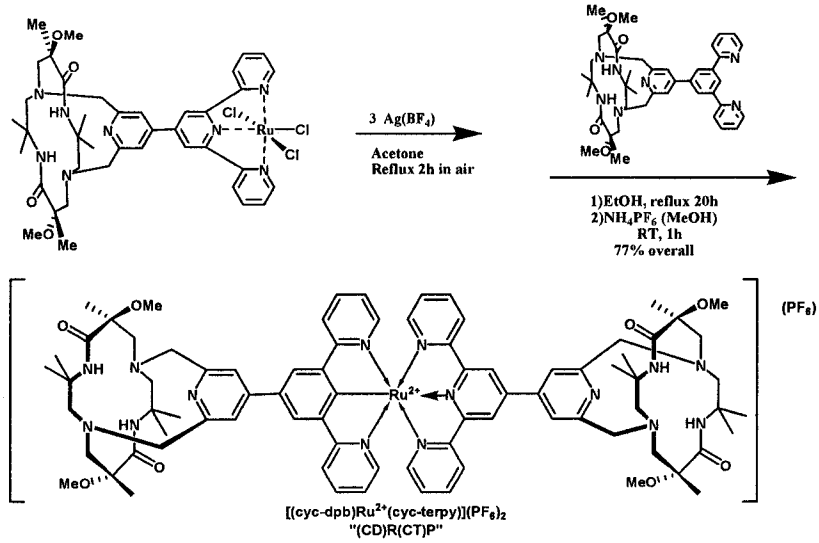

Scheme 12: Synthesis of heteroleptic bis(dioxocyclam) 14.

The cyclometallating polypyridyl/dioxocyclam ligand has been proven applicable for coordination in both ligating sites. Recently, Hegedus *et al.*[97] demonstrated methodology for coordinating metallated dioxocyclams similar to these to complexes including ruthenium pthalocyanines via bridging cyanides with some success. The cobalt and copper bimetallic species and their derivatives might prove useful in such arrays. However, it should prove possible to construct metallopolymers based on other strategies as well. Thus, the bimetallic complexes discussed thus far can only be extended in one direction; they are effectively capped on one end by (unfunctionalized) terpyridine, with no chance for further coordination. However, functionalized terpy ligands can allow propagation of the metallopolymer in a second direction. For this reason, a hybrid ruthenium complex of the original terpy-capped dioxocyclam with the cyclometallating dpb-capped dioxocyclam was investigated. As in the earlier variant "cdrtp" **11**, employing unsubstituted terpy, this eliminates the problems of ligand scrambling associated with non-cyclometallating ligands. Here, however, it has the benefit of generating two cyclam binding pockets that would be expected to exhibit somewhat distinct reactivity from one another. In other words, the electronics of a metal coordinated in the macrocycle bound to the cyclometallating ligand should be somewhat different from the case on the terpy-capped half of the molecule. Such subtle asymmetric differentiation could be useful in certain application. The synthesis is exactly analogous to that employed for cdrtp, but the yields are marginally higher here. This last fact is likely due to faster elution on chromatography columns, whereas the more polar **11** is somewhat more difficult to recover.

Attempts Towards Trimetallic Species

With the bis(polypyridine-dioxocyclam)Ru complex in hand, initial studies were made regarding the complexation of metals into the macrocyclic cavities. First attempts were made utilizing microwave irradiation of cdrctp **14** with cobaltous acetate hydrate and Hunig's base. TLC indicated that the starting material was consumed, and a discrete new product was formed (R_f = 0.6 on neutral Al plates with 10% MeOH/CH_2Cl_2, slightly less than starting material). However, the product gave broad proton NMR signals, and did not produce any characterizable ions under FAB or ES mass spec conditions. Ion exchange with cyanide did not improve the situation; the product now remained on the baseline in TLC and still failed to ionize in MS. In short, the products were intractable. This is not to suggest that the desired oligomers did not form; rather, that their isolation and characterization thus far remains elusive. In hindsight, this is not wholly unexpected. Cyanide linked oligomers[98] are known to be frequently intractable, with poor solubilities and ambiguous, mixed oxidation states.

Somewhat more promising results were achieved with the analogous cupration chemistry, shown in scheme 13. Refluxing the bis(dioxocyclam)Ru CDRCTP, **14**, overnight with excess copper (II) tetrafluoroborate in the presence of potassium carbonate in methanol consumed all of the starting material, and yielded two major products which were mobile on silica gel. Refluxing for up to three days did not change the products thus formed.

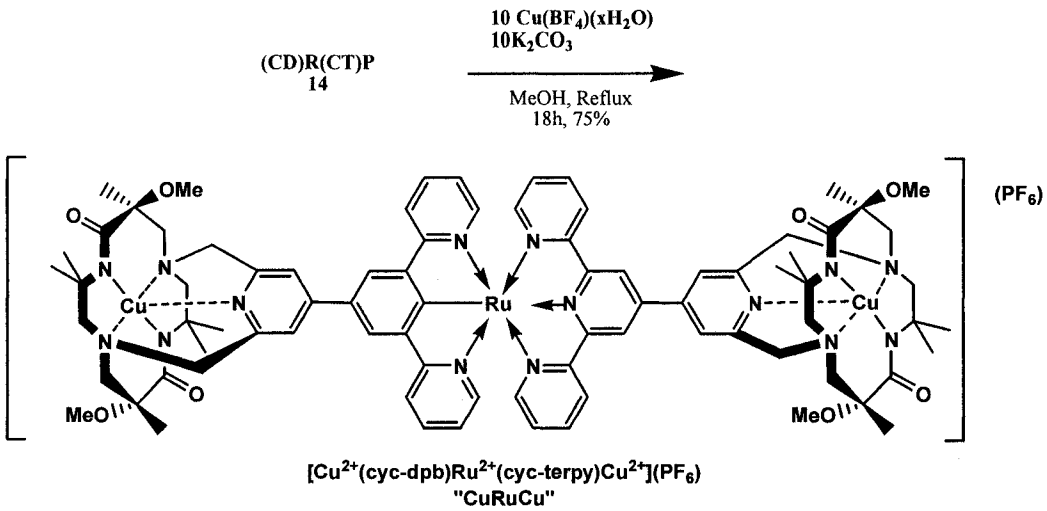

Scheme 13: Synthesis of trimetallic 15.

Mass spectral evidence showed formation of the desired trimetallic product **15** nearly as expected and shown. The expected isotopic distribution was observed, indicating incorporation of all three metals; the largest peak present is predicted ((+) electrospray) at *m/z* = 1783.49 (M + 1) for the structure **15** shown below, whereas 1782.13 was observed. Interestingly, this is NOT M + 1, but simply M^+, indicating that the complex as drawn is monocationic. This implies that one of the metals is oxidized (e.g. not all metals are in the (II) oxidation state as shown), and the parent ion forms by loss of an anion, rather than by gaining a cation. Consistent with this is the observation of a much larger distribution of peaks centered around 1928.07, which corresponds to the structure shown with the addition of another phosphate counterion and a proton (H^+ and $(PF_6)^-$; no net change in charge, thus still monocationic) (expected *m/z* = 1928.46). This corresponds to the bis-hexafluorophosphate salt as the neutral major product, which is protonated to form the observed parent cation. This requires that the neutral major product in fact contains one of the metals in an oxidation state one higher than that

shown, with an additional counterion to compensate. However, the possibility that this oxidation state change is an artifact of the MS experiment cannot yet be ruled out.

Thus this compound offers a fruitful area of study in order to establish its oxidation state, isolation procedures, and the ability of the metals to couple through these aromatic linkages. Once these details have been established, it will be possible to consider these species as trimetallic building blocks similar to the bimetallic species developed herein. At that point it may be feasible to address the complexation of other metals into the cyclam pocket to allow further extension of coordination arrays.

Electrochemical Studies

One of the goals of this project was to design bifunctional ligands containing dioxocyclams covalently linked to polypyridyl functionalities, and investigate the metal binding properties of both groups. Once this had been achieved, the question of the ability of the metal centers to "communicate" with each other, i.e. exhibit strong electronic coupling, arose. Cyclic voltammetry (CV) was selected as a convenient method to probe for this interaction. Professor Elliott in the CSU chemistry department provided instrumentation and expertise towards these ends. Utilizing this opportunity, I have screened numerous mono- and multi-metallic (Co and Cu) mono- and bis-dioxocyclams[99]. Unfortunately, in no case was the expected evidence forthcoming. While there is precedent for coupled metal centers which communicate and yet appear to yield only one redox wave,[100] this is somewhat rare, and tends to indicate minimal electronic coupling. In other words, for symmetrical bis(dioxocyclams) with metals in

both cavities, one would expect two responses for each redox step, if the metals are strongly coupled. Since redox at one metal center would change the electronic environment of the second metal center, this should shift the potential for the second metal, creating two redox waves. Although, as mentioned, Vahrenkamp and others have observed exceptions to this, our results tend to indicate a low level of communication between metal centers in these systems. Nevertheless, investigation of the present complexes seemed warranted, particularly given the huge couplings known in dpb systems. Further, examination of several cobalt dioxocyclams revealed unexpectedly that the metal does not exhibit reversible reductive behavior. In all cases, an associated re-oxidation is observed, but separated by a wide potential margin. This suggests that reduction produces a labile Co(II) center which rapidly exchanges ligands; hence the same chemical species is not present to be re-oxidized, resulting in a wide potential separation between the related redox waves. Such behavior is in fact precedented[101] and has been rationalized in a similar fashion by other researchers. This is another manifestation of similar behavior described in the section on cobalt terpyridine complexes. Others have observed this behavior in closely related systems (Co(III) cyclam)[102] and attributed it to slow axial ligand exchange. In the CV experiment, it must be recalled that a large excess of supporting electrolyte (ionic species; here, tetrabutyl ammonium hexafluorophosphate) is required relative to the analyte. Hence in our case, if Co(III) is reduced to a labile Co(II) product, then ligand exchange, apparently even of the tightly bound cyanide, becomes rapid. Although this exchange proceeds rapidly, the presence of several orders of magnitude larger concentrations of alternative axial ligands means that very little cyanide is re-complexed before the return scan of the

electrochemical experiment. Hence, the molecule has undergone changes in addition to the oxidation state, and its re-oxidation thus occurs at a different potential, and is observed as "irreversible."

Although cobalt was somewhat disappointing in these regards (no reversible redox, and apparently no communication between metal centers), copper appears more promising than initially reported. Scott David in the Hegedus group had previously reported that copper complexes of capped dioxocyclams (from the centrosymmetric isomer) only exhibited irreversible oxidations. Interestingly, however, magnetic measurements did indicate coupling between the metal centers, illustrating that CV is not absolute in its determinations in this regard. My work more recently has shown that in fact these compounds have reversible reduction behavior. Guilard and Kadish[103] have concurrently studied similar systems in great detail and assigned this behavior to a Cu(II)-Cu(I) couple. Thus, copper dioxocyclams are enjoying renewed interest.

Investigation of the free ligand cyclam-dpb as a control revealed an irreversible oxidation at +1.55V (all data reported relative to SCE), and no other response within the solvent window. Similar behavior was observed with other capped dioxocyclam ligands (with and without complexed metals), so this appears to be related to the dioxocyclam, not the polypyridyl functionality itself.

Next, the homoleptic Ru(cyc-terpy)$_2$ complex **5** was investigated. Ruthenium terpyridine complexes, both plain and simply-substituted have been extensively studied.[104] This complex undergoes a quasi-reversible oxidation centered at $E_{1/2}$= +1.3V (ΔE = 95 mV). This is essentially unchanged from the value for unsubstituted tpy complexes. The heteroleptic variant, Ru(cyc-terpy)(terpy), **7**, was not isolated in pure

form, so was not analyzed; however, nearly identical redox behavior would be expected, as substituents apparently have negligible effect on the metal-based electrochemistry.

Next, the cyclometallated CDRTP, **11**, was investigated. Collin and Sauvage[105] have compared Ru complexes of ligands of this type directly with their terpy analogs, and my results were in line with their precedent. Thus, a quasi-reversible oxidation is observed at $E_{1/2}$= 0.65V (ΔE = 100 mV), assigned to the Ru(III-II couple). Recall that the Ru(dioxocyclam-terpy)$_2$ complex exhibits this oxidation at 1.3V. Thus, the cyclometallated variant is more readily oxidized by approximately 0.65V. This is a dramatic demonstration of the enhanced electron density at the Ru metal center in the cyclometallated complexes, which in turn makes their oxidation more facile. This is yet another advantage of these second generation ligand systems. Given that most potential applications involve photoexcitation of the Ru center to generate a reducing equivalent, enhancement of ground-state reductive capacity should be beneficial. In addition, a quasi-reversible reduction is observed at E_P= -1.61V (ΔE = 160 mV), which may tentatively be assigned to Ru(II-I) couple. One further wave is observed at E_P= -2.16V, but this is approaching the edge of the solvent window, so the implications are as yet unclear.

The extended analog, CDRCTP, **14**, as expected, exhibits very similar behavior. The quasi-reversible oxidation occurs at $E_{1/2}$= 0.63V (ΔE = 98 mV), and the quasi-reversible reduction occurs at E_P= -1.44V (ΔE = 100 mV). Again, one further unassigned quasi-reversible wave is observed near the end of the acetonitrile solvent window, this time at E_P= -1.97V (ΔE = 100 mV) . Thus, within experimental error, the Ru center does

not appear to be electronically perturbed by the presence of substituents on the coordination terpy. This is consistent with NMR data as described above.

With the electrochemical properties of the polypyridyl segment firmly established, the next goal was to investigate the mixed-bimetallic systems. Analyses of pure "RuCo(CN)", the discrete bimetallic complex **12**, were thus performed as shown in figure 6. Interestingly, the CV simply reveals the redox waves of the individual components, with negligible disturbance from their behavior as separate entities. Thus, the Ru(III-II) quasi-reversible oxidation is observed here at $E_{1/2}$= 0.62V (ΔE = 92 mV), and the Ru(II-I) quasi-reversible reduction is observed at $E_{1/2}$= -1.51V (ΔE = 110 mV). The cobalt electrochemistry is identical to numerous cobalt dioxocyclams without additional metal appended: an essentially irreversible reduction (presumably CoIII-II) at E_P= -1.24V, and an associated, broad return oxidation centered at approximately 0.0V. The coupling of these two peaks is clearly illustrated in figure 6. The potential sweep begins in the anodic direction, beginning at -400 mV. No oxidation is observed at 0 V. After the ruthenium oxidation, the scan direction is reversed, allowing irreversible reduction of the cobalt center to form a Co(II) complex. When the scan direction is again reversed to the anodic direction, an oxidation is now observed at 0 V. This wave only appears after a cathodic scan to at least E_p for the Co reduction, consistent with oxidation of the just-formed Co(II) center. "Irreversibility" (very large ΔE) was observed with all cobalt dioxocyclams studied, and the peaks were observed at nearly identical potentials. This behavior is well precedented for other Co macrocycles[106] and is attributed to the lability of the Co(II) center. Rapid ligand exchange alters the electronic environment of

the metal center, and thus shifts the re-oxidation to different potentials, preventing a truly reversible redox couple.

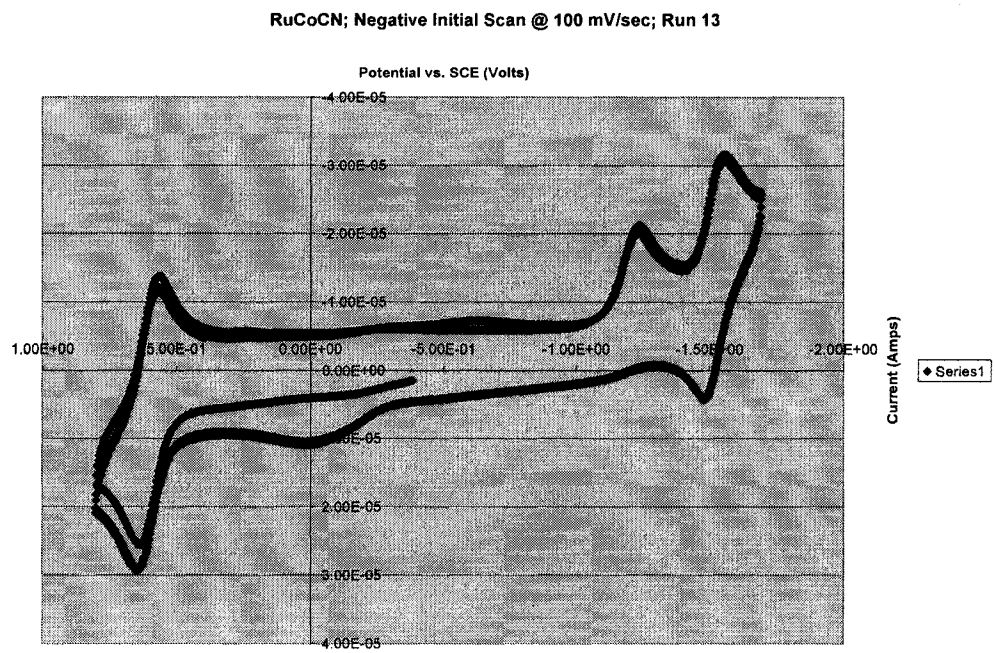

Figure 6: Cyclic voltammogram of RuCo(CN), 12

As discussed previously, this behavior does not preclude the possibility of intermetallic interactions, but does suggest that metal-metal coupling is rather weak.

Finally, "RuCu", **13**, the copper analog of **12** was investigated as illustrated in figure 7. The Ru(III-II) quasi-reversible oxidation couple is again cleanly observed at $E_{1/2}$= 0.65V (ΔE = 145 mV). The quasi-reversible reduction assigned to Ru(II-I) appears at -1.53V (ΔE = 150 mV), also very close to the copper-free analog **11**. Irreversible oxidation is again observed at a peak potential of +1.56V, similar to other complexes (and the free dioxocyclam ligand).

The remaining reductive behavior is more complex. An irreversible reduction is observed at E_p= -1.41V. This is nearly identical in potential to that observed in other

copper dioxocyclams studied in the Hegedus group, and close to the values reported by Guilard for simpler copper cyclam systems (-1.14V vs SCE). However, the reduction is now completely irreversible, and split into two peaks. In addition, the peak integration is quite a bit smaller than would be expected for a one electron process, suggesting that this may be an artifact of some trace impurity (either present in the product or produced under electrochemical conditions). This potential is strikingly close to that for oxygen reduction to superoxide, and may indicate catalysis of this process. Although solutions were purged with N_2 before analysis, and CV's were conducted under a flow of inert gas, trace oxygen contamination cannot be completely ruled out, and likely explain this response.

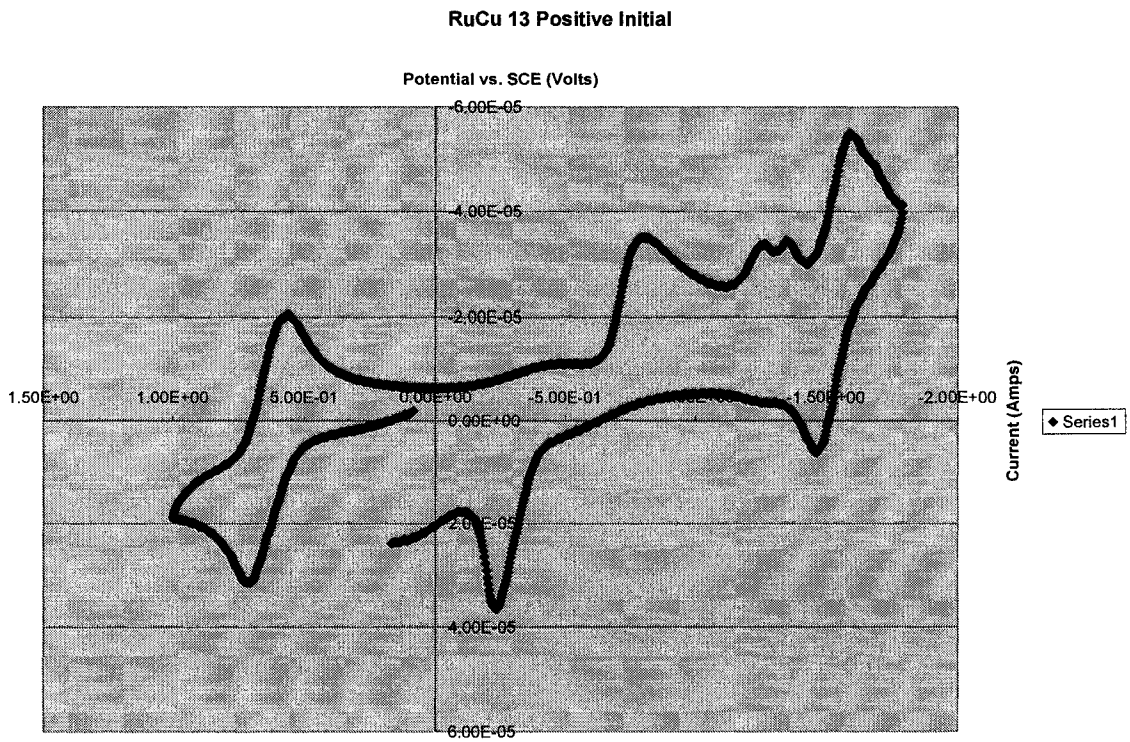

Figure 7: Cyclic Voltammogram of "RuCu", 13.

More interesting, however, is the irreversible reduction centered at E_P= -0.90V, and its associated oxidation at E_P= -0.44V. These peaks, unlike those centered at -1.41V, demonstrate current flow consistent with one electron processes. It is tempting to

propose that these peaks corresponds to the Cu (II – I) couple, occurring at substantially less negative potential and greater ΔE than in the cases without Ru covalently appended, implying metal-metal communication. The results are complex, however, and this conclusion cannot be drawn with certainty. It is clear, however, that the electrochemical behavior of the two covalently bound fragments is substantially different from the sum of its two parts. This is in contrast to the behavior observed with **12**, and illustrates that the two metal centers influence each other's physical properties. As such, this compound may warrant further study.

VI. Conclusions and Future Work

Several of the key targets of this project have been achieved. Thus, the coordination chemistry terpyridyl groups appended to dioxocyclams has been explored for the first time. Ru homoleptic (dioxocyclam-terpyridine)$_2$ complexes have been successfully synthesized, characterized, and their electrochemical properties explored. Heteroleptic Ru(dioxocyclam-terpy) complexes proved fluxional and difficult to purify. Cobalt analogs were also accessible, though much less robust, and prone to ligand exchange.

Building on this knowledge, a second generation ligand target was efficiently synthesized in good yield, replacing the pyridine nitrogen of the central aromatic ring in the appended terpy with a C-H group. These dpb-appended dioxocyclams were cleanly cyclometallated by ruthenium, generating heteroleptic Ru complexes which do not re-exchange, even under drastic conditions. Furthermore, the Ru complexes have favorable

electronic properties (allowing substantially improved metal/metal coupling, and more facile oxidation) relative to their terpy analogs. These materials are readily purifiable, and available in high yields and relatively large quantities; their handling is much simpler than the more ionic terpy complexes. Although homoleptic dpb complexes are not known (metal reduction is implicated), a coordination of two dioxocyclam functionalities was achieved by an approach involving coordination of dioxocyclam-terpy to ruthenium followd by cyclometallation by cyclam-dpb. This product then allowed initial studies attempting to coordinate metals into both cyclam cavities. While cobalt was somewhat ambiguous in this regard, copper appears more promising.

Complexation of copper and cobalt by (dioxocyclam-dpb)ruthenium intermediates resulted in the successful synthesis of heterobimetallic mixed, covalently bound polypyridyl/dioxocyclam products. Although initial studies of the physical properties have not conclusively demonstrated coupling of the metal centers, they certainly warrant further study. These bimetallic species may be thought of as robust "monomers", or subunits, which are sufficiently stable, characterizable, and discrete to now allow investigation of their use in arrays. Possible applications include coordination to ruthenium pthalocyanines, as has been successfully performed with similar systems in the Hegedus labs.

Future goals include screening other metals for complexation by the polypyridyl fragments, including Os, Fe, Pd, Pt. This will allow access to a diversity of arrays. Further, a key goal is a route to Ru-dioxocyclam complexes. Considerable synthetic effort has been expended by myself and numerous other Hegedus group members along these lines, but has yet to be rewarded with success. If this methodology is developed,

and applied to the cyclometallated dpb Ru complex presented here, mixed-valence species could be generated that are predicted to have novel properties. Fe is another target along these lines. Finally, it will be important to begin to investigate the ability to form larger supramolecular constructs utilizing the entities described herein as discrete building blocks.

VII. Experimental Section

General Procedures. THF and diethyl ether were distilled from sodium-benzophenone ketyl. CH_2Cl_2 and hexanes were distilled from CaH_2. Triethylamine was distilled from NaOH and stored over 4Å molecular sieves. Methanol was dried over molecular sieves. Acetonitrile was generally distilled over calcium hydride, but spectrophotometric grade solvent was used as received for electrochemical measurements. Commercially available reagents were used as received except where stated otherwise. Bromopyridine capped dioxocyclam (**3**) and terpyridine capped dioxocyclam (**2**) were prepared according to literature procedures[107]. All NMR spectra (300MHz for ^1H and 100 MHz for ^{13}C) were recorded in $CDCl_3$ or acetone-d_6. Chemical shifts are reported relative to residual non-deuterated chloroform (δ 7.27, ^1H) or $CDCl_3$ (δ 77.23, ^{13}C) in the former case, or to TMS (δ 0.0p) as an internal standard in the latter case. Although good quality proton spectra could be acquired with no special precautions, collection of useful carbon-NMR of all ruthenium containing species

required careful tuning of the probe. IR spectra were recorded on an Avatar 320 FT-IR. UV-vis spectra were recorded on an Agilent G1103A spectrometer. Electrochemical measurements were conducted with a Princeton Applied Research, model 75 universal programmer and a model 137 potentiostat, connected to an ADC. The data was then processed and analyzed using LabView software. The analyte was dissolved in a 0.1M solution of tetrabutylammonium hexafluorophosphate in dry, degassed acetonitrile, with measurements performed under inert gas flow. The working electrode was glassy carbon, the counter electrode was a Pt wire, and the reference electrode was SSCE. Potentials are reported relative to this reference. Data was obtained at a scan rate of 100mV/sec unless otherwise noted. X-ray crystallographic studies were performed on a Bruker Smart CCD diffractometer, and the intensity of the data set was integrated using Bruker SAINT software. Structures were solved using Bruker SHELXTL version 5.03 software. Microwave reactions were performed in a GE countertop microwave oven, model # JES1339WC, with a capacity of 1.3 ft^3 and an output of 1100 watts.

Dipyridyl Benzene-Capped Dioxoyclam (Cyc-dpb(H)) (8)

Synthesis An oven dried 20 mL pressure tube equipped with stir bar was cooled under nitrogen flow, and then charged with 10 mL freshly distilled THF via syringe. The solvent was degassed by sparging inert gas for 15 minutes. Dipyridyl phenyl boronic ester **9** (see scheme 5) (93 mg, 0.27 mmol), 4-bromopyridyl capped cyclam **2** (120 mg, 0.22 mmol), palladium tetrakis(triphenylphosphine) (7 mg, 0.006 mmol, 3mol%), and silver oxide (Ag_2O) (140 mg, 0.61 mmol) were weighed swiftly and added under nitrogen flow. The tube was then sealed with a screw cap fitted with an o-ring, and placed in an

oil bath at 80^0 C, where stirring was maintained for 15 hrs. The crude mixture was filtered through a pad of Celite, and concentrated *in vacuo* , then loaded onto a 1 x 17 cm neutral Alumin column packed with 25% hexane: 75% ethyl acetate. The eluent polarity was increased along a gradient until pure ethyl acetate and finally 10% MeOH: 90% ethyl acetate was used to wash the remaining product off the column. This yields relatively pure material still somewhat contaminated with PPh_3O (recovery weight higher than theoretical yield). Although this is sufficiently pure for use as an intermediate, analytically pure material may be obtained by further chromatography, this time over silica. A 1.0 x 15 cm silica gel column is slurry packed with CH_2Cl_2, and the eluent is gradually increased in polarity until 10% MeOH is used to flush the column, yielding (120 mg, 79%) **8** as a white powder.

^{1}H NMR ($CDCl_3$) δ 9.14 (s, 1H), 8.78 (d, J= 4.8 Hz, 2H), 8.62 (s, 1H), 8.38 (d, J= 1.5 Hz, 2H), 8.19 (s, 1H), 7.94-7.81 (m, 4H), 7.37-7.31 (m, 4H), 4.32-4.05 (m, 4H), 3.44 (s, 3H), 3.25 (d, J=13.5 Hz, 1H), 3.01-2.90 (m, 5H), 2.64-2.58 (m, 4H), 2.42 (d, J=14.4 Hz, 1H), 1.50 (s, 3H), 1.46 (s, 3H), 1.39 (s, 3H), 1.34 (s, 3H), 1.23 (s, 3H), 1.16 (s, 3H)

^{13}C NMR ($CDCl_3$) δ 173.53, 172.91, 163.54, 159.17, 156.79, 150.04, 149.63, 141.05, 139.65, 137.21, 126.26, 122.95, 121.09, 117.34, 117.17, 82.67, 79.70, 74.52, 72.83, 69.29, 67.35, 65.85, 64.80, 55.96, 54.91, 51.93, 50.44, 29.47, 27.92, 26.28, 25.67, 23.67, 23.53, 19.27.

FT-IT (film) 3235, 2985, 2930, 2826, 1657, 1585, 1561, 1519, 1453, 1368, 1132, 1102 cm^{-1}

LRMS (FAB^+, *m/z*) calc'd for $C_{41}H_{52}N_7O_4$ ($M + H^+$) 706.41 found 706.5

$[Ru^{II}(Cyclam\text{-}Terpy)_2](PF_6)_2$ (5)

Synthesis An oven dried 20 mL pressure tube equipped with stir bar was cooled under nitrogen flow, and then charged with 6 mL ethylene glycol. The solvent was degassed by sparging inert gas for 15 minutes. Terpy-capped cyclam **2** (71 mg, 0.1 mmol) and $RuCl_3(xH_2O)$ (13 mg, 0.05 mmol) were added under nitrogen flow. The tube was then sealed with a screw cap fitted with an o-ring, and placed in an oil bath at 140^0 C, where stirring was maintained for 3 hrs. The crude mixture was then cooled, diluted with 20 mL deionized water, and then filtered through a pad of Celite. Excess NH_4PF_6 (81 mg, 0.5 mmol, 10 equivalents) was added to the filtrate, and the suspension stirred for 1 hour at room temperature to affect anion exchange. Addition of 20 mL more water and cessation of stirring cause precipitation of a deep red precipitate. This was collected on a centrifuge, and the resultant solid rinsed with 2 x 50 mL more deionized water. After decanting the supernatant, the product is taken up in acetone/ether , and concentrated *in vacuo* 3 times to remove water azeotropically. The resultant powder is dried on a vacuum line over P_2O_5 to yield 71 mg (79%) **5** as a deep red powder. Purification was achieved by loading the product onto a 1.5 x 18 cm neutral alumina column, and eluting with a gradient of 0 – 10% MeOH in CH_2Cl_2, yielding 55 mg (61%).

^1H NMR (Acetone-d_6) δ 9.59 (s, 4H), 9.07-9.00 (m, 6H), 8.22-8.00 (m, 10H), 7.78 (d, J=5.6 Hz, 4H), 7.33 (t, J=6.8 Hz, 4H), 4.45-4.26 (m, 8H), 3.29 (s, 6H), 3.13-2.91 (m,

10H), 2.70-2.50 (m, 6H), 2.67 (s, 6H), 2.12 (s, 6H; coordinated acetone), 1.43-1.09 (m, 36H).

^{13}C NMR (Acetone-d_6) δ 173.84, 172.94, 165.29, 161.58, 159.25, 157.01, 153.62, 146.74, 146.37, 139.32, 128.92, 126.08, 122.77, 118.23, 118.07, 83.41, 80.31, 74.74, 73.47, 69.81, 67.91, 66.64, 66.11, 56.13, 55.53, 55.18, 51.59, 50.77, 32.07(coordinated acetone), 26.39, 25.73, 23.71, 19.67.

FT-IR (film) 3237, 2969, 2931, 2828, 1699, 1655, 1604, 1521, 1456, 1407, 1368, 1132, 1103.

UV-vis (Acetonitrile) λ_{max} (ε) 276 (4.1 x 10^4); 313 (2.6 x 10^4); 492 (1.2 x 10^4)

LRMS (ES^+, *m/z*) calc'd for $C_{80}H_{101}F_{12}N_{16}O_8P_2Ru$ (M + H^+) 1805.63 found 1806.2; calc'd for $C_{80}H_{100}F_6N_{16}O_8PRu$ (M – $(PF_6)^-$) 1659.66 found 1659.27

$[Co^{II}$(Cyclam-Terpy)$_2](PF_6)_2$ (6)

Synthesis A 20 mL round bottom flask was equipped with a stir bar and charged with 3 mL MeOH. Terpy-capped cyclam **2** (71 mg, 0.1 mmol) and $Co(OAc)_2(H_2O)_4$ (13 mg, 0.05 mmol) were added as solids. The reaction instantly turns red. Stirring was maintained for 1 hour at room temperature (longer times up to 24 hours at room temp. did not improve yields). Excess NH_4PF_6 (81 mg, 0.5 mmol, 10 equivalents) was added to the crude reaction mixture, and the solution stirred for 1 hour at room temperature to affect anion exchange. The solution was concentrated on a Rotovap, then dried on a vacuum pump for 1 hr. The solid thus obtained was suspended in 50 mL water and then precipitate on a centrifuge. The product was thus rinsed with 2 x 50 mL more deionized

water. After decanting the supernatant, the product is taken up in acetone/ether , and concentrated *in vacuo* 3 times to remove water azeotropically. The resultant powder is dried on a vacuum line over P_2O_5 to yield crude material in nearly quantitative yield. Purification was attempted by loading the product onto a 1.5 x 15 cm neutral alumina column, and eluting with a gradient of 0 – 8% MeOH in CH_2Cl_2, yielding 45 mg (51%) **6**. Apparently, substantial decomposition occurs under these column conditions.

FT-IR (film) 3239, 2964, 2931, 2829, 1711, 1659, 1602, 1543, 1520, 1455, 1438, 1364, 1120, 1098, 1057.

UV-vis (Acetonitrile) λ_{max} (ε) 452 (2.5 x 10^3); 518 (2.6 x 10^3)

LRMS (ES^+, *m/z*) calc'd for $C_{80}H_{101}F_{12}N_{16}O_8P_2Co$ ($M + H^+$) 1761.65 found 1762.20; calc'd for $C_{80}H_{100}F_6N_{16}O_8PCo$ ($M - (PF_6)^-$) 1616.69 found 1616.20

$[Ru^{II}$(Cyclam-Terpy)(Terpy)$](PF_6)_2$ (7)

Synthesis An oven dried 50 mL round bottom flask equipped with a stir bar and reflux condenser was cooled under nitrogen flow, and then charged with 25 mL absolute ethanol containing 1 mL triethylamine as a reductant. Terpy-capped dioxocyclam **2** (100 mg, 0.14 mmol) and $RuCl_3$(terpy) (63 mg, 0.14 mmol) were added as solids. The reaction was then placed in a preheated oil bath and refluxed vigorously for one hour under nitrogen. The crude mixture was then cooled and filtered through a pad of Celite. Excess NH_4PF_6 (230 mg, 1.4 mmol, 10 equivalents) was added to the filtrate, and the solution

stirred for 1 hour at room temperature to affect anion exchange. This mixture was then dried *in vacuo*, then washed and collected 3X with 50 mL deionized H_2O on a centrifuge. This was collected on a centrifuge, and the resultant solid rinsed with 2 x 50 mL more deionized water. After decanting the supernatant, the product is taken up in acetone/ether , and concentrated *in vacuo* 3 times to remove water azeotropically. Chromatography (best conditions involved CH_2Cl_2/MeOH on neutraul Al of the many systems tried) and crystallization in various solvents failed to completely separate the desired product from the homoleptic bis(cyclam-terpy)Ru(II) product, though the other homoleptic product could be successfully removed.

LRMS (ES^+, *m/z*) calc'd for $C_{55}H_{62}F_{12}N_{11}O_4P_2Ru$ ($M + H^+$) 1332.33 found 1332.13; calc'd for $C_{80}H_{100}F_6N_{16}O_8PRu$ ($M - (PF_6)^-$) 1186.36 found 1186.13

[(Cyclam-DPB)Ru^{II}(Terpy)](PF_6) (11)

Synthesis An oven dried 100 mL round bottom flask equipped with magnetic stir bar and reflux condenser was charged with 75 mL dry acetone, followed by Ru(terpy)Cl_3 (179 mg, 0.41 mmol) and Ag(BF_4) (237 mg, 1.22 mmol). The resultant suspension was placed into an oil bath and refluxed vigorously with stirring and without inert gas. After 2 hours, the mixture was cooled, filtered through a plug of Celite, and dried on a Rotovap. 200 mL absolute EtOH was degassed by sparging with N_2 for 30 minutes, then used to suspend the ruthenium intermediate in a 250 mL round bottom flask. DPB-capped

cyclam **8** (260 mg, 0.37 mmol) was then added as a solid under inert gas flow. The flask was fitted with an oven dried condenser sealed at the top with a rubber septum containing a N_2 inlet via a needle attached. The flask was covered with foil, placed in a preheated oil bath and reluxed for 20 hours with vigorous stirring. After this period, the flask was cooled, and stripped to dryness on a Rotovap. A 1.5 x 20 cm silica gel column was slurry packed with CH_2Cl_2 containing 1% TEA. The crude BF_4 salt was loaded with minimal MeOH and eluted in CH_2Cl_2 containing 1% TEA and a gradient of 0-10% MeOH. The purified borate salt is then dissolved in dry methanol with 5 equivalents NH_4PF_6 (301 mg, 1.85 mmol) and stirred for 1 hour to affect anion exchange, followed by removal of the solvent *in vacuo*. Washing with 3 x 50 mL deionized water with collection of the solid hexafluorophosphate salt on a centrifuge yields 332 mg (76%) relatively pure product. Additional purity is attained by chromatography over neutral alumina with 0-3% MeOH in CH_2Cl_2, affording 310 mg (71%) ultra pure product. X-ray quality crystal of the HPF_6 salt of this compound were obtained by layering diethyl ether onto a saturated solution of the product in acetone.

^{1}H NMR (Acetone-d_6) δ 9.13 (s, 1H), 9.03 (d, J=8.0 Hz, 2H), 8.88 (s, 2H), 8.70 (d, J=8.0 Hz, 2H), 8.49-8.39 (m, 4H), 7.87-7.73 (m, 6H), 7.24 (s, 4H), 7.11 (t, J=7.2 Hz, 2H), 6.79 (t, J= 8.0 Hz, 2H), 4.41-4.17 (m, 4H), 3.79 (s, 1H), 3.32 (s, 3H), 3.18-2.91 (m, 5H), 2.72 (s, 3H), 2.54 (m, 2H), 2.12 (s, 3H; 0.5 equivalent coordinated acetone) 1.48-1.11 (m, 18H)

^{13}C NMR (Acetone-d_6) δ 173.91, 173.03, 169.57, 164.27, 160.50, 160.12, 155.42, 153.84, 152.86, 151.87, 143.84, 136.59, 136.32, 133.60, 131.02, 127.52, 124.63, 123.46, 122.99,

121.04, 117.21, 117.09, 83.45, 80.37,74.78, 73.45, 69.79, 67.91, 66.78, 66.11, 56.16, 55.55, 55.31, 51.59, 50.76, 32.07 (coordinated acetone), 26.39, 25.77, 23.91, 23.73, 19.72

FT-IR (film) 3224, 2968, 2929, 2827, 1699, 1652, 1600, 1560, 1521, 1465, 1367, 1325, 1262, 1131, 1103, 1022.

UV-vis (Acetonitrile) λ_{max} (ε) 365 (3.1 x 10^4); 501 (2.5 x 10^4)

LRMS (ES^+, *m/z*) calc'd for $C_{56}H_{62}F_6N_{10}O_4PRu$ ($M + H^+$) 1185.37 found 1185.13; calc'd for $C_{56}H_{61}N_{10}O_4Ru$ ($M - (PF_6)^-$) 1039.39 found 1039.40

$[Co^{III}(CN)(Cyclam\text{-}DPB)Ru^{II}(Terpy)](PF_6)$ (12)

Synthesis An oven dried 20 mL pressure tube was cooled under nitrogen and charged with 6 mL MeOH which was degassed by sparging inert gas for 10 minutes. Freshly distilled *i*PrNEt$_3$ (0.34 mL, 1.94 mmol) was added by syringe, followed by degassing for 5 more minutes. Finally, CDRTP (**11**) (115 mg, 0.097 mmol) and $Co(OAc)_2$ $(H_2O)_4$ (242 mg, 0.97 mmol) were added quickly under a blanket of nitrogen. The solution was briefly sparged again, then sealed tightly with a screw cap. The reactor was irradiated in a commercial microwave oven for periods of two minutes at 20% power. The tube was cooled between each two minute session, and TLC (10% MeOH in CH_2Cl_2 ; neutral alumina plates) was used to monitor for disappearance of starting material periodically. Microwaving continued thusly until the starting complex was consumed. The crude mixture was diluted with methanol and filtered through Celite. The filtrate was stirred overnight open to air (to allow complete oxidation to Co^{III}). Rotary evaporation and vacuum drying yields 90 mg (71%) of the product with an acetate axial ligand on cobalt.

Ligand exchange is affected by dissolving the acetate product in methanol at room temperature in the presence of 2 equivalents sodium cyanide and stirring for 2 days. The crude product is filtered through Celite, then subjected to flash chromatography over neutral alumina with and eluent gradient from 0-10% MeOH in dichloromethane to yield the cyano product in 50-60% yield.

^{1}H NMR (Acetone-d_6) δ 9.09-9.06 (m, 4H), 8.74 (d, J=10.4 Hz, 2H), 8.51-8.38 (m, 4H), 7.85-7.75 (m, 4H), 7.33-7.27 (m, 4H), 7.14 (t, J=9.2 Hz, 2H), 6.86 (t, J=9.2 Hz, 2H), 5.99-5.95 (m, 1H), 5.21-4.75 (m, 4H), 3.87-3.58 (m, 4H), 3.39 (s, 3H), 3.28 (s, 3H), 3.14-3.00 (m, 4H), 1.72-1.40 (m, 18H).

^{13}C NMR (Acetone-d_6) δ 172.82, 169.12, 163.22, 160.96, 159.91, 155.35, 153.62, 152.77, 144.10, 136.41, 133.90, 128.44, 124.59, 123.39, 123.12, 122.73, 120.99, 116.29, 116.03, 82.47, 81.76, 80.14, 79.19, 71.07, 69.70, 68.88, 63.65, 63.13, 59.37, 55.49, 52.25, 51.98, 30.99 (coordinated acetone) 27.85, 27.45, 24.42, 23.20, 20.38

FT-IR (film) 2925, 1618, 1569, 1468, 1448, 1376, 1278, 1076

UV-vis (Acetonitrile) λ_{max} (ε) 279 (5.3 x 10^4); 314 (3.5 x 10^4); 398 (2.1 x 10^4); 501 (1.4 x 10^4)

LRMS (ES^+, *m/z*) calc'd for $C_{57}H_{59}CoN_{11}O_4Ru$ ($M-(PF_6)^-$) 1122.32 found 1122.4

[Cu^{II}(Cyclam-DPB)Ru^{II}(Terpy)]$(PF_6)_2$ (13)

Synthesis An oven dried 20 mL pressure tube equipped with stir bar was cooled under nitrogen and charged with 15 mL dry methanol. The solvent was sparged with inert gas for 15 minutes, and then charged with CDRTP **(11)** (50 mg, 0.038 mmol (assumes MW

of HPF_6 adduct) and 5 equivalents each $Cu(BF_4)_2(xH_2O)$ (freshly vacuum dried at 100^0C over P_2O_5) (45 mg, 0.19 mmol) and K_2CO_3 (26 mg, 0.19 mmol). The resultant suspension was degassed again briefly, then sealed tightly with a screw cap and lowered into an oil bath preheated to 80^0C, where it was stirred 18 hours. The crude mixture was then cooled, and stirred with excess NH_4PF_6 (62 mg, 0.38 mmol) for one hour. The solvent was then removed on a rotary evaporator, and the resultant solid was washed with 3 x 50 mL deionized water and collected on a centrifuge. The collected precipitate was dried over P_2O_5, yielding 45 mg (97%) bimetallic product **13**. Further purification could be affected by chromatography over neutral alumina utilizing a gradient of 0-8% MeOH in dichloromethane as the mobile phase.

FT-IR (film) 2970, 2928, 1699, 1670, 1580, 1467, 1448, 1381, 1354, 1278, 1069, 1022.

UV-vis (Acetonitrile) λ_{max} (ε) 314 (4.4×10^4); 389 (2.3×10^4); 500 (2.1×10^4)

LRMS (ES^+, *m/z*) calc'd for $C_{56}H_{60}CuF_6N_{10}O_4PRu$ ($M + H^+$) 1246.28 found 1246.00

$[Ru^{II}$(Cyclam-Terpy)(Cyclam-DPB)$](PF_6)$ (14)

Synthesis An oven dried 50 mL round bottom flask equipped with magnetic stir bar and reflux condenser was charged with 35 mL dry acetone, followed by Ru(cyclam-terpy)Cl_3 (91 mg, 0.1 mmol) and $Ag(BF_4)$ (58 mg, 0.3 mmol). The resultant suspension was placed into an oil bath and refluxed vigorously with stirring and without inert gas. After 2 hours, the mixture was cooled, filtered through a plug of Celite, and dried on a Rotovap. 100

mL absolute EtOH was degassed by sparging with N_2 for 30 minutes, then used to suspend the ruthenium intermediate in a 250 mL round bottom flask. DPB-capped cyclam **8** (64 mg, 0.091 mmol) was then added as a solid under inert gas flow. The flask was fitted with an oven dried condenser sealed at the top with a rubber septum containing a N_2 inlet via a needle attached. The flask was covered with foil, placed in a preheated oil bath and reluxed for 20 hours with vigorous stirring. After this period, the flask was cooled, and stripped to dryness on a Rotovap. A 1.5 x 20 cm silica gel column was slurry packed with CH_2Cl_2 containing 1% TEA. The crude BF_4 salt was loaded with minimal MeOH and eluted in CH_2Cl_2 containing 1% TEA and a gradient of 0-10% MeOH. The purified borate salt is then dissolved in dry methanol with 5 equivalents NH_4PF_6 and stirred for 1 hour to affect anion exchange, followed by removal of the solvent *in vacuo*. Washing with 3 x 50 mL deionized water with collection of the solid hexafluorophosphate salt on a centrifuge yields 115 mg (77%) relatively pure product.

^{1}H NMR (Acetone-d_6) δ 9.54 (s, 1H), 9.14-8.90 (m, 5H), 8.45-7.74 (m, 14H), 7.31-7.29 (m, 4H), 7.16 (t, J= 7.4 Hz, 2H), 6.79 (t, J=8.0 Hz, 2H), 4.45-4.18 (m, 8H), 3.67-2.51 (m, 28H), 1.47-1.11 (m, 36H).

^{13}C NMR (Acetone-d_6) δ 173.93, 173.03, 169.55, 165.26, 164.29, 161.40, 160.52, 160.16, 155.48, 154.40, 152.91, 151.80, 147.48, 143.62, 142.42, 136.79, 136.39, 131.40, 127.72, 125.01, 123.02, 121.40, 121.17, 117.89, 117.25, 83.45, 80.31, 74.85, 73.45, 69.79, 67.93,

66.67, 66.09, 58.11, 56.16, 55.55, 55.22, 53.56, 51.61, 50.76, 49.90, 47.09, 32.07 (coordinated acetone), 26.41, 25.77, 23.71, 21.93, 12.69

FT-IR (film) 3115, 2971, 2835, 1661, 1629, 1604, 1575, 1525, 1463, 1364, 1103, 1023.

UV-vis (Acetonitrile) λ_{max} (ε) 413 (2.5 x 10^4); 509 (2.9 x 10^4); 550 (2.9 x 10^4)

LRMS (ES^+, *m/z*) calc'd for $C_{80}H_{101}F_6N_{15}O_8PRu$ ($M + H^+$) 1658.67 found 1658.6; calc'd for $C_{80}H_{100}N_{15}O_8Ru$ ($M - (PF_6)^-$) 1512.69 found 1512.60

$[Cu^{II}$(Cyclam-DPB)Ru^{II}(Cyclam-Terpy)$Cu^{II}](PF_6)$ (15)

Synthesis An oven dried 20 mL pressure tube equipped with a magnetic stir bar was cooled under nitrogen and charged with 10 mL dry methanol. The solvent was degassed by vigorously bubbling nitrogen for 15 minutes, then charged with (CD)R(CT)P (**14**) (60 mg, 0.036 mmol), $Cu(BF_4)\cdot xH_2O$ (dried overnight under vacuum at 100°C over P_2O_5) (250 mg, 0.72 mmol), and K_2CO_3 (100 mg, 0.72 mmol). The tube was sealed, and lowered into a preheated oil bath set to 80°C, and stirred for 18 hrs. An aliquot was removed for TLC analysis (10% MeOH in CH_2Cl_2 on neutral Al plates), which revealed the absence of starting material. To ensure that the reaction went to completion, it was stirred for 72 hours total, but no further conversion was observed. The crude reaction was then cooled and filtered through a pad of Celite. The filtrate was stirred with excess NH_4PF_6 (60 mg, 0.36 mmol) for 1 hour, after which the solvent was removed by rotary evaporation. The resultant solid was washed with 3 X 50 mL deionized water and collected on a centrifuge. 49 mg crude product was isolated and a sample was submitted for mass spectral analysis.

LRMS (ES^+, *m/z*) calc'd for $C_{81}H_{97}Cu_2F_6N_{15}O_8PRu$ $(M + H^+)$ 1783.50 found 1782.13.

IX. References

[1] Staudinger, H. *Chem. Ber.* , **1924**, *57*, 1203.
[2] Stevens, M.P. *Polymer Chemistry, 3rd ed.;* Oxford University Press: New York, 1999; pp. 3-6.
[3] Voet, D.; Voet, J.G. *Biochemistry, 2nd ed.*; Wiley: New York, 1995; pp. 105-212.
[4] A) Lehn, J.M. *Supramolecular Chemistry: Concepts and Perspectives*, VCH: Weinheim, 1995.
B) Biomimicry: Philp, D; Stoddart, J.F. *Angew. Chem. Int. Ed.*, **1996**, *35*, 1154-1196.
C) Lehn, J.M. *Angew. Chem. Int. Ed.*, **1988**, *27*, 89-112.
D) Pedersen, C.J. *Angew. Chem. Int. Ed.*, **1988**, *27*, 1021-1027.
E) Cram, D.J. *Angew. Chem. Int. Ed.*, **1988**, *27*, 1009-1020.
[5] Balzani, V.; Scandola, F. *Supramolecular Photochemistry;* Horwood: Chichester, U.K., 1991.
[6] Gust, D.; Moore, T.A.; Moore, A.L. *Acc. Chem. Res.*, **1993**, *26*, 198.
[7] O'Regan, B.; Gratzel, M. *Nature,* **1991**, *353,* 738.
[8] Sauvage, J.-P.; Collin, J.-P.; Chambron, J.-C.; Guilerez, S.; Coudret, C.; Balzani, V.; Barigelletti, F.; De Cola, L.; Flamigni, L. *Chem. Rev.*, **1994**, *94*, 993-1019.
[9] Eddoaudi, M.; Moler, D.B.; Li, H.; Chen, B.; Reineke, T.M.; O'Keeffe, M.; Yaghi, O.M. *Acc. Chem. Res.,* **2001**, *34*, 319-330.
[10] A) Maddox, J. *Nature*, **1988**, *335*, 201.
B) Ball, P. *Nature*, **1996**, *381*, 648-650.
[11] Zaworotko, M.J., in *Crystal Engineering*, Kluwer: Netherlands, 1999; pp. 383-408.
[12] Machida, R.; Kimura, E.; Kodama, M. *Inorg. Chem.*, **1983**, *22*, 2055-2061.
[13] A) Kimura, E.; Koike, T.; Machida, R.; Nagai, R.; Kodama, M. *Inorg. Chem.*, **1984**, *23*, 4181-4188.
B) Meyer, M.; Fremond, L.; Espinosa, E.; Guilard, R.; Ou, Z.; Kadish, K.M. *Inorg. Chem.*, **2004**, *43*, 5572-5587.
[14] Constable, E.C.; Kulke, T.; Neuburger, M.; Zehnder, M. *New J. Chem.*, **1997**, *21*, 1091-1102, esp. p. 1095.
[15] Laine, P.; Bedioui, F.; Ochsenbein, P.; Marvaud, V.; Bonin, M.; Amouyal, E. *J. Am. Chem. Soc.*, **2002**, *124*, 1364-1377.
[16] A) Hegedus, L.S.; McGuire, M.A.; Schultze, L.M.; Yijun, C.; Anderson, O.P. *J. Am. Chem. Soc.*, **1984**, *106*, 2680.
B) Hegedus, L.S.; deWeck, G.; D'Andrea, S. *J. Am. Chem. Soc.*, **1988**, *106*, 2122.
C) Hegedus, L.S.; Montgomery, J.; Narukawa, Y.; Snustad, D.C. *J. Am. Chem. Soc.*, **1991**, *113*, 5784.
[17] Betschart, C.; Hegedus, L.S. *J. Am. Chem. Soc.*, **1992**, *114*, 5010-5017.
[18] Hegedus, L.S.; Moser, W.H. *J. Org. Chem.* , **1994**, *59*, 7779-7784.
[19] Hegedus, L.S.; Sundermann, M.J.; Dorhout, P.K. *Inorg.Chem.*, **2003**, *42*, 4346-4354.
[20] Andrew Bolig, unpublished results; see also:
A)Gil, J.M.; David, S.; Reiff, A.; Hegedus, L., Hegedus, L.S., submitted.
B) Reiff, A.L.; Garcia-Frutos, E.; Gil, J.M., Hegedus, L.S., submitted.
[21] Curtis, N.F. *Coord. Chem. Rev.*, **1968**, *3*, 3.
[22] Blake, A.J.; Gould, R.O.; Hyde, T,I,; Schroder, M. *J.Chem. Soc., Chem. Comm.*, **1987**, 431.
[23] Robinson, G. H.; Sangokoy , S. A.; Pennington, W.T.; Self, M. F. *J.Coord. Chem.*, **1989**, *19*, 287.
[24] Denat, F., Brandes, S.; Guilard, R. *Synlett*, **2000**, *5*, 561-574 (and references therein).
[25] A) Koola, J. D.; Kochi, J. K. *Inorg. Chem.*, **1987**, *26*, 908.
B) Nam, W.; Ho, R.; Valentin, J. S. *J. Am. Chem. Soc.*, **1991**, *113*, 7052.
[26] Chen, X.; Rokita, S. E.; Burrows, C. J. *J. Am. Chem. Soc.*, **1991**, *113*, 5884.

[27] A) Li, H.-L.; Anderson, W.C.; Chambers, J.Q.; Hobbs, D.T. *Inorg. Chem.*, **1989**, *28*, 863-868.
B) Kang, C.; Anson, F.C. *Inorg. Chem.*, **1995**, *34*, 2771-2780.
[28] Schwarzenbach, G. *Helv. Chim. Acta*, **1952**, *35*, 2344.
[29] Cabbiness, D.K.; Margerum, D.W. *J. Am. Chem. Soc.*, **1969**, *91*, 6540.
[30] Kimura, E.; Koike, T.; Machida.; Nagai, R.; Kodama, M. *Inorg. Chem.* **1984**, *23*, 4181-4188.
[31] Sigel, H.; Martin, R. B. *Chem. Rev.*, **1982**, *82*, 385.
[32] Chin, M.; Wone, D.; Nguyen, Q.; Nathan, L. C.; Wagenknecht, P. S. *Inorg. Chim. Acta*, **1999**, *292*, 254-259.
[33] A) Kimura, E. *J. Coord. Chem.*, **1986**, *15*, 1.
B) Sigel, H.; Martin, R. B. *Chem. Rev.*, **1982**, *82*, 385.
[34] Collins, T.J. *Acc. Chem. Res.*, **2002**, *35*, 782-790.
[35] Kimura, E.; Koike, T.; Machida, R.; Nagai, R.; Kodama, M. *Inorg. Chem.*, **1984**, *23*, 4181-4188.

[36] Denat, F.; Brandes, S.; Guilard, R. *Synlett,* **2000**, *5*, 561-574.
[37] A)Brandes, S.; Denat, F.; Lacour, S.; Rabiet, F.; Barbette, F.; Pullumbi, P.; Guilard, R. *Eur. J. Org. Chem.* **1998**, 2349.
B)Denat, F.; Lacour, S.; Brandes, S.; Guilard, R. *Tet. Lett.*, **1997**, *38*, 4417
[38] Wynn, T.; Hegedus, L.S. *J. Am. Chem. Soc.,* **2000**, *122*, 5034-5042.
[39] Hegedus, L.S.; Sundermann, M.J.; Dorhout, P.K. *Inorg.Chem.*, **2003**, *42*, 4346-4354.
[40] Reiff, A.; Garcia-Frutos, E.; Gil, J.S.; Hegedus, L.S., *submitted.*
[41] Achmatowicz, M.; Hegedus, L.S.; David, S. *J. Org. Chem.*,**2003**, *68*, 7661-7666.
[42] Lauffer, R.B. *Chem. Rev.* **1987,** *87*, 901.
[43] Brugel, T.; Hegedus, L.S. *J. Org. Chem.,* **2003**, *68*, 8409-8415.
[44] a)Nam, W.; Ho, R.; Valentine, J.S. *J. Am. Chem. Soc.* **1991**, *113*, 7052-7054
b)Wagler, T.R.; Fang, Y; Burrows, C.J. *J. Org. Chem.*, **1989**, *54*, 1584-1589.
[45] Hsiao, Y.; Hegedus, L.S. *J. Org. Chem.*, **1997**, *62*, 3586-3591.
[46] Kimura, E.; Koike, T.; Machida, R.; Nagai, R.; Kodama, M. *Inorg. Chem.*, **1984**, *23*, 4181-4188.
[47] A) Hegedus, L.S.; Sundermann, M.J.; Dorhout, P.K. *Inorg. Chem.*, **2003**, *42*, 4346-4354.
B) Achmatowicz, M.; Hegedus, L.S.; David, S. *J. Org. Chem.*, **2003**, *68*, 7661-7666.
C)Wynn, T.; Hegedus, L.S. *J. Am. Chem. Soc.*, **2000**, *122*, 5034-5042.
[48] Meyer, M.; Fremond, L.; Espinosa, E.; Guilard, R.; Ou, Z.; Kadish, K.M. *Inorg. Chem.*, **2004**, *43*, 5572-5587.
[49] Hegedus, L.S.; Sundermann, M.J.; Dorhout, P.K. *Inorg. Chem.*, **2003**, *42*, 4346-4354.
[50] B) Reiff, A.L.; Garcia-Frutos, E.; Gil, J.M., Hegedus, L.S., *Inorg. Chem.*, submitted.
[51] A) Juris, A.; Balzani, V.; Barigelletti, F.; Campagna, S.; Belser, P.; Von Zelewsky, A. *Coord. Chem. Rev.,* **1988**, *84*, 85.
B) Krausz, E.; Ferguson, J. *Prog. Inorg. Chem.*, **1989**, *37*, 293.
[52] Blau, F. *Ber. Dtsch. Chem. Ges.*, **1888**, *21*, 1077-1078.
[53] Meyer, T. J. *Acc. Chem. Res.*, **1989**, *22*, 163-170.
[54] Kalyanasundaram, K. *Coord. Chem. Rev.* **1982**, *46*, 159-244.
[55] A) Constable, E.C.; Kulke, R.; Neuburger, M.; Zehnder, M. *New. J. Chem.*, **1997**, *21*, 1091-1102.
B) Thummel, R.P.; Hegde, V.; Jahng, Y. *Inorg. Chem.*, **1989**, *28*, 3264-3267.
[56] Constable, E.C. *Adv. Inorg. Chem. Radiochem.*, **1986**, *30*, 69.
[57] Morgan, S.G.; Burstall, F.H. *J. Chem. Soc.* **1931**, 20-30.
[58] McWhinnie, W.R.; Miller, J.D. *Adv. Inorg. Chem. Radiochem.*, **1969**, *12,* 135-215.
[59] Constable, E.C. *Adv. Inorg. Chem. Radiochem.*, **1986**, 30, 69-121.
[60] Schubert, U.S.; Eschbaumer, C. *Angew. Chem. Int. Ed.* **2002**, *41*, 2892.
[61] A) Creutz, C. ; Chou, M.; Netzel, T.L.; Okumura, M.; Sutin, M. *J. Am. Chem. Soc.*, **1980**, *102*, 1309.
B) Winkler, J.R.; Netzel, T.L.; Creutz, C.; Sutin, N. *J. Am. Chem. Soc.*, **1987**, *109*, 2381.
[62] Sauvage, J.-P.; Collin, J.-P.; Chambron, J.-C.; Guilerez, S.; Coudret, C.; Balzani, V.; Barigelletti, F.; De Cola, L.; Flamigni, L. *Chem. Rev.*, **1994**, *94*, 993-1019.
[63] Phifer, C.C.; McMillin, D.R. *Inorg. Chem.*, **1986**, *25*, 1329.
[64] Constable, E.C.; Cargill-Thompson, A.M.W.; Tocher, D.A.; Daniels, M.A.M. *New J. Chem.*, **1992**, *16*, 855-867.

[65] Passalacqua, R.; Loiseau, F.; Campagna, S.; Fang, Y.-Q.; Hanan, G.S. *Angew. Chem. Int. Ed.*, **2003**, *42*, 1608.
[66] Hammarstrom, L.; Barigelletti, F.; Flamigni, L.; Indelli, M. T.; Armaroli, N.; Calogero, G.; Guardigli, M.; Sour, A.; Collin, J.-P.; Sauvage, J.-P. *J. Phys. Chem. A*, **1997**, *101*, 9061-9069.
[67] Baranoff, E.; Collin, J.-P.; Flamigni, L.; Sauvage, J.-P. *Chem. Soc. Rev.*, **2004**, *33*, 147-155.
[68] A) Creutz, C.; Taube, H. *J. Am. Chem. Soc.*, **1969**, *91*, 3988.
B) Creutz, C. *Prog. Inorg. Chem.*, **1983**, *30*, 1.
C) Richardson, D.E.; Taube, H. *Coord. Chem. Rev.*, **1984**, *60*, 107.
[69] Kaim, W.; Klein, A.; Glockle, M. *Acc. Chem. Res.*, **2000**, *33*, 755-763.
[70] A) Launay, J.-P. *Chem. Soc. Rev.*, **2001**, *30*, 386-397.
B) Collin, J. P.; Laine, P.; Launay, J.-P.; Sauvage, J.-P.; Sour, A. *Chem. Comm*, **1993**, 434-435.
C) Powers, M.J.; Meyer, T.J. *J. Am. Chem. Soc.*, **1980**, *102*, 1289 and references therein.
[71] Beley, M.; Collin, J.-P.; Louis, R.; Metz, B.; Sauvage, J.-P. *J. Am. Chem. Soc.*, **1991**, *113*, 8521-8522.
[72] Patoux, C.; Launay, J.-P.; Beley, M.; Chodorowski,-Kimmes, S.; Collin, J.-P.; James, S.; Sauvage, J.-P. *J. Am. Chem. Soc.*, **1998**, *120*, 3717-3725.)
C) Constable, E. C.; Cargill Thompson, A.M.W.; Greulich, S. *Chem. Comm.*, **1993**, 1444-1446.
[73] Beley, M.; Collin, J.-P.; Sauvage, J.-P. *Inorg. Chem.*, **1993**, *32*, 4539-4534.
[74] Patoux, C.; Launay, J.-P.; Beley, M.; Chodorowski,-Kimmes, S.; Collin, J.-P.; James, S.; Sauvage, J.-P. *J. Am. Chem. Soc.*, **1998**, *120*, 3717-3725.)
[75] Launay, J.P. *Chem. Soc. Rev.*, **2001**, *30*, 386-397.
[76] Constable, E.C.; Cargill-Thompson, A.M.W.; Tocher, D.A.; Daniels, M.A.M. *New J. Chem.*, **1992**, *16*, 855-867.
[77] Wendling, J. J. Synthesis of Quinoxaline Dioxocyclams and Analysis of Their DNA Binding and Cleaving Properties and Progress Toward the Synthesis of Ruthenium (II) Terpyridine-Capped Dioxocyclams. Ph.D. Dissertation, Colorado State University, Fort Collins, CO, 2003.
[78] Achmatowicz, M.; Hegedus, L.S.; David, S. *J. Org. Chem.*,**2003**, *68*, 7661-7666.
[79] Aspley, C.J.; Williams, J.A. *New J. Chem.*, **2001**, *25*, 1136-1147.
[80] Reddy, Y.K.; Falck, J.R. *Org Lett.*, **2002**, *4*, 969-971.
[81] Sullivan, B.P.; Calvert, J. M.; Meyer, T. J. *Inorg. Chem.*, **1980**, *19*, 1404-1407.
[82] Flamigni, L.; Barigelletti, F.; Armaroli, N.; Collin, J.-P.; Sauvage, J.-P.; Williams, J.A.G. *Chem. Eur. J.*, **1998**, *4*, 1744.
[83] Constable, E.C.; Cargill Thompson, A.M.W.; Tocher, D.A.; Daniels, M.A.M. *New J. Chem.*, **1992**, *16*, 855-867.
[84] Constable, E.C.; Kulke, T.; Neuburger, M.; Zehnder, M. *New J. Chem.*, **1997**, *21*, 1091-1102.
[85] Constable, E.C.; Kulke, T.; Neuburger, M.; Zehnder, M. *New J. Chem.*, **1997**, *21*, 1091-1102.
[86] Constable, E.C.; Cargill Thompson, A.M.W.; Tocher, D.A.; Daniels, M.A.M. *New J. Chem.*, **1992**, *16*, 855-867.
[87] Chavarot, M.; Pikramenou, Z. *Tet. Lett.*, **1999**, *40*, 6865-6868.
[88] Jouaiti, A.; Geoffrey, M.; Collin, J.-P. *Inorg. Chim. Acta*, **1996**, *245*, 69-73.
[89] Ishiyama, T.; Murata, M.; Miyaura, N. *J. Org. Chem.*, **1995**, *60*, 7508.
[90] Jouaiti, A.; Geoffrey, M.; Collin, J.-P. *Inorg. Chim. Acta*, **1996**, *245*, 69-73.
[91] Beley, M.; Collin, J.P.; Louis, R.; Metz, B.; Sauvage, J.-P. *J. Am. Chem. Soc.*, **1991**, *113*, 8521-8522.
[92] Beley, M.; Collin, J.-P.; Louis, R.; Metz, B.; Sauvage, J.-P. *J. Am. Chem. Soc.*, **1991**, *113*, 8521-8522.
[93] Jeffrey, G.A. *An Introduction to Hydrogen Bonding;* Oxford University Press: New York, 1997; pp. 12-16.
[94] Hubin, T.J.; McCormick, J.M.; Collinson, S.R.; Alcock, N.W.; Busch, D.H. *Chem. Comm.*, **1998**, 1675-1676.
[95] Reiff, A.L.; Garcia-Frutos, E.; Gil, J.M., Hegedus, L.S., *Inorg.Chem.*,submitted.
[96] Hegedus, L.S.; Sundermann, M.J.; Dorhout, P.K. *Inorg. Chem.*, **2003**, *42*, 4346-4354.
[97] Reiff, A.L.; Garcia-Frutos, E.; Gil, J.M., Hegedus, L.S., *Inorg.Chem.*,submitted.
[98] Albores, P.; Slep, L.D.; Weyhermuller, T.; Baraldo, L.M. *Inorg. Chem.*, **2004**, *43*, 6762-6773.
[99] A)Gil, J.M.; David, S.; Reiff, A.; Hegedus, L., Hegedus, L.S., *Inorg.Chem.*, submitted.
B) Reiff, A.L.; Garcia-Frutos, E.; Gil, J.M., Hegedus, L.S., *Inorg.Chem.*,submitted.
[100] Geiss, A.; Kolm, J.J.; Janiak, D.; Vahrenkamp, H. *Inorg. Chem.*, **2000**, *39*, 4037.
[101] Nagata, T.; Kikuzawa, Y; Osuka, A.; *Inorg. Chim. Acta.*, **2003**,*342*, 139-144.

[102] Kang, C.; Anson, F. *J. Electroanal. Chem.* , **1996**, *407*, 233-236.
[103] Meyer, M.; Fremond, L.; Espinosa, E.; Guilard, R.; Ou, Z.; Kadish, K.M. *Inorg. Chem.*, **2004**, *43*, 5572-5587.
[104] See, for example: Patoux, C.; Launay, J.-P.; Beley, M.; Chodorowski-Kimmes, S.; Collin, J.-P.; James, S.; Sauvage, J.-P. *J. Am. Chem. Soc.*, **1998**, *120*, 3717-3725.
[105] Patoux, C.; Launay, J.-P.; Beley, M.; Chodorowski-Kimmes, S.; Collin, J.-P.; James, S.; Sauvage, J.-P. *J. Am. Chem. Soc.*, **1998**, *120*, 3717-3725.
[106] A) Kang, C.; Anson, F. C. *J. Electroanal. Chem.*, **1996**, *407*, 233-236.
B) Nagata, T.; Kikuzawa, Y.; Osuka, A. *Inorg. Chim. Acta*, **2003**, *342*, 139-144.
[107] A) Achmatowicz, M.; Hegedus, L.S.; David, S. *J. Org. Chem.*,**2003**, *68*, 7661-7666.
B) Wendling, J. J. Synthesis of Quinoxaline Dioxocyclams and Analysis of Their DNA Binding and Cleaving Properties and Progress Toward the Synthesis of Ruthenium (II) Terpyridine-Capped Dioxocyclams. Ph.D. Dissertation, Colorado State University, Fort Collins, CO, 2003.

IX. Appendix B

Table 1. Crystal data and structure refinement for lsh148.

Identification code	lsh148	
Empirical formula	C64 H68 F12 N10 O7 P2 Ru	
Formula weight	1480.29	
Temperature	173(2) K	
Wavelength	0.71073 Å	
Crystal system	Monoclinic	
Space group	P2(1)/c	
Unit cell dimensions	a = 17.7224(17) Å	α= 90°.
	b = 25.328(2) Å	β= 94.583(2)°.
	c = 14.9698(14) Å	γ = 90°.
Volume	6698.1(11) $Å^3$	
Z	4	
Density (calculated)	1.468 Mg/m^3	
Absorption coefficient	0.375 mm^{-1}	
F(000)	3040	
Crystal size	0.40 x 0.40 x 0.20 mm^3	
Theta range for data collection	1.98 to 23.26°.	
Index ranges	-19<=h<=19, -28<=k<=28, -16<=l<=16	
Reflections collected	42560	
Independent reflections	9626 [R(int) = 0.0581]	
Completeness to theta = 23.26°	99.9 %	
Absorption correction	multi-scan	
Max. and min. transmission	0.9288 and 0.8645	
Refinement method	Full-matrix least-squares on F^2	
Data / restraints / parameters	9626 / 0 / 843	
Goodness-of-fit on F^2	1.042	
Final R indices [I>2sigma(I)]	R1 = 0.0714, wR2 = 0.1758	
R indices (all data)	R1 = 0.0938, wR2 = 0.1921	
Extinction coefficient	0.00138(19)	
Largest diff. peak and hole	2.668 and -0.761 $e.Å^{-3}$	

Table 2. Atomic coordinates (x 10^4) and equivalent isotropic displacement parameters ($Å^2$x 10^3) for lsh148. U(eq) is defined as one third of the trace of the orthogonalized U^{ij} tensor.

	x	y	z	U(eq)
C(61)	3407(14)	6828(11)	9856(17)	231(10)
Ru(1)	2626(1)	3736(1)	-2371(1)	31(1)
N(1)	3456(3)	3370(2)	-1501(3)	35(1)
N(2)	1839(3)	4313(2)	-2802(3)	33(1)
N(3)	3408(3)	4054(2)	-3171(3)	37(1)
N(4)	2586(3)	3221(2)	-3410(3)	35(1)
N(5)	1793(3)	3217(2)	-2040(3)	34(1)
N(6)	3256(3)	5908(2)	3895(3)	31(1)
N(7)	1031(3)	6283(2)	2847(3)	33(1)
N(8)	1497(4)	6467(4)	4744(5)	85(2)
N(9)	2996(6)	6727(4)	2505(7)	139(5)
N(10)	2183(3)	5618(2)	2613(3)	31(1)
C(1)	2633(3)	4184(2)	-1313(4)	33(1)
C(2)	3091(3)	4053(2)	-530(4)	34(1)
C(3)	3014(3)	4332(2)	255(4)	36(1)
C(4)	2480(3)	4741(2)	273(4)	34(1)
C(5)	2032(3)	4871(2)	-501(4)	33(1)
C(6)	2103(3)	4593(2)	-1290(4)	33(1)
C(7)	1668(3)	4674(2)	-2156(4)	33(1)
C(8)	1143(4)	5074(3)	-2351(4)	40(2)
C(9)	804(4)	5120(3)	-3211(4)	44(2)
C(10)	992(4)	4768(3)	-3861(4)	41(2)
C(11)	1490(4)	4373(3)	-3639(4)	38(2)
C(12)	3879(4)	2943(2)	-1683(4)	39(2)
C(13)	4425(4)	2733(3)	-1081(5)	45(2)
C(14)	4553(4)	2965(3)	-260(5)	50(2)
C(15)	4128(4)	3400(3)	-47(4)	46(2)
C(16)	3582(4)	3599(2)	-668(4)	36(2)
C(17)	2382(3)	5039(2)	1112(4)	32(1)
C(18)	2960(3)	5083(2)	1803(4)	33(1)
C(19)	2855(3)	5377(2)	2559(4)	32(1)

C(20)	1612(3)	5595(2)	1970(4)	32(1)
C(21)	1701(3)	5296(2)	1224(4)	34(1)
C(22)	3419(4)	5438(2)	3362(4)	37(2)
C(23)	895(3)	5878(3)	2156(4)	37(2)
C(24)	3231(3)	5774(2)	4854(4)	36(1)
C(25)	2709(4)	6109(3)	5387(4)	43(2)
C(26)	2640(4)	5850(3)	6296(4)	53(2)
C(27)	3454(5)	6782(4)	5947(7)	84(3)
C(28)	1873(7)	6083(5)	4874(5)	101(5)
C(29)	708(4)	6492(4)	4452(4)	56(2)
C(30)	216(4)	6229(3)	5128(4)	52(2)
C(31)	532(8)	7102(4)	4460(5)	123(5)
C(32)	484(3)	6235(3)	3531(4)	36(1)
C(33)	1051(4)	6826(3)	2487(5)	44(2)
C(34)	1723(5)	6986(3)	1987(5)	56(2)
C(35)	1681(5)	7573(3)	1806(7)	80(3)
C(36)	1459(6)	6737(5)	571(8)	124(5)
C(37)	2438(5)	6901(5)	2569(14)	165(10)
C(38)	3759(4)	6628(3)	2885(5)	50(2)
C(39)	4169(5)	7153(3)	3008(6)	72(2)
C(40)	4285(7)	6291(4)	2185(8)	108(4)
C(41)	3776(3)	6354(3)	3790(4)	40(2)
C(42)	3800(4)	4507(3)	-3031(5)	48(2)
C(43)	4282(4)	4701(3)	-3654(6)	60(2)
C(44)	4358(4)	4423(4)	-4436(6)	62(2)
C(45)	3967(4)	3964(3)	-4580(5)	53(2)
C(46)	3495(3)	3783(3)	-3959(4)	39(2)
C(47)	3048(4)	3297(3)	-4073(4)	41(2)
C(48)	3060(4)	2930(3)	-4759(5)	61(2)
C(49)	2591(5)	2500(4)	-4755(6)	74(3)
C(50)	2119(4)	2426(3)	-4077(5)	61(2)
C(51)	2118(4)	2798(3)	-3400(4)	41(2)
C(52)	1663(4)	2799(3)	-2619(4)	41(2)
C(53)	1140(4)	2409(3)	-2462(5)	54(2)
C(54)	746(4)	2438(3)	-1706(6)	56(2)
C(55)	858(4)	2858(3)	-1143(5)	53(2)

C(56)	1377(4)	3238(3)	-1324(4)	43(2)
C(57)	1415(6)	4444(4)	3550(7)	89(3)
C(58)	1802(5)	3938(4)	3765(6)	71(2)
C(59)	2307(6)	3726(5)	3123(7)	105(4)
O(1)	2514(4)	7141(2)	3481(4)	66(2)
O(2)	1599(3)	5591(2)	4654(3)	47(1)
O(3)	1902(4)	6628(3)	1316(4)	103(2)
O(4)	2853(4)	6651(2)	5417(4)	83(2)
O(5)	1655(4)	3681(3)	4441(5)	97(2)
P(1)	4621(1)	1143(1)	7716(2)	59(1)
P(2)	9733(1)	6086(1)	8979(2)	63(1)
F(1)	4555(6)	1504(2)	8524(5)	168(4)
F(2)	5383(4)	894(2)	8062(6)	153(4)
F(3)	4157(3)	700(2)	8191(3)	89(2)
F(4)	4619(4)	783(3)	6868(5)	140(3)
F(5)	3874(3)	1361(3)	7232(5)	128(3)
F(6)	5084(3)	1581(3)	7256(5)	112(2)
F(7)	9834(4)	6694(2)	9210(4)	113(2)
F(8)	9768(5)	6231(2)	7952(4)	124(2)
F(9)	8850(3)	6170(3)	8867(5)	126(2)
F(10)	9641(3)	5493(2)	8696(5)	108(2)
F(11)	10613(3)	6009(2)	9073(5)	117(2)
F(12)	9716(4)	5968(3)	10000(4)	135(3)
C(62)	2700(20)	6394(15)	8670(30)	338(18)
O(6)	3025(12)	6138(8)	10233(15)	289(9)
C(63)	5020(20)	9810(15)	5520(20)	337(17)
C(60)	3209(18)	6379(13)	9390(20)	238(11)
O(7)	4090(20)	5353(19)	9280(30)	550(20)
C(64)	3790(20)	5844(16)	9620(20)	296(15)

Table 3. Bond lengths [Å] and angles [°] for lsh148.

C(61)-C(60)	1.37(3)	C(4)-C(5)	1.391(8)
Ru(1)-C(1)	1.947(6)	C(4)-C(17)	1.487(8)
Ru(1)-N(4)	2.028(5)	C(5)-C(6)	1.389(8)
Ru(1)-N(3)	2.066(5)	C(6)-C(7)	1.468(8)
Ru(1)-N(5)	2.067(5)	C(7)-C(8)	1.391(9)
Ru(1)-N(2)	2.086(5)	C(8)-C(9)	1.381(9)
Ru(1)-N(1)	2.101(5)	C(9)-C(10)	1.381(9)
N(1)-C(12)	1.357(8)	C(10)-C(11)	1.359(9)
N(1)-C(16)	1.377(8)	C(12)-C(13)	1.375(9)
N(2)-C(11)	1.361(7)	C(13)-C(14)	1.365(9)
N(2)-C(7)	1.382(7)	C(14)-C(15)	1.388(9)
N(3)-C(42)	1.349(8)	C(15)-C(16)	1.383(9)
N(3)-C(46)	1.385(8)	C(17)-C(21)	1.394(8)
N(4)-C(47)	1.349(8)	C(17)-C(18)	1.401(8)
N(4)-C(51)	1.356(8)	C(18)-C(19)	1.379(8)
N(5)-C(56)	1.349(8)	C(19)-C(22)	1.509(8)
N(5)-C(52)	1.377(8)	C(20)-C(21)	1.369(8)
N(6)-C(41)	1.473(8)	C(20)-C(23)	1.503(8)
N(6)-C(22)	1.474(7)	C(24)-C(25)	1.526(8)
N(6)-C(24)	1.480(7)	C(25)-O(4)	1.396(9)
N(7)-C(23)	1.462(7)	C(25)-C(26)	1.524(9)
N(7)-C(32)	1.472(8)	C(25)-C(28)	1.615(14)
N(7)-C(33)	1.478(8)	C(27)-O(4)	1.318(10)
N(8)-C(28)	1.186(11)	C(28)-O(2)	1.367(14)
N(8)-C(29)	1.432(10)	C(29)-C(30)	1.539(10)
N(9)-C(37)	1.095(15)	C(29)-C(32)	1.547(9)
N(9)-C(38)	1.446(12)	C(29)-C(31)	1.579(14)
N(10)-C(20)	1.341(7)	C(33)-C(34)	1.512(10)
N(10)-C(19)	1.347(7)	C(34)-O(3)	1.409(10)
C(1)-C(6)	1.401(8)	C(34)-C(37)	1.495(16)
C(1)-C(2)	1.411(8)	C(34)-C(35)	1.511(11)
C(2)-C(3)	1.387(8)	C(36)-O(3)	1.340(11)
C(2)-C(16)	1.467(8)	C(37)-O(1)	1.49(2)
C(3)-C(4)	1.405(8)	C(38)-C(39)	1.520(10)

C(38)-C(41)	1.520(9)	C(58)-C(59)	1.466(13)
C(38)-C(40)	1.688(14)	P(1)-F(1)	1.528(6)
C(42)-C(43)	1.402(10)	P(1)-F(2)	1.542(6)
C(43)-C(44)	1.382(11)	P(1)-F(5)	1.558(6)
C(44)-C(45)	1.363(11)	P(1)-F(4)	1.563(7)
C(45)-C(46)	1.377(9)	P(1)-F(6)	1.571(6)
C(46)-C(47)	1.465(9)	P(1)-F(3)	1.592(5)
C(47)-C(48)	1.388(9)	P(2)-F(12)	1.559(6)
C(48)-C(49)	1.370(12)	P(2)-F(10)	1.565(6)
C(49)-C(50)	1.378(11)	P(2)-F(11)	1.567(6)
C(50)-C(51)	1.384(9)	P(2)-F(9)	1.576(6)
C(51)-C(52)	1.473(9)	P(2)-F(8)	1.586(7)
C(52)-C(53)	1.386(9)	P(2)-F(7)	1.587(6)
C(53)-C(54)	1.379(11)	C(62)-C(60)	1.35(4)
C(54)-C(55)	1.362(11)	O(6)-C(60)	1.47(3)
C(55)-C(56)	1.373(10)	O(6)-C(64)	1.86(4)
C(57)-C(58)	1.475(13)	C(63)-C(63)#1	1.84(6)
C(58)-O(5)	1.249(11)	O(7)-C(64)	1.45(5)

C(1)-Ru(1)-N(4)	175.3(2)	C(16)-N(1)-Ru(1)	115.5(4)
C(1)-Ru(1)-N(3)	106.4(2)	C(11)-N(2)-C(7)	117.5(5)
N(4)-Ru(1)-N(3)	77.9(2)	C(11)-N(2)-Ru(1)	127.3(4)
C(1)-Ru(1)-N(5)	97.7(2)	C(7)-N(2)-Ru(1)	115.2(4)
N(4)-Ru(1)-N(5)	78.1(2)	C(42)-N(3)-C(46)	117.6(6)
N(3)-Ru(1)-N(5)	155.8(2)	C(42)-N(3)-Ru(1)	127.1(5)
C(1)-Ru(1)-N(2)	78.7(2)	C(46)-N(3)-Ru(1)	115.2(4)
N(4)-Ru(1)-N(2)	103.43(19)	C(47)-N(4)-C(51)	122.0(5)
N(3)-Ru(1)-N(2)	90.61(19)	C(47)-N(4)-Ru(1)	119.1(4)
N(5)-Ru(1)-N(2)	92.66(19)	C(51)-N(4)-Ru(1)	118.9(4)
C(1)-Ru(1)-N(1)	78.1(2)	C(56)-N(5)-C(52)	117.1(6)
N(4)-Ru(1)-N(1)	99.87(19)	C(56)-N(5)-Ru(1)	127.7(4)
N(3)-Ru(1)-N(1)	93.55(19)	C(52)-N(5)-Ru(1)	115.2(4)
N(5)-Ru(1)-N(1)	92.85(19)	C(41)-N(6)-C(22)	114.2(5)
N(2)-Ru(1)-N(1)	156.69(18)	C(41)-N(6)-C(24)	110.3(5)
C(12)-N(1)-C(16)	117.8(5)	C(22)-N(6)-C(24)	111.3(5)
C(12)-N(1)-Ru(1)	126.7(4)	C(23)-N(7)-C(32)	110.7(5)

C(23)-N(7)-C(33)	113.7(5)	C(19)-C(18)-C(17)	120.7(5)
C(32)-N(7)-C(33)	111.5(5)	N(10)-C(19)-C(18)	118.1(5)
C(28)-N(8)-C(29)	127.5(11)	N(10)-C(19)-C(22)	116.0(5)
C(37)-N(9)-C(38)	149.2(18)	C(18)-C(19)-C(22)	125.8(5)
C(20)-N(10)-C(19)	123.9(5)	N(10)-C(20)-C(21)	118.7(5)
C(6)-C(1)-C(2)	119.7(5)	N(10)-C(20)-C(23)	116.6(5)
C(6)-C(1)-Ru(1)	119.3(4)	C(21)-C(20)-C(23)	124.7(5)
C(2)-C(1)-Ru(1)	120.3(4)	C(20)-C(21)-C(17)	120.9(5)
C(3)-C(2)-C(1)	119.7(6)	N(6)-C(22)-C(19)	111.6(5)
C(3)-C(2)-C(16)	128.2(5)	N(7)-C(23)-C(20)	111.8(5)
C(1)-C(2)-C(16)	112.1(5)	N(6)-C(24)-C(25)	116.5(5)
C(2)-C(3)-C(4)	120.3(5)	O(4)-C(25)-C(26)	114.9(6)
C(5)-C(4)-C(3)	119.9(5)	O(4)-C(25)-C(24)	116.5(6)
C(5)-C(4)-C(17)	119.2(5)	C(26)-C(25)-C(24)	108.9(5)
C(3)-C(4)-C(17)	121.0(5)	O(4)-C(25)-C(28)	102.3(6)
C(6)-C(5)-C(4)	120.3(6)	C(26)-C(25)-C(28)	105.7(6)
C(5)-C(6)-C(1)	120.1(5)	C(24)-C(25)-C(28)	107.4(5)
C(5)-C(6)-C(7)	127.0(5)	N(8)-C(28)-O(2)	121.5(12)
C(1)-C(6)-C(7)	112.8(5)	N(8)-C(28)-C(25)	121.8(12)
N(2)-C(7)-C(8)	121.0(5)	O(2)-C(28)-C(25)	116.5(6)
N(2)-C(7)-C(6)	113.3(5)	N(8)-C(29)-C(30)	111.7(6)
C(8)-C(7)-C(6)	125.6(5)	N(8)-C(29)-C(32)	115.4(6)
C(9)-C(8)-C(7)	119.4(6)	C(30)-C(29)-C(32)	106.6(6)
C(10)-C(9)-C(8)	119.4(6)	N(8)-C(29)-C(31)	103.3(8)
C(11)-C(10)-C(9)	119.5(6)	C(30)-C(29)-C(31)	107.2(6)
C(10)-C(11)-N(2)	123.1(6)	C(32)-C(29)-C(31)	112.4(6)
N(1)-C(12)-C(13)	123.2(6)	N(7)-C(32)-C(29)	116.6(5)
C(14)-C(13)-C(12)	118.8(6)	N(7)-C(33)-C(34)	118.3(5)
C(13)-C(14)-C(15)	119.7(6)	O(3)-C(34)-C(37)	95.4(10)
C(16)-C(15)-C(14)	119.9(6)	O(3)-C(34)-C(35)	121.1(7)
N(1)-C(16)-C(15)	120.6(6)	C(37)-C(34)-C(35)	105.9(8)
N(1)-C(16)-C(2)	113.8(5)	O(3)-C(34)-C(33)	114.2(7)
C(15)-C(16)-C(2)	125.6(6)	C(37)-C(34)-C(33)	109.7(8)
C(21)-C(17)-C(18)	117.6(5)	C(35)-C(34)-C(33)	108.9(7)
C(21)-C(17)-C(4)	119.9(5)	N(9)-C(37)-O(1)	103.2(15)
C(18)-C(17)-C(4)	122.4(5)	N(9)-C(37)-C(34)	138(2)

O(1)-C(37)-C(34)	119.0(10)	F(1)-P(1)-F(2)	95.7(5)
N(9)-C(38)-C(39)	108.5(7)	F(1)-P(1)-F(5)	92.3(5)
N(9)-C(38)-C(41)	112.4(7)	F(2)-P(1)-F(5)	171.7(5)
C(39)-C(38)-C(41)	108.5(6)	F(1)-P(1)-F(4)	175.4(5)
N(9)-C(38)-C(40)	112.9(8)	F(2)-P(1)-F(4)	88.8(5)
C(39)-C(38)-C(40)	103.6(7)	F(5)-P(1)-F(4)	83.3(4)
C(41)-C(38)-C(40)	110.5(6)	F(1)-P(1)-F(6)	90.1(4)
N(6)-C(41)-C(38)	118.5(5)	F(2)-P(1)-F(6)	87.8(4)
N(3)-C(42)-C(43)	121.9(7)	F(5)-P(1)-F(6)	90.0(3)
C(44)-C(43)-C(42)	119.4(7)	F(4)-P(1)-F(6)	91.3(4)
C(45)-C(44)-C(43)	119.0(7)	F(1)-P(1)-F(3)	89.6(3)
C(44)-C(45)-C(46)	120.4(7)	F(2)-P(1)-F(3)	91.8(4)
C(45)-C(46)-N(3)	121.7(6)	F(5)-P(1)-F(3)	90.5(3)
C(45)-C(46)-C(47)	123.6(6)	F(4)-P(1)-F(3)	89.1(4)
N(3)-C(46)-C(47)	114.8(5)	F(6)-P(1)-F(3)	179.4(4)
N(4)-C(47)-C(48)	119.6(6)	F(12)-P(2)-F(10)	94.1(4)
N(4)-C(47)-C(46)	112.9(5)	F(12)-P(2)-F(11)	89.1(4)
C(48)-C(47)-C(46)	127.5(6)	F(10)-P(2)-F(11)	89.3(3)
C(49)-C(48)-C(47)	119.0(7)	F(12)-P(2)-F(9)	91.9(4)
C(48)-C(49)-C(50)	121.0(7)	F(10)-P(2)-F(9)	91.2(4)
C(49)-C(50)-C(51)	118.9(7)	F(11)-P(2)-F(9)	178.8(5)
N(4)-C(51)-C(50)	119.5(6)	F(12)-P(2)-F(8)	177.4(5)
N(4)-C(51)-C(52)	112.5(5)	F(10)-P(2)-F(8)	88.4(4)
C(50)-C(51)-C(52)	128.0(6)	F(11)-P(2)-F(8)	90.0(4)
N(5)-C(52)-C(53)	121.4(6)	F(9)-P(2)-F(8)	88.9(4)
N(5)-C(52)-C(51)	115.2(5)	F(12)-P(2)-F(7)	89.0(4)
C(53)-C(52)-C(51)	123.3(6)	F(10)-P(2)-F(7)	176.9(4)
C(54)-C(53)-C(52)	119.4(7)	F(11)-P(2)-F(7)	90.4(4)
C(55)-C(54)-C(53)	119.4(7)	F(9)-P(2)-F(7)	89.1(4)
C(54)-C(55)-C(56)	119.5(7)	F(8)-P(2)-F(7)	88.5(3)
N(5)-C(56)-C(55)	123.1(7)	C(60)-O(6)-C(64)	61.0(16)
O(5)-C(58)-C(59)	121.2(10)	C(62)-C(60)-C(61)	121(4)
O(5)-C(58)-C(57)	120.4(9)	C(62)-C(60)-O(6)	122(3)
C(59)-C(58)-C(57)	118.2(9)	C(61)-C(60)-O(6)	88(2)
C(36)-O(3)-C(34)	108.1(9)	O(7)-C(64)-O(6)	145(3)
C(27)-O(4)-C(25)	113.8(7)		

Symmetry transformations used to generate equivalent atoms:

#1 -x+1,-y+2,-z+1

Table 4. Anisotropic displacement parameters ($Å^2 x\ 10^3$) for lsh148. The anisotropic displacement factor exponent takes the form: $-2\pi^2[\ h^2\ a^{*2}U^{11} + ... + 2\ h\ k\ a^*\ b^*\ U^{12}\ ]$

	U^{11}	U^{22}	U^{33}	U^{23}	U^{13}	U^{12}
Ru(1)	34(1)	33(1)	25(1)	-7(1)	2(1)	0(1)
N(1)	39(3)	29(3)	37(3)	-7(2)	4(2)	0(2)
N(2)	37(3)	37(3)	26(3)	-5(2)	3(2)	-3(2)
N(3)	35(3)	35(3)	40(3)	0(2)	2(2)	3(2)
N(4)	33(3)	41(3)	30(3)	-10(2)	1(2)	2(2)
N(5)	33(3)	39(3)	31(3)	-2(2)	-2(2)	5(2)
N(6)	34(3)	34(3)	25(3)	-6(2)	-3(2)	5(2)
N(7)	27(3)	42(3)	29(3)	0(2)	-1(2)	4(2)
N(8)	78(5)	125(7)	53(4)	-7(4)	8(4)	-5(5)
N(9)	125(8)	127(8)	148(9)	99(7)	-96(7)	-91(7)
N(10)	35(3)	35(3)	22(3)	-4(2)	4(2)	3(2)
C(1)	39(3)	33(3)	28(3)	-5(3)	0(3)	-1(3)
C(2)	38(3)	36(3)	27(3)	-2(3)	-4(3)	3(3)
C(3)	40(4)	40(4)	28(3)	0(3)	-2(3)	4(3)
C(4)	40(4)	36(3)	27(3)	-5(3)	1(3)	1(3)
C(5)	36(3)	36(3)	27(3)	-5(3)	-1(3)	4(3)
C(6)	38(3)	33(3)	28(3)	-3(3)	-1(3)	5(3)
C(7)	36(3)	41(4)	22(3)	0(3)	3(3)	0(3)
C(8)	43(4)	47(4)	31(3)	-5(3)	2(3)	5(3)
C(9)	47(4)	45(4)	37(4)	4(3)	-4(3)	5(3)
C(10)	46(4)	49(4)	26(3)	3(3)	-5(3)	-3(3)
C(11)	45(4)	46(4)	23(3)	-5(3)	2(3)	-6(3)
C(12)	43(4)	31(3)	43(4)	-10(3)	11(3)	-3(3)
C(13)	47(4)	34(4)	54(4)	1(3)	11(3)	8(3)
C(14)	49(4)	49(4)	50(4)	5(3)	-3(3)	14(3)
C(15)	58(4)	46(4)	34(4)	-2(3)	-3(3)	10(3)
C(16)	39(4)	33(3)	36(3)	-4(3)	0(3)	2(3)
C(17)	37(3)	33(3)	24(3)	-4(2)	3(3)	-1(3)

C(18)	36(3)	33(3)	29(3)	-3(3)	1(3)	4(3)
C(19)	33(3)	33(3)	28(3)	-2(3)	-4(3)	5(3)
C(20)	30(3)	42(4)	24(3)	-3(3)	-2(3)	-3(3)
C(21)	36(3)	39(4)	25(3)	-7(3)	-1(3)	-2(3)
C(22)	39(4)	40(4)	30(3)	-8(3)	-6(3)	8(3)
C(23)	31(3)	53(4)	26(3)	-9(3)	-3(3)	3(3)
C(24)	36(3)	43(4)	26(3)	-3(3)	-7(3)	9(3)
C(25)	50(4)	47(4)	30(3)	-2(3)	-2(3)	14(3)
C(26)	51(4)	78(5)	29(4)	0(3)	-1(3)	11(4)
C(27)	60(6)	108(8)	82(6)	4(6)	-13(5)	10(5)
C(28)	135(9)	136(10)	40(5)	47(6)	52(5)	106(9)
C(29)	26(4)	112(7)	28(4)	-7(4)	-1(3)	1(4)
C(30)	38(4)	82(5)	36(4)	-10(4)	9(3)	2(4)
C(31)	227(14)	113(9)	32(4)	-43(5)	26(6)	-120(9)
C(32)	30(3)	48(4)	29(3)	-6(3)	-2(3)	2(3)
C(33)	34(4)	47(4)	50(4)	6(3)	1(3)	12(3)
C(34)	68(5)	47(4)	52(5)	9(4)	14(4)	2(4)
C(35)	66(5)	66(6)	105(7)	45(5)	-12(5)	-3(4)
C(36)	73(7)	145(11)	145(11)	70(9)	-48(7)	3(7)
C(37)	20(5)	106(10)	370(30)	166(14)	29(9)	16(5)
C(38)	51(4)	50(4)	49(4)	-1(3)	2(3)	-3(3)
C(39)	50(5)	74(6)	90(6)	17(5)	-2(4)	-16(4)
C(40)	113(9)	113(9)	98(8)	54(7)	-3(7)	-14(7)
C(41)	29(3)	49(4)	41(4)	-6(3)	-6(3)	-2(3)
C(42)	41(4)	43(4)	59(4)	-2(3)	-3(3)	3(3)
C(43)	40(4)	48(4)	92(6)	20(4)	4(4)	-6(3)
C(44)	45(4)	76(6)	68(6)	25(5)	14(4)	5(4)
C(45)	43(4)	70(5)	48(4)	4(4)	13(3)	11(4)
C(46)	37(4)	46(4)	35(3)	-2(3)	8(3)	7(3)
C(47)	37(4)	54(4)	31(3)	-13(3)	2(3)	6(3)
C(48)	48(4)	85(6)	51(5)	-31(4)	15(4)	5(4)
C(49)	57(5)	91(7)	75(6)	-60(5)	12(4)	0(5)
C(50)	56(5)	53(5)	72(5)	-32(4)	2(4)	-10(4)
C(51)	37(4)	40(4)	45(4)	-14(3)	-1(3)	-1(3)
C(52)	35(4)	38(4)	48(4)	0(3)	-1(3)	3(3)
C(53)	43(4)	42(4)	75(5)	-1(4)	-3(4)	-7(3)

C(54)	42(4)	48(5)	79(6)	18(4)	8(4)	-4(3)
C(55)	41(4)	67(5)	53(4)	20(4)	11(3)	5(4)
C(56)	40(4)	52(4)	37(4)	5(3)	0(3)	7(3)
C(57)	121(9)	60(6)	84(7)	-2(5)	6(6)	-8(6)
C(58)	62(5)	99(7)	52(5)	-13(5)	3(4)	-12(5)
C(59)	75(7)	151(11)	93(8)	-25(7)	27(6)	-7(7)
O(1)	93(5)	59(4)	47(3)	-14(3)	5(3)	-8(3)
O(2)	60(3)	29(3)	50(3)	-6(2)	-4(2)	4(2)
O(3)	89(5)	151(7)	68(4)	24(5)	-6(4)	-4(5)
O(4)	96(5)	76(4)	77(4)	-22(3)	9(4)	0(4)
O(5)	110(6)	106(6)	76(5)	4(4)	23(4)	17(4)
P(1)	58(1)	52(1)	63(1)	0(1)	-15(1)	-3(1)
P(2)	62(1)	54(1)	75(2)	-5(1)	7(1)	15(1)
F(1)	344(12)	69(4)	103(5)	-38(4)	91(6)	-70(6)
F(2)	92(4)	86(4)	262(9)	37(5)	-99(5)	-4(3)
F(3)	123(4)	60(3)	82(3)	10(3)	-1(3)	-31(3)
F(4)	127(6)	168(7)	126(6)	-67(5)	21(4)	-48(5)
F(5)	71(4)	178(7)	134(6)	72(5)	4(4)	18(4)
F(6)	83(4)	109(5)	143(5)	38(4)	14(4)	-26(3)
F(7)	169(6)	58(3)	108(4)	-28(3)	-9(4)	31(4)
F(8)	197(7)	95(4)	86(4)	-11(3)	45(5)	-14(4)
F(9)	72(4)	144(6)	162(6)	10(5)	5(4)	42(4)
F(10)	89(4)	56(3)	177(6)	-4(3)	3(4)	-6(3)
F(11)	65(3)	100(4)	187(7)	-72(4)	5(4)	7(3)
F(12)	169(7)	156(6)	84(4)	45(4)	28(4)	66(5)

Table 5. Hydrogen coordinates (x 10^4) and isotropic displacement parameters ($Å^2$x 10^3) for lsh148.

	x	y	z	U(eq)
H(60)	1729	6771	4838	102
H(61)	2967	6577	1974	167
H(10)	2120(30)	5840(20)	3100(40)	26(15)
H(3)	3323	4246	782	43
H(5)	1675	5150	-490	40
H(8)	1019	5314	-1897	48
H(9)	445	5392	-3353	52
H(80)	775	4802	-4460	49
H(11)	1600	4126	-4089	46
H(12)	3793	2780	-2254	46
H(13)	4709	2433	-1235	54
H(14)	4931	2828	164	59
H(15)	4212	3562	526	56
H(18)	3429	4909	1750	39
H(21)	1293	5264	775	40
H(22A)	3404	5119	3744	44
H(22B)	3935	5468	3158	44
H(23A)	675	6045	1597	44
H(23B)	524	5619	2353	44
H(24A)	3751	5802	5146	43
H(24B)	3073	5400	4897	43
H(26A)	3143	5817	6613	79
H(26B)	2414	5499	6209	79
H(26C)	2317	6068	6650	79
H(27A)	3336	6753	6573	126
H(27B)	3599	7146	5821	126
H(27C)	3873	6544	5840	126
H(30A)	283	5845	5108	78
H(30B)	-317	6316	4974	78
H(30C)	370	6358	5733	78

H(31A)	570	7248	3858	185
H(31B)	898	7280	4884	185
H(31C)	19	7159	4642	185
H(32A)	390	5855	3629	43
H(32B)	-1	6393	3288	43
H(33A)	1020	7073	2995	53
H(33B)	589	6877	2080	53
H(35A)	2087	7675	1433	120
H(35B)	1740	7766	2375	120
H(35C)	1190	7659	1494	120
H(36A)	976	6882	735	186
H(36B)	1365	6412	223	186
H(36C)	1712	6996	211	186
H(39A)	4214	7316	2421	108
H(39B)	4675	7094	3305	108
H(39C)	3882	7387	3377	108
H(40A)	4448	6530	1723	163
H(40B)	3981	6004	1900	163
H(40C)	4730	6142	2525	163
H(41A)	4298	6225	3940	48
H(41B)	3672	6623	4243	48
H(42)	3748	4700	-2495	58
H(43)	4553	5020	-3539	72
H(44)	4679	4550	-4867	75
H(45)	4020	3767	-5112	64
H(48)	3388	2975	-5225	73
H(49)	2591	2249	-5226	89
H(50)	1800	2125	-4075	73
H(53)	1054	2125	-2872	64
H(54)	399	2167	-1579	68
H(55)	580	2887	-628	64
H(56)	1446	3529	-926	52
H(57A)	966	4472	3888	133
H(57B)	1263	4458	2907	133
H(57C)	1760	4737	3713	133
H(59A)	2784	3924	3170	158

H(59B)	2066	3760	2514	158
H(59C)	2410	3353	3257	158